

Exchange Rate Disconnect Revisited*

Ryan Chahrour
Cornell University

Vito Cormun
Santa Clara University

Pierre De Leo
University of Maryland

Pablo Guerrón-Quintana
Boston College

Rosen Valchev
Boston College

November 21, 2025

Abstract

We find that variation in expected US productivity explains over half of US dollar/G7 exchange rate fluctuations. These fluctuations reflect both partly-anticipated changes in productivity and noise that affects beliefs without affecting realized productivity. This “noisy news” is primarily related to medium-to-long-run TFP growth, and causes significant deviations from uncovered interest parity. Together, these disturbances generate several well-known exchange rate puzzles, including predictable excess returns, low [Backus-Smith](#) correlations, and excess volatility. We examine leading classes of open-economy models and find that the incomplete markets framework best matches the qualitative patterns we identify in the data.

JEL Codes: D8, F3, G1

Keywords: Exchange Rate Disconnect, TFP News, Excess Returns, Excess Volatility

*We thank Adrien Auclert, Gurdip Bakshi, Antonio Coppola, Max Croce, Charles Engel, Tarek Hassan, Oleg Itskhoki, Rohan Kekre, Moritz Lenel, Yang Liu, Dmitry Mukhin, Francesco Pappadà, Mikkel Plagborg-Møller, Stephanie Schmitt-Grohé, Daniele Siena, Andreas Stathopoulos, Jenny Tang as well as participants at numerous seminars and conferences for helpful comments. This paper previously circulated under “Exchange Rate Disconnect Redux”.

Emails: ryan.chahrour@cornell.edu; vcormun@scu.edu; deleop@umd.edu; pguerron@gmail.com; valchev@bc.edu

The real exchange rate—the relative price of consumption across countries—plays a crucial role in clearing markets for goods and financial assets in open-economy models. As a result, these models typically imply that exchange rates are tightly linked to cross-country differentials in macro aggregates, real interest rates, and other asset prices in the economy. However, in the data, real exchange rates appear largely “disconnected” from these macro fundamentals: they exhibit virtually no correlation with current and past macro quantities (*e.g.*, Meese and Rogoff, 1983) or interest rates (*e.g.*, Fama, 1984), and are also surprisingly volatile (*e.g.*, Rogoff, 1996). Consequently, a large literature has proposed structural models to explore the shocks and mechanisms capable of generating these empirical features. Yet, direct empirical evidence on the origins of these patterns remains limited.

This paper aims to uncover the main empirical drivers of exchange rate fluctuations without relying on a structural model. Our key finding is that noisy news about future TFP accounts for more than half of the overall variation in *both* real exchange rates and many macro variables. Thus, our results indicate that the exchange rate is indeed connected to macro fundamentals: the apparent disconnect documented in previous literature arises because the effects of news manifest at *different horizons* for exchange rates and macro aggregates. Specifically, we find that the response of the exchange rate leads that of many macro variables by two years or more, resulting in low contemporaneous correlations between the exchange rate and macro aggregates, even though both sets of variables ultimately react to the same underlying source of fluctuations. Moreover, the conditional responses to noisy news reproduce a number of famous exchange rate puzzles, suggesting that these well-known empirical regularities have a common and fundamental origin.

We begin by documenting the main comovement patterns associated with exchange rate fluctuations using a reduced-form approach. In particular, following Uhlig (2003), we employ a VAR framework to isolate the dynamic covariances associated with the bulk of real exchange rate movements. This approach reveals that US/G7 real exchange rate appreciations are typically associated with future improvements in macro variables—such as US consumption, output, and utilization-adjusted TFP—while their contemporaneous comovement with these macro variables is weak. The resulting lead-lag structure unfolds over three to five years. These patterns suggest that the exchange rate, as a forward-looking asset price, responds to news about future macro fundamentals.

We then seek to directly identify disturbances to expectations about future US TFP and estimate their effects on the real exchange rate and other international macro variables. To do so, we follow Chahroud and Jurado (2022) to separately identify two orthogonal, structural disturbances: (i) changes in productivity that may be partly anticipated, and (ii) expectational “noise” disturbances that move expectations of productivity, *but never*

materialize in realized productivity. We use this approach to extract the disturbances driving expectations about future US TFP and then trace out their effects on the real exchange rate and other macro aggregates.

We find that anticipated future TFP changes and noise in TFP expectations both play an important role in driving exchange rates in the data. Noise disturbances give rise to volatile but relatively short-lived fluctuations in the exchange rate, while partly-anticipated TFP changes drive longer-run changes in the exchange rate. As a result, expectational noise appears more relevant at higher frequencies, while lower-frequency movements in exchange rates predominantly reflect true technological disturbances. Taken together, the two disturbances account for more than half of the variation in the level of the real exchange rate, while explaining a comparable fraction of the variation in real macro aggregates. However, echoing the reduced-form evidence mentioned above, the effects on macro aggregates is delayed relative to the response of exchange rates. We also study the impulse responses of a number of other variables, such as the trade balance and equity prices, and find that the US current account deteriorates and US and foreign equity prices rise in anticipation of an improvement of future US productivity. Thus, noisy news about future TFP prove to be the rare structural disturbances that drive a large portion of both real exchange rates, international business cycles and also other asset prices.

Noisy news also generate a number of well-known “exchange rate puzzles,” suggesting that a constellation of famous anomalies share a common fundamental origin. First, these disturbances cause significant fluctuations in expected excess currency returns, generating violations of uncovered interest parity (UIP) that are consistent with both the classic Forward Premium Puzzle (Fama, 1984) and the recently documented reversal at longer horizons (Engel, 2016; Valchev, 2020). Our results therefore speak to the time variation in the currency risk premium and complement the evidence of time-series predictability in Kremens and Martin (2019). In that vein, we also document that trading strategies that exploit the predictable component of excess returns associated with our identified disturbances are indeed profitable (out of sample). Second, the conditional responses of exchange rates and cross-country consumption differentials exhibit a weak negative correlation, in line with the famous Backus and Smith (1993) puzzle. Third, the conditional responses imply that the exchange rate is highly persistent and more volatile than other macro quantities, two well-known features of exchange rate dynamics that the literature calls the “PPP Puzzle” and the excess volatility of the exchange rate (*e.g.*, Rogoff, 1996).

Two features of our analysis help explain why other studies that have examined the forward-looking nature of exchange rates have generally struggled to establish a robust correlation between exchange rates and future macro aggregates. First, our estimates suggest

that the information driving the exchange rate is mainly *medium-to-long horizon* news—specifically news about TFP changes roughly three to five years in advance. The bulk of existing studies have concentrated on much shorter horizons, seeking lead-lag relationships at horizons of one to two years ([Engel and West, 2005](#)). Indeed, we find that extending the forecast horizon of [Engel and West](#)'s regressions reveals stronger evidence of Granger causality. Second, unlike previous literature, we separately identify and account for expectational noise. Because expectational noise weakens the correlation between expectations and *realized* fundamentals, it reduces the statistical power of empirical approaches that focus on the lead-lag relationship between exchange rates and *realized* future macro aggregates.

We conclude the paper with a discussion of the implications of our results for several popular types of open-economy models. We find that models with *complete asset markets* fail to replicate our key finding that higher expected home TFP is associated with relatively high current home consumption and an appreciated exchange rate. For example, in a benchmark complete-market model, consumption and the exchange rate do not respond to news of future TFP, and move only after the actual TFP improvement. Complete markets models with recursive preferences do generate expectational effects (*e.g.*, [Colacito and Croce, 2013](#)). However, in these models, complete risk sharing implies that high expected home productivity causes a *fall* in current home consumption and a *depreciation* of the real exchange rate, contrary to our evidence.

By contrast, models with *incomplete markets* can generate the pattern of an appreciated exchange rate and increased consumption differential when home productivity is expected to improve. Positive news about future TFP raises expected household income, prompting external borrowing, higher interest rate differentials, and an exchange rate appreciation. In this sense, the comovement upon arrival of news mirrors that generated by demand disturbances ([Kekre and Lenel, 2024](#)). Nevertheless, the benchmark incomplete-market model produces a key counterfactual implication: the exchange rate depreciates sharply once the TFP improvement occurs, whereas in the data it remains appreciated for several years following the productivity increase. We show that a simple extension—allowing global demand for the home good to increase as its supply expands—reconciles the model with the data.

We highlight that a successful candidate model must account for the sharp rise in expected foreign currency returns that follows a home TFP improvement, which helps sustain an appreciated exchange rate even as interest rate differentials turn negative. The extended incomplete-market framework, which ties currency premia to external borrowing, naturally delivers this feature. In the anticipation phase, the home economy borrows to front-load consumption, raising demand for foreign currency and thereby depressing expected excess foreign-currency returns. Once the TFP increase materializes, the home economy shifts to

lending to the foreign economy, which only later reaps the productivity gains. At that point, demand for foreign currency declines and expected excess returns rise. It is the expectation of persistently higher excess foreign currency returns—rather than the anticipated path of interest rate differentials—that accounts for the persistent real exchange rate appreciation both before and after the TFP improvement in the model.

Related literature This paper is related to several strands of the international finance and macro literatures. First, we speak to the exchange rate determination puzzle, which is characterized by the consistently low empirical correlations between current or past macroeconomic fundamentals and current exchange rates (Meese and Rogoff, 1983; Cheung et al., 2005; Rogoff and Stavkareva, 2008; Rossi, 2013). A related observation is that the exchange rate is both “excessively” volatile and overly persistent, relative to macroeconomic fundamentals (Obstfeld and Rogoff, 2000; Chari et al., 2002; Sarno, 2005; Corsetti et al., 2008a; Steinsson, 2008).¹

Contrary to this strand of literature, we find that there is a strong connection between exchange rates and macroeconomic fundamentals, albeit one that relates current exchange rates to future fundamentals. Our evidence is consistent with the argument of Engel and West (2005) that exchange rates are forward-looking and therefore should lead, rather than lag behind, macroeconomic variables. We contribute to this discussion in a number of ways. First, we show that the link between current exchange rates and future fundamentals runs specifically through *imperfect* and *noisy* anticipation of future productivity. Second, we show that the expectations reflected in exchange rates primarily concern TFP at medium-to-long horizons (three to five years in the future). Third, our analysis explicitly accounts for expectational noise, *i.e.*, fluctuations in expectations that are not associated with actual subsequent changes in fundamentals. We argue that ignoring this component of expectations leads one to underestimate the forward-looking nature of exchange rates.²

Another contribution of this paper is to show that a large number of famous exchange rate puzzles have a common fundamental origin in noisy news about future TFP. These empirical moments have received extensive theoretical attention, although few mechanisms

¹There is some evidence of contemporaneous relationships between exchange rates and specific variables, including commodity prices (Chen et al., 2010; Ayres et al., 2020), external imbalances (Gourinchas and Rey, 2007), order flow and microstructure dynamics (Evans and Lyons, 2002, 2008), as well as proxies for global risk (Lilley et al., 2020) and monetary factors (Engel and Wu, 2024) in recent decades. Hassan et al. (2016) further link exchange rate stochastic properties to cross-country differences in capital-output ratios.

²A related literature uses survey expectations to measure surprises in macroeconomic announcements and examines their effects on exchange rates (Andersen et al., 2003; Faust et al., 2007; Engel et al., 2008; Stavkareva and Tang, 2020). While there are important conceptual differences between our analysis and this literature—including in the definition of “news”—we find that revisions in expectations of future US TFP are partly linked to information revealed in macroeconomic announcements (see Section 4.3).

have been linked to news about future TFP.³ The conditional moments that we identify provide discipline for candidate models of exchange rate determination. Against these moments, we evaluate how leading classes of complete- and incomplete-markets open-economy models perform and relate our findings to recent insights on the sources of exchange rate fluctuations (Colacito and Croce, 2013; Itsikhoki and Mukhin, 2021; Kekre and Lenel, 2024).

A related literature examines the relationship between cross-country productivity differences and international business cycle comovement or exchange rate dynamics (Corsetti et al., 2014; Beaudry and Portier, 2014; Siena, 2015; Levchenko and Pandalai-Nayar, 2020; Huo et al., 2023, 2025; Gornemann et al., 2025). Most closely related to our analysis is Nam and Wang (2015), who adopt the Barsky and Sims (2011) approach to identify TFP news shocks in an open-economy context. In contrast to this paper, we depart from the conventional “news shock” framework to separately identify the effects of partly-anticipated TFP improvements and expectational noise disturbances. This distinction offers both practical advantages in terms of identification assumptions and conceptual advantages for interpretation.⁴ Our approach helps explain why previous studies found only a weak link between exchange rates and future realized fundamentals, clarifies the distinct roles of technological and noise disturbances in generating various exchange rate puzzles, and provides a natural framework for confronting model predictions with the data.

1 Data and basic empirical framework

Our empirical analysis centers on a VAR

$$Y_t = C(L)Y_{t-1} + u_t, \quad (1)$$

where the column vector Y_t contains data on the US and a trade-weighted aggregate for the other G7 economies. Going forward, we refer to the US and the other G7 economies as the “home” and “foreign” economies, respectively, and use the $*$ notation to denote foreign variables. For our baseline analyses, the vector Y_t contains eight variables: the

³The deep body of theoretical work on exchange rate puzzles includes, among others, Devereux and Engel (2002); Jeanne and Rose (2002); Gourinchas and Tornell (2004); Kollmann (2005); Bacchetta and van Wincoop (2006); Corsetti et al. (2008b); Alvarez et al. (2009); Bacchetta and Van Wincoop (2010); Verdelhan (2010); Burnside et al. (2011); Ilut (2012); Bansal and Shaliastovich (2012); Colacito and Croce (2013); Hassan (2013); Karabarbounis (2014); Farhi and Gabaix (2015); Gabaix and Maggiori (2015); Engel (2016); Valchev (2020); Itsikhoki and Mukhin (2021); Kekre and Lenel (2024); Candian and De Leo (2025).

⁴Regarding identification, the news shock literature (Barsky and Sims, 2011) relies on joint assumptions about the invertibility of the data generating process and the relative persistence of news shocks relative to surprises. By contrast, our approach relies on the weaker recoverability condition of Chahrour and Jurado (2022) and imposes no assumptions about persistence.

nominal exchange rate S_t expressed in units of US dollar per foreign currency, Fernald's (2012) series on utilization-adjusted US TFP, the US real consumption and investment, foreign real consumption and investment, the nominal interest rate differential, and the CPI price level differential between the US and a trade-weighted aggregate for the other G7 economies. In summary,

$$Y_t \equiv \left[\ln(S_t), \ln(TFP_t), \ln(C_t), \ln(C_t^*), \ln(I_t), \ln(I_t^*), \ln\left(\frac{1+i_t}{1+i_t^*}\right), \ln\left(\frac{CPI_t}{CPI_t^*}\right) \right]' . \quad (2)$$

We follow Engel (2016) in constructing the trade-weighted aggregates of the other G7 economies. The weight for each of the six countries is the sum of the country's world trade divided by the sum of world trade for all six countries combined.⁵ In addition, in Appendix B, we conduct the analysis using six separate bilateral VARs between the US and each other G7 country separately. The conclusions emerging from these bilateral VARs are similar, and the VAR with a trade-weighted aggregate serves as a useful benchmark to summarize the results.

For our benchmark results, we use quarterly data for 1978:Q4-2008:Q2. The sample stops in 2008:Q2 out of abundance of caution, to guard against a possible structural break in the aftermath of the financial crisis, which is a potential pitfall as argued by Baillie and Cho (2014) and Du et al. (2018). However, in Appendix B we conduct our analysis on an extended sample through the end of 2018 and the results remain very similar.

We describe the data and their sources in detail in Appendix A. As a brief overview, the exchange rate is the average of the daily exchange rates within a quarter, obtained from *Datastream*. The interest rate differential is the average of daily Eurodollar rates within a quarter, obtained from *Datastream*.⁶ The CPI indices and the consumption and investment series are from the *OECD* database. Lastly, the US TFP is from John Fernald's website.

We do not have a comparable utilization-adjusted quarterly TFP series for countries other than the US. Some recent papers have constructed utilization-adjusted TFP for foreign economies (*e.g.*, Huo et al., 2023; Comin et al., 2023), but we find that these measures are not suitable for our purposes. Most such measures of adjusted foreign TFP can only be constructed at annual frequencies (Huo et al., 2023) or over a very short sample period (Comin et al., 2023), which limits the scope of the analysis. In Appendix B, we consider

⁵We use the average of the 1978 and 2008 weights. The weights are: Germany: 29.45%; Japan: 18.43%; France: 15.99%; United Kingdom: 13.99%; Italy: 12.30%; Canada: 9.84%. For the transition to the Euro, *Datastream* uses a Country's currency/Euro conversion rate to construct a synthetic exchange rate for the whole period. For example in the case of Italy, the post 1998 exchange rate values are rescaled by 1936.27, which is the Lira/Euro exchange rate.

⁶Note that these interest rate differentials are not forward discount-implied interest rate differentials, but actual eurodollar rates.

alternative specifications that include the foreign Solow residual as part of Y_t . All of our main results and conclusions remain unchanged.

We estimate the VAR in (1) using four lags and Bayesian methods with a Minnesota prior. This commonly used prior assumes all series in Y_t are mutually-independent random walks. This choice of prior is conservative, since we are looking for relationships between the exchange rate and other macro variables.

Following the established convention (*e.g.*, Sims et al., 1990; Eichenbaum and Evans, 1995), we estimate the VAR in levels and do not impose any cointegration assumptions *ex ante*. Nevertheless, in Appendix B we show that our results remain qualitatively similar if we estimate a Vector Error Correction Model (VECM) that imposes the same cointegration relationships as Engel (2016), where the real exchange rate and interest rate differential are assumed stationary. More generally, we have found the results to be robust to imposing a variety of other potential cointegration relationships.

We use our VAR to perform two different identification exercises. The first is descriptive. The goal of this exercise is to isolate the comovement of macro variables and the real exchange rate, conditional on a reduced-form shock that explains the most of the unconditional variance in the real exchange rate. The second exercise is structural, and is intended to quantify the role of productivity expectations in driving macro and real exchange rate fluctuations. This approach allows us to separately identify the disturbances that drive actual changes in TFP and the noise that influences expectations, but never affects TFP.

2 The main driver of real exchange rate fluctuations

We begin with an agnostic empirical approach that isolates the main source of exchange rate fluctuations in the data while imposing minimal ex-ante assumptions on the nature of the underlying structural disturbances. To do so, we follow the max-share approach of Faust (1998) and Uhlig (2003) to extract the reduced-form shock that explains the largest share of the variation in the real exchange rate. This approach has been applied by Angeletos et al. (2020) to extract a so-called “main business cycle shock”. We apply it to exchange rates and, in parallel to Angeletos et al.’s terminology, we refer to the shock we extract as the “main exchange rate shock”.⁷

To apply the max-share procedure, write the moving average representation of the VAR

⁷Kurmann and Otrok (2013), Basu et al. (2021), Cormun and De Leo (2024), Chahrour et al. (2023), and Boer et al. (2025) also contain applications of the max-share approach.

in (1):

$$Y_t = \sum_{k=0}^{\infty} B_k A_0 \varepsilon_{t-k}, \quad (3)$$

where the $\{B_k\}$ correspond to the coefficients in the $MA(\infty)$ representation of $B(L) \equiv (I - LC(L))^{-1}$ and A_0 is the structural matrix relating reduced-form residuals and the underlying shocks, such that $u_t = A_0 \varepsilon_t$. The (log) real exchange rate is the difference between the log nominal exchange rate and the log of relative CPIs,

$$q_t \equiv s_t + p_t^* - p_t.$$

Using the VAR variables reported in (2), we can therefore construct $q_t = e_q' Y_t$, where $e_q = [1, 0, 0, 0, 0, 0, 0, -1]'$.

The h -step ahead forecast error for the real exchange rate is given by

$$q_{t+h} - \mathbb{E}_{t-1} q_{t+h} = e_q' \left[\sum_{\tau=0}^h B_\tau A_0 \varepsilon_{t+h-\tau} \right],$$

where $h \geq 0$. The contribution of the first element ε_{1t} to the forecast error variance of the real exchange rate is then,

$$\text{var}(q_{t+h} - \mathbb{E}_{t-1}(q_{t+h}) | \varepsilon_{i,t+\tau} = 0 \forall i \neq 1, \tau = 0, \dots, h) = e_q' \left[\sum_{\tau=0}^h B_\tau A_0 e_1 e_1' A_0' B_\tau' \right] e_q \quad (4)$$

where e_1 is the selection vector so that $A_0 e_1$ selects the first column of A_0 , and $\varepsilon_{k,t}$ is the k^{th} shock in the vector ε_t .

We choose the rotation matrix A_0 by maximizing (4) subject to $A_0 A_0' = \mathbb{E}(u_t u_t')$. This requires us to specify a horizon h at which the forecast error variance in (4) is computed, and for that we choose $h = 100$ quarters, which effectively gives us the unconditional variance of q_t . This procedure yields a partially identified system, in that the above maximization problem uniquely determines only the first column of A_0 and thus the first element of the shock vector of ε_t (which is what we are interested in). The resulting series ε_{1t} represents the reduced-form innovation that accounts for the largest share of fluctuations in q_t . It should not be interpreted as a structural shock— ε_{1t} likely reflects a linear combination of multiple underlying structural shocks (Dieppe et al., 2021; Dou et al., 2025). We will address the question of its structural origin in the following sections.

Table 1 reports the share of the forecast error variance of each macro variable that is explained by the main exchange rate shock, across horizons from 1 to 100 quarters. We

Table 1: Share of forecast error variance explained by the main exchange rate shock (ε_1)

| | Forecast Horizon (Quarters) | | | | | |
|----------------------------|-----------------------------|------|------|------|------|------|
| | Q1 | Q4 | Q12 | Q24 | Q40 | Q100 |
| Home TFP | 0.03 | 0.06 | 0.20 | 0.37 | 0.45 | 0.43 |
| Home Consumption | 0.02 | 0.04 | 0.21 | 0.47 | 0.51 | 0.40 |
| Foreign Consumption | 0.01 | 0.04 | 0.06 | 0.21 | 0.36 | 0.30 |
| Home Investment | 0.29 | 0.34 | 0.32 | 0.40 | 0.42 | 0.41 |
| Foreign Investment | 0.06 | 0.08 | 0.15 | 0.22 | 0.34 | 0.33 |
| Interest Rate Differential | 0.40 | 0.39 | 0.30 | 0.34 | 0.35 | 0.39 |
| Real Exchange Rate | 0.50 | 0.69 | 0.82 | 0.73 | 0.70 | 0.68 |
| Expected Excess Returns | 0.47 | 0.33 | 0.34 | 0.44 | 0.45 | 0.47 |

Notes: The table reports the variance shares accounted for by the main exchange rate shock.

find that this shock is indeed a dominant driver of exchange rate fluctuations—it explains roughly 70% of variance of the real exchange rate.

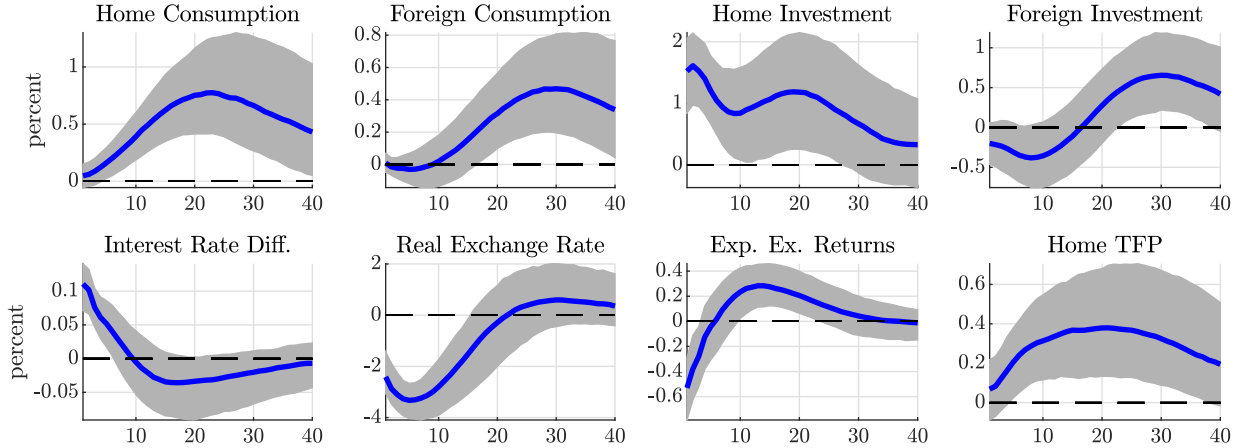
To examine the comovement patterns associated with this variation, Figure 1 presents the impulse response functions of the exchange rate and other macroeconomic variables following a one-standard deviation increase in the main exchange rate shock. The responses reveal a clear comovement: high interest rates along with an appreciation of the real exchange rate, which exhibits persistent, hump-shaped dynamics—continuing to appreciate for about 5 quarters after the initial impact before gradually returning to its long-run mean.

These dynamics are reflected in the non-monotonic behavior of expected excess returns of holding foreign bonds, defined as $\mathbb{E}_t \lambda_{t+1} \equiv \mathbb{E}_t \Delta q_{t+1} + r_t^* - r_t$, and computed using VAR-implied expectations. Expected excess foreign currency returns are initially negative and remain so for around 5 quarters before turning significantly positive and staying elevated for several years thereafter.

The joint behavior of these variables displays the defining features of exchange rate dynamics. The hump-shaped, persistent appreciation of the real exchange rate—with a half-life of about 3 years—echoes the estimates of Steinsson (2008) based on a univariate reduced-form innovation to the exchange rate. The observed comovement with the interest rate differential reflects the classic Forward Premium Puzzle: the high-interest rate currency (the USD) initially earns high returns, but over the medium run, the direction of the UIP violation reverses, with the USD subsequently earning low returns for an extended period (Engel, 2016; Valchev, 2020).

Importantly, Table 1 also shows that the main exchange rate shock explains a substantial

Figure 1: Impulse Response Functions to the main exchange rate shock (ε_1)



Notes: The figure reports the impulse responses to the main exchange rate shock, along with the 16–84th percentile bands. Each period is a quarter.

share of the overall variation in several key macroeconomic aggregates. At long horizons, it accounts for roughly 40% of the forecast error variance of consumption (both home and foreign) and home TFP, while contributing only modestly to their short-run fluctuations (see Table 1). Figure 1 shows that the responses of other macro aggregates systematically lag those of the exchange rate. For instance, home and foreign consumption peak only around 20–30 quarters after the initial response of the exchange rate. (The increase in the home consumption differential, along with the appreciated exchange rate, echoes the well-known empirical violation of the [Backus and Smith \(1993\)](#) condition.) Likewise, while the main exchange rate shock has little immediate effect on US TFP, productivity subsequently rises significantly, peaking at an increase of about 0.4% roughly 20 quarters after the initial impulse. Thus, both consumption and TFP exhibit pronounced medium- to long-run responses, but respond relatively little in the short run. This difference in the timing of responses implies that exchange rates are only weakly (conditionally) correlated with current and lagged macroeconomic aggregates, consistent with the empirical regularities highlighted in the literature on the “exchange rate disconnect” (*e.g.*, [Meese and Rogoff, 1983](#)).

The main exchange rate shock at different frequencies Some authors using the max-share approach have targeted specific frequencies instead. To understand the implication of focusing on different frequency bands, Appendix B.2 reports variance decomposition values when the shock is selected to explain the most of the 2–1000 and 6–32 periodicities in the real exchange rate, respectively.

The first of these, reported in Table B.1, essentially targets the unconditional variances in

the data and delivers results extremely similar to our Table 1. By contrast, the contribution of the shock to other macro aggregates, reported in Table B.2, is about half as large when the maximization targets the 6–32 business cycle frequencies. This observation is consistent with Miyamoto et al.’s (2023) finding that the relationship between exchange rates and fundamentals appears weak when the max-share approach targets the business cycle range. As we explain below, our main empirical results will rationalize these contrasting results. We find that noise in the expectation of future TFP drive a lot of the high frequency variation in the exchange rate, and this fact obscures the connection between exchange rates and *realized* fundamentals.

Taking stock Taken together, this evidence sheds new light on the “exchange rate disconnect”. Our results confirm that most real exchange rate variation is essentially unrelated *contemporaneously* to aggregate consumption or TFP—two key macro variables often examined in this context. Instead, we find that the exchange rate *leads* these aggregates, suggesting that the observed “disconnect” reflects differences in the timing of responses rather than a true separation between exchange rates and fundamentals. This evidence challenges the emerging view that exchange rate fluctuations are primarily driven by currency market-specific financial or risk shocks that are unrelated to macro fundamentals.

While this empirical approach provides a compact statistical summary of the data with minimal assumptions, it does not identify the structural origins of the reduced-form innovation ε_{1t} . The observed lead–lag relationship between exchange rates and macroeconomic aggregates suggests the possibility that these variables are responding to news about future TFP. The basic idea is that when information about future productivity arrives, forward-looking asset prices—such as the exchange rate—adjust immediately, whereas it takes time for the news, and the subsequent realization of productivity improvements, to be reflected in macroeconomic quantities. To examine this hypothesis, the next section introduces structural assumptions that allow us to identify innovations to expectations about future TFP and to assess their role in driving exchange rate dynamics.

3 Expectations of TFP and exchange rates

We follow the approach of Chahrou and Jurado (2022) to identify two distinct types of disturbances to expected TFP. The first type of disturbance captures all realized changes to TFP, and may be imperfectly anticipated at an arbitrary horizon. The second disturbance captures the noise in expectations that leads agents’ forecasts about future TFP to fluctuate even when realized TFP subsequently does not change.

Our identification strategy can be applied under general information and time series structures. We assume that the process for home productivity admits a $\text{MA}(\infty)$ representation,

$$a_t = \sum_{k=0}^{\infty} \delta_k \varepsilon_t^a, \quad (5)$$

where ε_t^a are the innovations in TFP's univariate Wold representation; we impose no additional assumptions on the time-series dynamics of a_t .

One key goal of our analysis is to identify the degree to which the future increments to TFP, ε_{t+k}^a , are forecastable, *i.e.* whether $\mathbb{E}_t(\varepsilon_{t+k}^a) \neq 0$. There are different ways to model the time- t information set underlying this conditional expectation, and we seek an empirical approach that is both general and flexible. To motivate our approach to identification, we describe a concrete information structure that embodies our key identifying assumptions. As we discuss below, this structure encompasses a wide range of processes and information assumptions used elsewhere in the literature.

Specifically, assume that each period agents perfectly observe current and past productivity, along with an additional signal about future productivity,

$$\eta_t = \sum_{k=1}^{\infty} \zeta_k a_{t+k} + v_t. \quad (6)$$

Again, we put no ex ante restrictions on the weights ζ_k in the signal. The process $v_t \perp a_{t+k}, \forall k$ represents informational noise. It also follows an arbitrary $\text{MA}(\infty)$ process,

$$v_t = \sum_{k=0}^{\infty} \nu_k \varepsilon_{t-k}^v. \quad (7)$$

Evidently, the information structure in (5)-(7) allows for a wide range of signal structures with noisy information about future TFP. But this structure also encompasses a range of processes in which *there is no explicit expectational noise*, including the well-known “long-run risk” process often considered in international asset pricing models (Colacito and Croce, 2011, 2013). Intuitively, Beveridge-Nelson, long-run risk, and other processes that decompose a scalar fundamental into separate components observed by agents all provide those agents with information above and beyond the observation of the fundamental history, and they can all be represented as including noisy observations of future realizations (Chahrour and Jurado, 2018). In Appendix C.2 and C.3, we provide an explicit mapping to (5)-(7) for the information structures of Blanchard et al. (2013) and Colacito and Croce (2013). Hence, we work with a very general representation, while imposing minimal structural assumptions.

We separately identify the true technological disturbances ε_t^a and the expectational noise disturbances ε_t^v using the approach of Chahrour and Jurado (2022). The economic assumption behind this identification approach can be easily stated: they are (i) the productivity disturbances ε_t^a are orthogonal to other structural disturbances (as is standard) and (ii) the expectational noise innovations ε_t^v are orthogonal to ε_t^a (intuitively, the procedure captures rational expectations errors—unrelated to actual TFP by construction).⁸ Below we relay the key intuition of the identification strategy, and provide full details in Appendix B.1.

To get some intuition for how the procedure works, consider the illustrative case where productivity a_t and the signal η_t are both directly observed by the econometrician. As in standard VAR analysis, the joint process for $[a_t, \eta_t]$ has many potential representations that deliver the same autocovariances; identification requires some theoretical restrictions. The (very minimal) restrictions implied by (5)-(7) can be represented as placing zeros in the two-sided MA representation of $[a_t, \eta_t]$ in the following way:

$$\begin{bmatrix} a_t \\ \eta_t \end{bmatrix} = \cdots + \begin{bmatrix} 0 & 0 \\ * & 0 \end{bmatrix} \begin{bmatrix} \varepsilon_{t+1}^a \\ \varepsilon_{t+1}^v \end{bmatrix} + \begin{bmatrix} * & 0 \\ * & * \end{bmatrix} \begin{bmatrix} \varepsilon_t^a \\ \varepsilon_t^v \end{bmatrix} + \begin{bmatrix} * & 0 \\ * & * \end{bmatrix} \begin{bmatrix} \varepsilon_{t-1}^a \\ \varepsilon_{t-1}^v \end{bmatrix} + \cdots \quad (8)$$

The identification assumption that the noise disturbances ε_t^v are not related to TFP at any lead or lag implies that the upper-right elements of all lead and lag coefficient matrices are zero. In addition, since ε_t^a is the Wold innovation to TFP, the upper left corner of all *lead* matrices is zero, *i.e.* technological disturbances naturally move TFP only after they realize. Chahrour and Jurado (2022) show this gives enough zero restrictions to identify the system—intuitively, the number of remaining unrestricted coefficients is equal to the number of moments one can estimate from data. With estimates for the unrestricted $*$ coefficients in (8), one can subsequently recover time series estimates of the disturbances ε_t^a and ε_t^v .

Of course, the above illustrative example implausibly assumes that the econometrician directly observes the relevant signal η_t . However, because expectations reflect the information contained in the signals, the same identification can be achieved by replacing η_t in the observation vector with the forecasts of future TFP, $\mathbb{E}_t(a_{t+k})$. When we implement this approach in practice, we use the forecast of future TFP implied by our estimated VAR in eq. (1). Formally, the key assumption needed for replacing η_t with the VAR-implied $\mathbb{E}_t(a_{t+k})$ is that the forward-looking variables in the VAR, *e.g.* exchange rates and interest rates, reflect the forward information about TFP that agents receive through the unobserved signals η_t . Moreover, if the data in our VAR fail to capture some of agents' forward information, this

⁸We also follow Chahrour and Jurado (2022)'s choice to refer to structural “disturbances” in this context, rather than “shocks”, because the ε_t^a and ε_t^v do not necessarily enter people's information sets at the same time as they are realized.

will only bias us *against* finding anticipation effects in our estimation.

For the actual implementation of this procedure we need to specify a target “horizon” k for the VAR-expectation $\mathbb{E}_t(a_{t+k})$. We set $k = 20$, in line with the observation from Section 2 that TFP appears most forecastable at medium-to-long horizons. However, in principle, if agents only observe one signal η_t about future TFP, the choice of horizon k is irrelevant, as any choice will yield identical estimation results (Chahrou and Jurado, 2022). In practice, we find that our estimation yields similar results for a wide range of k ’s.

Last, we note that when there are more than two variables in the VAR, as in our baseline application, the procedure imposes only a subset of the restrictions implied by the signal structure (5)-(7). In particular it does not impose the restriction that other variables besides the target expectation, $\mathbb{E}_t(a_{t+k})$, have a zero response prior to the occurrence of the noise disturbance ε_t^v . Because we do not impose these additional over-identifying restrictions *ex ante*, one can use these additional restrictions as an *ex post* test of the information assumptions that motivate our identification approach. In our main application, we find small responses of other variables before the occurrence of a noise disturbance, suggesting that equations (5)-(7) provide a good description of the empirical process of expectations.

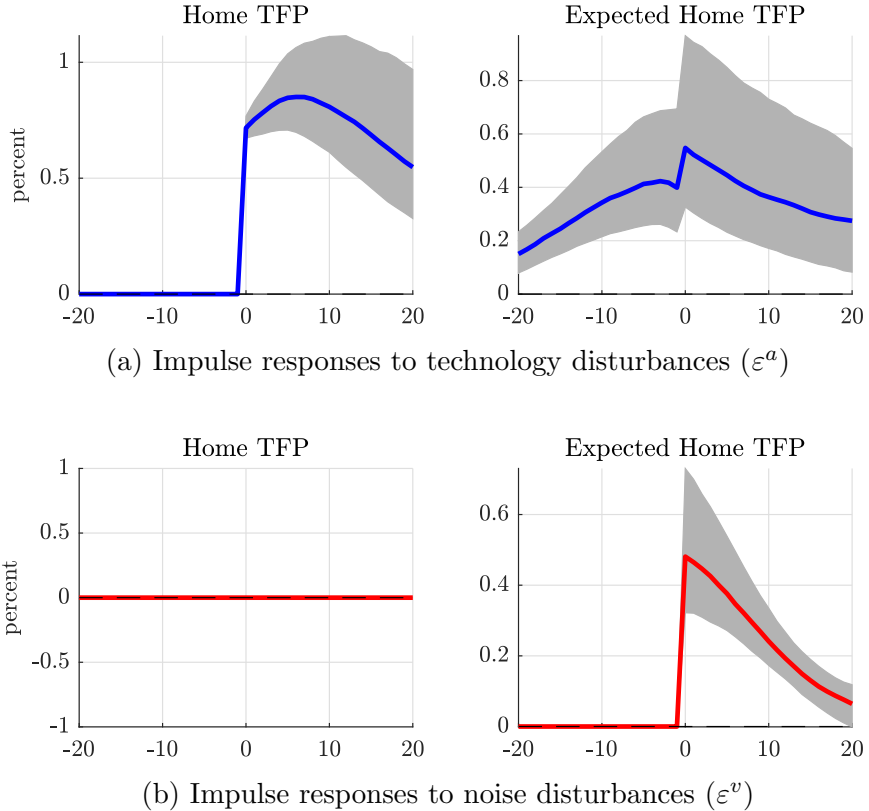
3.1 The dynamic effects of technological and noise disturbances

After we separately identify the technological and noise disturbances, ε_t^a and ε_t^v , we compute the resulting impulse responses of a number of variables of interest.

To begin, Figure 2 plots the impulse response of TFP itself, a_t , as well as the impulse response of the 20-quarter ahead expectation of TFP, $\mathbb{E}_t(a_{t+20})$. Since our approach allows technological disturbances to be potentially anticipated, we plot each impulse response beginning 20 quarters *before* the actual change in productivity, which we normalize to occur at $t = 0$, and then trace the evolution of the responses up to 20 quarters after the realization of the disturbance. Hence, the x -axis spans from -20 to $+20$. The extent to which TFP anticipation is present in the data can be assessed by examining whether the estimated TFP forecast $\mathbb{E}_t(a_{t+20})$ responds significantly prior to the actual TFP improvement (which occurs at time 0).

We find strong evidence of anticipation in the data. In response to a one standard deviation technological disturbance, ε_t^a , expected TFP rises by about 0.2% even 20 quarters before the actual 0.75% increase at $t = 0$, implying that roughly one-quarter of the improvement is foreseen five years in advance (see Figure 2a). The forecast continues to rise as the TFP improvement approaches, consistent with greater short-term predictability. That said, the further upward revision in expectations at $t = 0$ indicates that the realization of the

Figure 2: Dynamic responses of TFP and TFP expectations



Notes: The figure displays responses to a one standard deviation impulse in the technological disturbance (Figure 2b) and noise disturbance (Figure 2b) at time $t = 0$. The shaded areas are 16–84th percentile bands. Each period is a quarter.

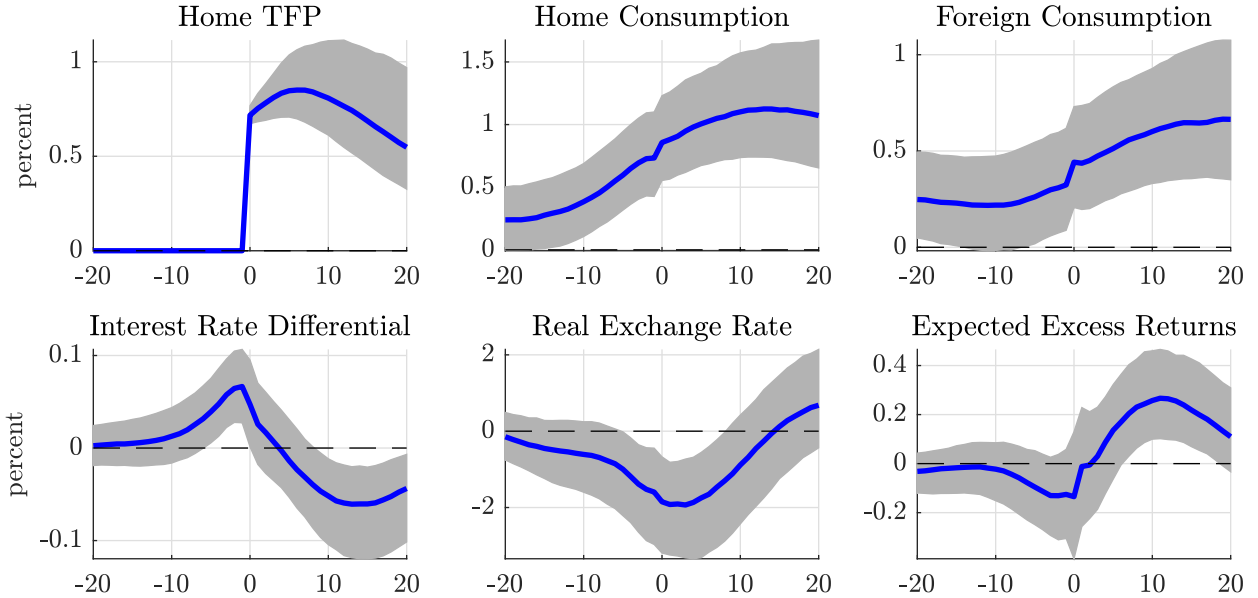
technological disturbance still comes as a partial surprise to agents. After the TFP increase materializes, both TFP and TFP expectations remain persistently elevated.

We also find evidence of expectational noise in expectations of TFP. While expectational noise disturbances, ε_t^v , have no effect on actual TFP at any lead or lag by assumption, they move expected TFP substantially: a one-standard deviation increase in ε_t^v —an “optimistic” revision about future TFP—raises $\mathbb{E}_t(a_{t+20})$ by roughly 0.5% (see Figure 2b). These expectational effects are mean-reverting, as agents gradually recognize that their initial optimism was unwarranted and expectations return to trend.

Overall, the results in Figure 2 support the hypothesis of a noisy-information paradigm, where future movements in TFP are partially anticipated, but expectations are noisy and sometimes move even though there is no actual change in productivity.

We now turn to the effects of these two disturbances on the rest of the endogenous variables

Figure 3: Impulse responses to technology disturbances (ε^a)



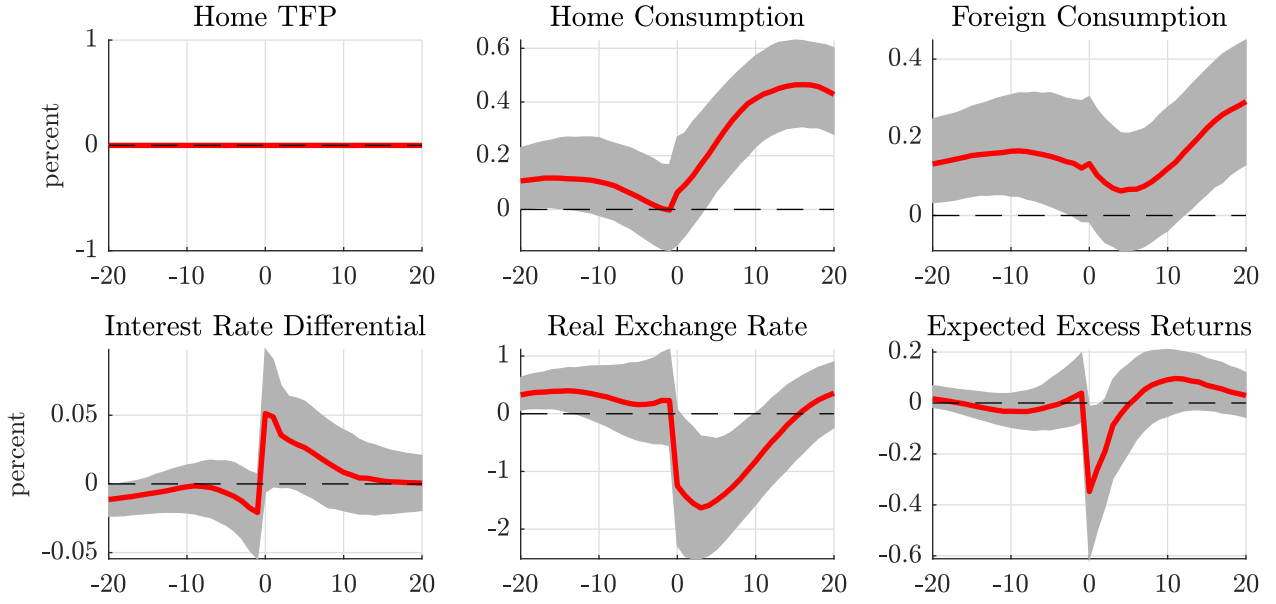
Notes: The figure displays IRFs to a one standard deviation impulse in the technological disturbance at time $t = 0$. The shaded areas are 16–84th percentile bands. Each period is a quarter.

in the VAR. Figure 3 plots the responses of selected variables to a technological improvement (an increase in ε_t^a at $t = 0$). Here, we focus on describing the comovement patterns induced by our disturbances, and defer a more theoretical interpretation of them until Section 5.

Technological disturbances give rise to significant responses in exchange rates, interest rates, and consumption differentials. The real exchange rate responds with a pronounced hump-shaped fashion. In anticipation of the TFP improvement, the real exchange rate steadily appreciates, and, only gradually depreciates back to its long-run mean after the TFP increase materializes. The three-month real interest rate differential also rises in anticipation of the TFP improvement, while it declines steadily and remains significantly below its long-run mean for around 10–20 quarters following the actual TFP increase. We also observe a significant increase in US consumption preceding the TFP improvement. Although foreign consumption also rises, its response is considerably weaker, leading to a large and positive consumption differential (not shown). Notably, the exchange rate appears to lead consumption, as its peak response occurs earlier than the peak in consumption. Technological disturbances, which are partly anticipated, are indeed strongly reflected in the real exchange rate, and, with different timing, in relative consumption.

The timing differences are even clearer in the impulse responses to the expectational noise disturbance, ε_t^v , shown in Figure 4. Following an improvement in expectations (period 0 on the x -axis), the real exchange rate immediately appreciates sharply. This directly speaks

Figure 4: Impulse responses to noise disturbances (ε^v)



Notes: The figure displays IRFs to a one standard deviation impulse in the expectational disturbance at time $t = 0$. The shaded areas are 16–84th percentile bands. Each period is a quarter.

to anticipation effects on the exchange rate, as the expectational noise disturbance has no impact on TFP at any horizon. The exchange rate response is also persistent, returning to its long-run mean only after about 12 quarters. The interest rate differential—another asset price—also jumps on impact following the upward revision in expectations. By contrast, the consumption response is gradual and delayed without a significant change at time 0. Delayed consumption effects relative to the immediate exchange rate response are consistent with an information structure in which agents receive news about medium- to long-term TFP prospects; as a forward-looking asset price, the exchange rate reacts immediately, whereas home (and, to a smaller extent, foreign) consumption responds only as the expected TFP improvement approaches.⁹

The US trade balance also responds significantly to technological and noise disturbances, as shown in Appendix Figure B.1. We find that the trade balance (as a percentage of US GDP) deteriorates, albeit modestly, in anticipation of future TFP gains, while it improves following the actual realization of higher TFP. As we discuss in Section 5 these dynamics are consistent with the intertemporal approach to the current account and implied consumption smoothing behavior. The evidence is also consistent with the observation that survey-based

⁹As noted above, responses of real variables prior to a noise disturbance are zero under the information assumptions in (6)–(7), but our procedure does not impose these restrictions *ex ante*. We interpret the small pre- $t = 0$ responses in Figure 4 as evidence that the baseline information structure is consistent with the data.

Table 2: Variance Decomposition

| | Periodicities of 2–100 Quarters | | | Periodicities of 6–32 Quarters | | |
|----------------------------|---------------------------------|-------|-------|--------------------------------|-------|-------|
| | Both | Tech. | Noise | Both | Tech. | Noise |
| Home TFP | 1.00 | 1.00 | 0.00 | 1.00 | 1.00 | 0.00 |
| Home Consumption | 0.70 | 0.54 | 0.16 | 0.30 | 0.10 | 0.20 |
| Foreign Consumption | 0.63 | 0.49 | 0.14 | 0.30 | 0.13 | 0.17 |
| Home Investment | 0.62 | 0.46 | 0.15 | 0.42 | 0.29 | 0.13 |
| Foreign Investment | 0.68 | 0.43 | 0.25 | 0.45 | 0.14 | 0.31 |
| Interest Rate Differential | 0.57 | 0.46 | 0.11 | 0.37 | 0.23 | 0.14 |
| Real Exchange Rate | 0.64 | 0.45 | 0.20 | 0.36 | 0.14 | 0.22 |
| Expected Excess Returns | 0.50 | 0.35 | 0.15 | 0.37 | 0.19 | 0.18 |

Notes: The table reports the estimated variance shares (at periodicities between 2 and 100 quarters and between 6 and 32 quarters) explained by technological disturbances (“Tech”), expectational disturbances (“Noise”), and the combination of both.

expectations of US GDP growth relative to the rest of the world are significantly correlated with the US current account (Engel and Rogers, 2006; Hoffmann et al., 2019). Overall, the identified disturbances imply a weak correlation between changes in the exchange rate and the trade balance, a feature of exchange rate dynamics recently emphasized in the literature (Mac Mullen and Woo, 2025; Bodenstein et al., 2024).

Variance decomposition To quantify the role of technology and noise disturbances, Table 2 reports the contribution of these disturbances to various endogenous variables. We report these variance decompositions both over a wide band of frequencies (2–100 quarters) and over the higher business cycle frequency (6–32 quarters) many models target. As per our identification restrictions, technological disturbances account for 100% of the variation in TFP, while expectational noise disturbances are orthogonal to TFP.

We estimate that the two disturbances together explain around 60% of the low-frequency variation in the levels of the real exchange rate, as well as US and foreign real consumption and investment. Noisy news about future TFP therefore represents a key common driver of both exchange rates and real quantities, highlighting a fundamental link between exchange rates and the broader macroeconomy. At business-cycle frequencies, the two disturbances remain important, accounting for 30–45% of the variation in real aggregates and 36% of the variation in the exchange rate.¹⁰

¹⁰The evidence that US TFP-related disturbances explain over 50% of the variation in the real exchange rate and in foreign real variables is consistent with the notion that the US is a dominant source of technological progress and international spillovers, a view supported by the fact that US inventors account for the vast

The relative importance of the technological disturbance ε_t^a and the noise disturbance ε_t^v varies across frequencies. At lower frequencies, true technological disturbances dominate, explaining about two-thirds of the exchange rate variation captured by the two disturbances combined (45% versus 64% in total). By contrast, at the higher business-cycle frequencies, expectational noise is the main driver, accounting for roughly two-thirds of the variation generated by both disturbances (22% versus 36% in total). This pattern mirrors the impulse responses discussed above: noise disturbances generate short-lived, volatile exchange rate movements, while partly-anticipated TFP changes yield more persistent effects. Similar frequency patterns appear in the variance decompositions of other real variables.

We emphasize that the variance contribution of technological disturbances reflects both movements in anticipation of and reactions to realized TFP changes (*i.e.*, before and after time 0 in Figure 3). To isolate the pure anticipation effect, we compute the variance associated with the leading terms in the impulse responses—those occurring prior to the TFP realization. This anticipation channel emerges as the dominant source of exchange rate fluctuations: $t < 0$ movements account for 34% of the variation in the exchange rate, compared with only 11% for $t \geq 0$ movements. Importantly, our analysis does not necessarily suggest that an anticipated TFP change has a stronger *impulse response* than an equal-sized unanticipated change. Rather, it shows that most TFP changes are anticipated, so the anticipated component of TFP explains a larger share of exchange rate *variance* than the unanticipated component.

4 Extensions and empirical implications

In this section, we present additional empirical results and relate them to previous findings on the link between exchange rates and fundamentals. Section 4.1 shows that news and noise disturbances generate exchange rate fluctuations exhibiting many well-known puzzles, suggesting a common fundamental origin. Section 4.2 examines the effects of these disturbances on other asset prices, while Section 4.3 explores why prior studies have struggled to identify robust correlations between exchange rates and macroeconomic fundamentals. Finally, Section 4.4 reports robustness tests for the identification of our disturbances.

4.1 Common origin in exchange rate puzzles

The exchange rate literature has traditionally been organized around a series of “puzzles,” that is empirical exchange rate patterns that are at odds with standard international

majority of foreign patents in all major advanced economies (*e.g.*, Eaton and Kortum, 1999).

models. Given the prominent role the two identified disturbances play in driving exchange rate dynamics, it is natural to ask whether they reproduce some of these classic puzzles. The answer is yes. This leads us to conclude that many well-known exchange rate puzzles may share a common and fundamental origin in noisy news about TFP.

The Forward Premium Puzzle Our results indicate that the identified noisy news disturbances generate significant deviations from interest rate parity and reproduce the dynamics characteristic of the Forward Premium Puzzle (Fama, 1984; Hassan and Mano, 2019). Indeed, Figures 3 and 4 show a pronounced negative time-series comovement between interest rate differentials and expected excess currency returns.

Formally, consider the following version of the Fama regression:

$$\lambda_{t+1} = \alpha + \beta_\lambda(r_t - r_t^*) + u_{t+1}. \quad (9)$$

Because we employ trade-weighted variables, equation (9) estimates a specific version of what Hassan and Mano (2019) denote as Dollar β (as the US dollar is the base-currency). Unlike Hassan and Mano (2019), who use simple averages of foreign variables, we use trade-weighted averages—an approach that we consider more appropriate for our context.¹¹ Nevertheless, using simple averages yields very similar results for β_λ and other related estimates.

Estimating equation (9) in our raw dataset, we obtain a significantly negative estimate of $\beta_\lambda = -2.43$, consistent with earlier evidence (*e.g.*, Engel, 2014). We then compute the β_λ implied by a counterfactual dataset in which only the two noisy news disturbances we identify, ε_t^a and ε_t^v , are active. To construct these series, we simulate from our estimated VAR while setting the variances of all other disturbances to zero.

In this counterfactual simulation, we estimate $\beta_\lambda = -2.20$, indicating that the combination of disturbances to TFP and to expectations thereof both qualitatively and quantitatively reproduces the canonical Forward Premium Puzzle relationship. Panel A of Table 3 also reveals that both disturbances give rise to the comovement associated with the Forward Premium Puzzle. In addition, it is useful to examine how much of the raw covariance $\text{cov}(\lambda_{t+1}, r_t - r_t^*)$ —the numerator in the β_λ expression—our identified disturbances can explain. As shown in the table, the two disturbances together account for roughly two-thirds of the total covariance: the raw covariance equals -1.30 , whereas in the counterfactual data driven only by our two disturbances, it is -0.82 . Hence, the majority of the negative comovement between interest rate differentials and excess currency returns that underlies the

¹¹This approach is consistent with standard practice in the empirical international macroeconomics literature, where foreign countries are typically weighted by their economic size (GDP) or their trade relevance with respect to the United States (*e.g.*, Engel, 2016; Miyamoto et al., 2023; Corsetti et al., 2014).

Table 3: Exchange Rate Related Puzzles and TFP Expectations

Panel A: Forward Premium Puzzle Moments

| | Technology | Noise | Both | Unconditional |
|--|-------------------------|-------------------------|-------------------------|-------------------------|
| Fama β_λ | -2.08 [-3.34, -1.29] | -2.96 [-4.33, -1.68] | -2.20 [-3.47, -1.42] | -2.43 [-3.41, -1.66] |
| $\text{cov}(\lambda_{t+1}, r_t - r_t^*)$ | -0.68 [-2.10, -0.21] | -0.14 [-0.31, -0.06] | -0.82 [-2.41, -0.27] | -1.30 [-2.91, -0.69] |
| Engel β_Λ | 9.29 [-1.82, 22.20] | 9.19 [-8.88, 24.93] | 9.54 [-0.95, 20.27] | 5.49 [-1.37, 13.12] |
| $\text{cov}(\sum_{k=0}^{\infty} \mathbb{E}_t(\lambda_{t+k+1}), r_t - r_t^*)$ | 0.87 [-0.12, 4.19] | 0.24 [-0.23, 0.90] | 1.11 [-0.35, 5.09] | 1.25 [-0.27, 5.20] |
| $\sigma(r_t - r_t^*)/\sigma(\Delta q_t)$ | 0.37 [0.24, 0.64] | 0.13 [0.08, 0.22] | 0.25 [0.16, 0.42] | 0.17 [0.13, 0.27] |
| $\rho(r_t - r_t^*)$ | 0.99 [0.98, 1.00] | 0.93 [0.84, 0.97] | 0.98 [0.96, 0.99] | 0.95 [0.91, 0.98] |

Panel B: Backus-Smith Puzzle Moments

| | Technology | Noise | Both | Unconditional |
|--|------------------------|------------------------|-------------------------|-------------------------|
| $\text{corr}(\Delta q_t, \Delta(c_t - c_t^*))$ | -0.31 [-0.65, 0.06] | -0.38 [-0.74, 0.10] | -0.35 [-0.65, -0.01] | -0.27 [-0.38, -0.16] |
| $\text{cov}(\Delta q_t, \Delta(c_t - c_t^*))$ | -0.08 [-0.36, 0.01] | -0.12 [-0.37, 0.03] | -0.20 [-0.73, 0.04] | -0.70 [-1.13, -0.39] |

Panel C: Excess Volatility and Persistence

| | Technology | Noise | Both | Unconditional |
|---|----------------------|-----------------------|----------------------|----------------------|
| $\rho(q_t)$ | 0.99 [0.98, 0.99] | 0.96 [0.93, 0.98] | 0.98 [0.96, 0.99] | 0.96 [0.94, 0.98] |
| $\sigma(\Delta q_t)/\sigma(\Delta c_t)$ | 4.03 [2.50, 6.19] | 8.14 [4.95, 12.71] | 5.67 [3.66, 7.65] | 6.04 [4.96, 6.92] |

Notes: The table reports the estimated moments conditional on technological disturbances (Technology), expectational disturbances (Noise), and the sum of both disturbances, along the moments estimated from the raw data (Unconditional). The moments including **Engel** β_Λ , $\text{cov}(\sum_{k=0}^{\infty} \mathbb{E}_t(\lambda_{t+k+1}), r_t - r_t^*)$, and $\rho(q_t)$ are computed on the data filtered over [2–100] quarter periodicities. The values in brackets represent the 16–84 percentile bands. The moments in the table are defined in the text.

Forward Premium Puzzle can be attributed to the noisy-news disturbances we identify.

In addition to the “classic” Forward Premium Puzzle, the conditional responses of the exchange rate to our identified disturbances replicate the [Engel \(2016\)](#) finding that the puzzle reverses at longer horizons. Specifically, while regression (9) shows a negative association between interest rate differentials and one-quarter-ahead excess currency returns, it is well established that the correlation between today’s interest rate differential and currency ex-

cess returns two or more years ahead turns *positive*. We observe the same pattern in the impulse responses in Figure 3: periods of high expected excess currency returns following TFP improvements are preceded—several years earlier—by periods of high interest rates.

To summarize this relationship, we follow Engel (2016) and examine the coefficient β_Λ from the regression:

$$\sum_{k=0}^{\infty} \mathbb{E}_t(\lambda_{t+k+1}) = \alpha_0 + \beta_\Lambda(r_t - r_t^*) + \varepsilon_t.$$

In the raw data, we estimate $\beta_\Lambda = 5.49$, indicating that the overall sum $\sum_{k=0}^{\infty} \text{cov}(\lambda_{t+k+1}, r_t - r_t^*)$ is positive, even though the first term in the sum (*i.e.*, the coefficient in regression (9)) is negative. In our counterfactual simulation—where only the two noisy-news disturbances, ε_t^a and ε_t^v , are active—we find $\beta_\Lambda = 9.54$. Furthermore, these two disturbances together account for almost all of the total $\text{cov}(\sum_{k=0}^{\infty} \mathbb{E}_t \lambda_{t+k+1}, r_t - r_t^*)$ observed in the data. Hence, the long-horizon “reversal” of the Forward Premium Puzzle also largely arises as a consequence of the dynamic responses to the noisy-news disturbances we identify.

In addition, we note that our two disturbances not only replicate empirically relevant regression coefficients (β 's), but also generate interest rate differential dynamics that closely match their unconditional empirical counterparts. This can be seen from the moments $\sigma(r_t - r_t^*)/\sigma(\Delta q_t)$ and $\text{autocorr}(r_t - r_t^*)$ reported in Table 3.

Our results speak to the time variation in the currency risk premium, but they reflect in-sample predictability relationships. In Appendix B.3, instead, we construct out-of-sample trading strategies that exploit the predictable component of excess returns associated with the identified disturbances. Specifically, we consider a simple strategy in which a US investor takes a position in foreign currency proportional to the VAR-implied expectation of the foreign excess return. Our preferred specification yields a Sharpe ratio broadly comparable to those obtained from alternative currency market trading strategies that exploit time variation in return predictability (Lustig et al., 2014; Hassan and Mano, 2019; Burnside et al., 2011; Menkhoff et al., 2012; Moskowitz et al., 2012). This evidence complements the time-series predictability documented by Kremens and Martin (2019).

The Backus-Smith Puzzle The classic international risk-sharing condition of Backus and Smith (1993) predicts that relative consumption across countries should be strongly positively correlated with real exchange rates. In the data, however, this condition is largely violated: the unconditional correlation is in fact mildly negative (Kollmann, 1995; Corsetti et al., 2008b). We also observe this negative relationship in our impulse responses. As shown in Figure 3, in anticipation of a US TFP improvement (*i.e.*, for $t < 0$), the US dollar *appreciates* even though US consumption is relatively high. The impulse responses to the

expectational noise disturbances in Figure 4 display a similar pattern.

To quantify this relationship, we consider the moment

$$\text{corr}(\Delta q_t, \Delta c_t - \Delta c_t^*),$$

computed both in the raw data and in a counterfactual simulation where only the noisy-news disturbances are active. The results, reported in Panel B of Table 3, confirm the empirical pattern: the correlation in the data is mildly negative at -0.27 , while in the counterfactual driven solely by the two identified disturbances, it equals -0.35 . In addition, examining the underlying covariance, $\text{cov}(\Delta q_t, \Delta c_t - \Delta c_t^*)$, we find that the two disturbances together account for roughly 30% of this moment in the data. Thus, the noisy-news disturbances play a substantial role in generating the Backus-Smith puzzle.

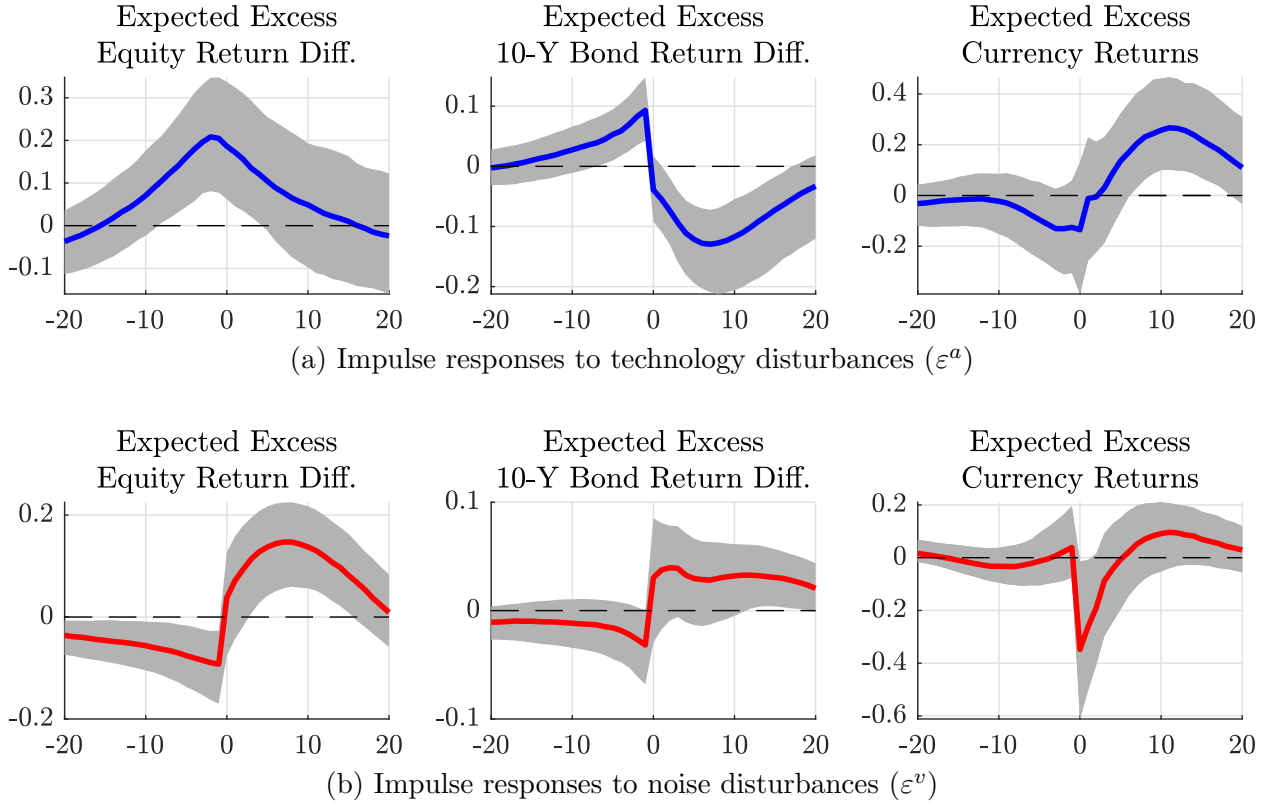
Excess volatility and persistence Two additional well-known exchange rate “puzzles” concern the excess persistence and volatility of the real exchange rate (*e.g.* Chari et al., 2002). We next examine the extent to which these phenomena are accounted for by the noisy-news disturbances we identify.

Panel C of Table 3 reports additional moments related to persistence and volatility. Two results stand out. First, the real exchange rate exhibits pronounced persistence when conditioned on the identified disturbances: its autocorrelation is approximately 0.98, compared with 0.96 in the unconditional data. Second, fluctuations in the real exchange rate remain highly volatile relative to macroeconomic aggregates. The standard deviation of quarterly exchange rate growth is about 5.7 times that of consumption growth under the two disturbances, closely matching the ratio of about 6 observed in the raw data. Notably, noise disturbances alone generate substantially higher “excess volatility” in exchange rates than technological disturbances: the ratio of the standard deviation of quarterly exchange rate growth to that of consumption is approximately 8 under noise disturbances, compared with about 4 under technological disturbances. This pattern is intuitive: expectational noise alters beliefs about future productivity—and thus asset prices—without corresponding movements in realized fundamentals, generating large exchange rate fluctuations but comparatively muted responses in consumption and output.

4.2 Technology, noise, and other asset prices

Do other asset prices respond to news about future productivity? In Appendix Figure B.2, we present the response of home and foreign equity prices to technological and noise disturbances. Indeed, we find a significant increase in equity prices, initially home and subse-

Figure 5: Technology, noise, and asset returns



Notes: The figure displays responses to a one standard deviation impulse in the technological disturbance (Figure 5a) and noise disturbance (Figure 5b) at time $t = 0$. The shaded areas are 16–84th percentile bands. Each period is a quarter.

quently foreign, in anticipation of future improvements in home productivity.¹² This finding is consistent with Beaudry and Portier's (2006) evidence that equity prices incorporate, at least in part, news about future economic fundamentals.

Figure 5 displays the responses of *risk premia* for home and foreign assets, measured as VAR-implied expected quarterly excess return differentials for equities and long-term bonds. These differentials are defined as the expected excess foreign return (in foreign currency) minus the expected excess home return (in home currency), that is, $(\mathbb{E}_t r_{t+1}^{x,*} - r_t^*) - (\mathbb{E}_t r_{t+1}^x - r_t)$, where r_{t+1}^x denotes the return on either equities or long-term bonds between periods t and $t+1$. We find substantial cross-country variation in both equity and bond returns in response to our identified disturbances, suggesting that they influence risk premia across asset classes.

We emphasize that the fact that equity risk premia respond to noisy news about TFP

¹²We estimate the impulse response of equities and long-term bonds (which are not directly included in the VAR), by projecting those returns on the VAR and its lags, and then using the VAR impulse responses. In any case, the results reported in this section are unchanged if instead we alternatively add equity or bond prices in our VAR and repeat the whole identification procedure.

does not imply a strong contemporaneous correlation across equity and currency returns. The variation driven by technology and noise disturbances implies a correlation between equity and currency expected excess returns of only about -0.10 . This aligns with empirical evidence showing negative, albeit mild, correlations between equity and currency returns (*e.g.*, Verdelhan, 2010; Hau and Rey, 2006). The low correlation arises because equity and currency returns are negatively correlated in response to fluctuations in TFP expectations but positively correlated following actual TFP improvements (see Figure 5).

In contrast, the implied correlation between bond and currency returns is a robust -0.50 , consistent with evidence of strong negative comovements between long-term bonds and exchange rates (*e.g.*, Lustig et al., 2019; Greenwood et al., 2023; Gourinchas et al., 2022; Lloyd and Marin, 2020; Kekre and Lenel, 2024). Overall, noisy-news disturbances are reflected across multiple asset classes. Nonetheless, these disturbances explain only about 50% of the business-cycle variation in equity and bond returns, with the remainder likely reflecting idiosyncratic factors that weaken the overall relationship between currency and other asset returns (Burnside, 2011; Chernov and Creal, 2023; Chernov et al., 2023).

4.3 Exchange rates and future fundamentals

Our empirical results reveal a connection between exchange rate fluctuations and imperfectly-forecasted changes in future TFP. In this section we discuss possible explanations for why this relationship has largely been overlooked in the empirical literature. Along the way, we provide further intuition on the key empirical features that drive our results.

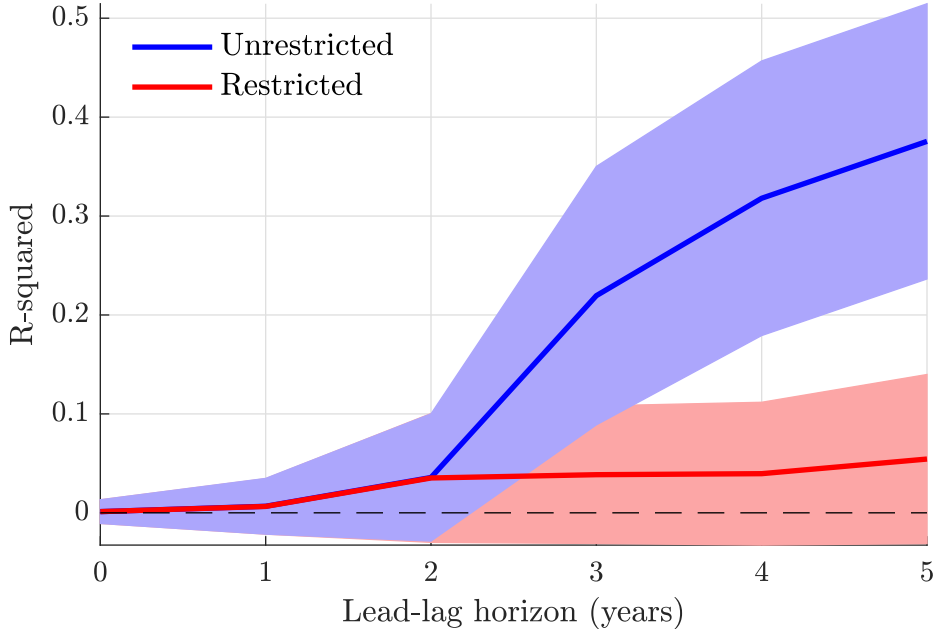
Our initial observation is that many previous studies start with the premise that TFP disturbances arrive as pure surprises, as they typically do in macroeconomic theories. From that point of view, one would only look for a relationship between the exchange rate and current and past TFP (or current and past macro aggregates more generally). Regressions of the real exchange rate changes on past variables, however, typically reveal a very weak relationship.

According to our empirical estimates, however, the real exchange rate *leads* TFP changes, rather than lag them. Do simpler empirical approaches also capture the same relationship? To explore this question, we consider the following simple exercise, in which we regress the annual change in the real exchange rate at time t on leads and lags of the annual change in TFP:

$$\Delta q_t = \alpha + \beta_0 \Delta TFP_t + \sum_{k=1}^h \beta_k^{lag} (\Delta TFP_{t-k}) + \sum_{k=1}^h \beta_k^{lead} (\Delta TFP_{t+k}) + \varepsilon_t. \quad (10)$$

If we included just the constant and the first term on the right-hand side, the regression would

Figure 6: Real exchange rate growth and leads and lags of TFP growth



Notes: The figure reports the R^2 of regression (10). The right-hand side includes either present and past TFP ('Restricted'), or present, past and future TFP ('Unrestricted').

estimate the standard relationship between contemporaneous changes in the exchange rate and TFP. If we include also the first summation term on the right-hand side, then we would also consider the additional explanatory power of lagged changes in TFP of up to h years in the past. Once we include the second summation term, we also consider a potential correlation with *future* TFP changes, of up to h -years ahead.

Figure 6 reports the R^2 from two versions of regression (10): a "Restricted" backward-looking version including only current and lagged TFP growth (red line), and an "Unrestricted" version including all right-hand-side terms (blue line).

The R^2 of the purely backward-looking regression is statistically indistinguishable from zero regardless of the number of lags, reflecting the typical "disconnect" result. The picture changes once terms capturing *future* TFP growth are included. The relationship between exchange rate changes and TFP growth remains insignificant if only TFP growth up to two years ahead is included, but becomes increasingly significant when including growth three to five years out. Hence, a simple regression reveals that exchange rates do lead TFP, consistent with the predictive patterns underlying our VAR results.¹³

¹³Appendix Table B.5 reports p-values from a Wald test of Granger causality based on (10), for both the aggregate of the other G7 countries and individual countries across annual horizons. We reject the null in favor of exchange rates Granger-causing TFP for most countries at horizons beyond two years.

These results further highlight that exchange rates contain substantial information about future TFP growth in the *medium- to long-run*. The long-horizon nature of the noisy news we identify is particularly relevant in relation to the existing literature. While the existing literature recognizes that, as a forward-looking asset price, the exchange rate should lead macroeconomic fundamentals, it has also generally struggled to find robust correlations between exchange rates and future fundamentals.

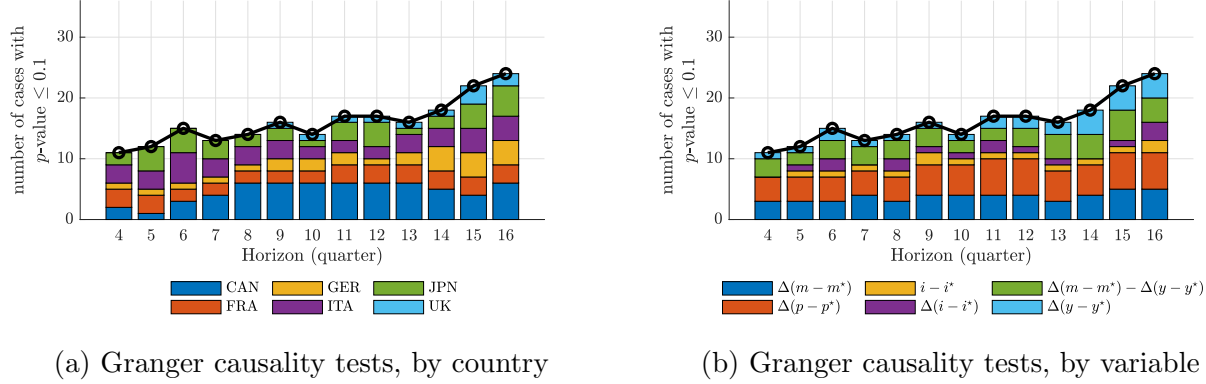
[Engel and West \(2005\)](#) find a weak predictive relationship between exchange rates and future “macroeconomic fundamentals” using Granger causality regressions. Their regressions focus on quarterly exchange rate changes and forecast horizons of up to one year for variables such as GDP and interest rate differentials.¹⁴ We offer three observations with regard to this evidence. First, given the low frequency nature of the news we estimate, we observe that *short-horizon* regressions tend to yield limited predictive power in finite samples. Second, we note that Granger causality should not be expected to manifest for *all* macroeconomic fundamental considered by [Engel and West \(2005\)](#), even when TFP expectations are important drivers of exchange rates. Finally, we observe that the expectational *noise* disturbances we estimate play the role of measurement error in Granger causality regressions, reducing their ability to identify the link between exchange rates and future productivity.

To the first observation, Figure 7 summarizes the significance of Granger causality tests for a range of variables and countries, using the 1974:Q1-2001:Q3 sample and variables originally considered by [Engel and West](#). All regressions are estimated with [Newey and West \(1987\)](#) standard errors to account for serial correlation in errors. Consistent with our hypothesis that lower-frequency relationships are key, the figure shows that the predictive relationships studied in [Engel and West \(2005\)](#) strengthen at longer horizons, which they did not consider. A similar pattern emerges when we extend the sample through 2018:Q4 (see Appendix Figure B.9). This pattern is intuitive and consistent with noisy-news view: long-horizon exchange rate changes reflect accumulated information about future macro movements, when the influence of transitory noise tends to average out.

To the second observation, Figure 7 shows that Granger causality results are not uniformly significant: the strength of the exchange rate-fundamentals relationship is stronger for output, money, and price differentials, but weaker for interest rate differentials. This pattern makes sense, however, because different macro variables respond to news at different horizons. For example, if both exchange rates and interest rate differentials respond to news about future TFP at the same time, the current exchange rate would *not* contain information about future interest differentials (independent of current interest differentials) and exchange

¹⁴[Sarno and Schmeling \(2014\)](#) adopt a more non-parametric approach, but still limit their null hypothesis to testing predictive relationships to a maximum of two years ahead.

Figure 7: Bivariate Granger causality tests *á la* Engel and West (2005) (1974:Q1–2001:Q3)



Notes: For each horizon, we report the number of cases in which the p -value from a Wald test of Granger causality is below 0.1. There are 36 cases per horizon: 6 countries (each compared to the US) and 6 macroeconomic fundamentals, following the data and methodology of Engel and West (2005). Each test is based on a bivariate VAR estimated using the quarterly change in the nominal exchange rate, Δs , and one fundamental variable, f . The horizon on the x -axis indicates the number of lags included in the VAR. The reported p -value corresponds to a Wald test of the joint significance of the lags of Δs in predicting f . The variables are defined as follows: Δm is the percentage change in M1 (M2 for the United Kingdom); Δy is the percentage change in real GDP; Δp is the percentage change in consumer prices; and i is the short-term government interest rate. Newey-West standard errors are computed using a data-driven bandwidth, a Bartlett kernel, and prewhitening. Panel (a) highlights the case in which p -value from the Wald test of Granger causality is below 0.1, *by country*, while Panel (b) highlights the corresponding cases *by variable*.

rate changes would *not* Granger-cause interest differentials.¹⁵ In general, we should expect stronger evidence of the exchange rate Granger causing slower-moving fundamentals, such as TFP or consumption differentials, and this is what our regressions show.

Finally, we observe that expectational noise (i.e. ε_t^v) generates changes in TFP forecasts that do not materialize. Since exchange rates respond to expectations regardless of their ex-post accuracy, however, simple correlations between realized fundamentals and exchange rates are likely to underestimate the role of expected TFP fluctuations. In Granger causality regressions, noise disturbances play the role of measurement error, and may bias these regressions towards zero. This is especially true at high frequencies, where our results indicate the impact of the expectational noise disturbances on the exchange rate is the strongest.

This final observation also helps explain why studies using survey-based macro expectations, including those based on macro announcements, often find a stronger connection between exchange rates and fundamentals (e.g., Engel et al., 2008; Stavrakeva and Tang, 2020). To connect our findings to this literature, we compare the quarterly trade-weighted exchange rate changes implied by our technology and noise disturbances with the “exchange

¹⁵This example is motivated by our empirical evidence that interest differentials move contemporaneously with exchange rates (see, *e.g.*, Figure 1).

rate news index” of [Stavrova and Tang \(2020\)](#), which aggregates daily announcement effects to a quarterly frequency. Over the overlapping 2002–2018 sample, the two series are correlated at approximately 40%, indicating that TFP news partly overlaps with macro announcements but also contains distinct information; similarly, macro announcements reflect revisions in future TFP expectations, but not exclusively.

4.4 Additional observations on the identification of news

Proxies of technological innovation In our baseline analysis, our measure of total factor productivity is [Fernald](#) utilization-adjusted TFP. The literature has often considered various proxies of technological innovation such as the number of patent applications, the value of granted patents, the adoption of new ICT standards, or R&D expenditure. In Appendix Figure [B.10](#) we plot the responses of these proxies of technological innovation to our identified disturbances. We make two observations. First, these measures rise in response to both technology disturbances and expectational noise. This result is natural: since not every innovation has the same impact on eventual productivity, these measures are best interpreted as a noisy signal of future productivity and should be responsive to both technological *and* noise disturbances. Since they contain informational noise, however, it would be incorrect to use these series as direct proxies for *realized* TFP in our identification strategy. Second, Appendix Figure [B.10](#) shows that these variables react relatively little *in anticipation* of realized productivity. This pattern suggests these variables capture a relatively small share of anticipated TFP movements. Using these series as direct proxies for *expected* TFP changes would also likely give misleading results.^{[16](#),[17](#)}

Estimation of VAR without exchange rate The reader may wonder whether it is conceptually appropriate to include the real exchange rate in our structural VAR procedure, since any identified disturbance is allowed to load on the reduced-form residuals from all variables in the VAR, including those from the exchange rate equation. We argue that it is indeed conceptually correct to include the exchange rate in the VAR. The reason is that we want to test the hypothesis that the exchange rate responds to the structural disturbances of interest. If the exchange rate does respond to the disturbances, then its reduced-form

¹⁶Nevertheless, in a robustness check we included these variables in our baseline VAR. The resulting impulse responses remained largely unchanged, indicating that these alternative TFP news measures contribute little additional information to the formation of TFP expectations.

¹⁷To ensure that our procedure does not inadvertently capture the endogenous productivity effects of non-technological disturbances, we verify that the correlations between our identified technology and noise disturbances and US monetary policy shocks—measured using the “high-frequency approach” of [Gertler and Karadi \(2015\)](#)—are close to zero and statistically insignificant.

residuals contain information about those disturbances, as well as any others that influence the economy. It is then the role of the identification procedure to extract the information from the set of reduced-form residuals of all variables and map this into structural disturbances.

A distinct, but related, question is how precisely the exchange rate contributes to our estimates of fundamental and noise disturbances. To answer this question, we use the baseline VAR estimates to compute the coefficients of a restricted VAR system that excludes the exchange rate. The details of this procedure are described in Appendix B.4. Since there is no exchange rate equation in the restricted VAR, no reduced-form exchange rate residual will contribute to the estimated disturbance. At the same time, because the exchange rate is included in the estimation of the unrestricted system, it is possible to compute the exchange rate response to the disturbance without doing any additional estimation step, and the results are directly comparable to our baseline.

Appendix Figure B.7 compares the resulting structural disturbances to the baseline, while Appendix Figure B.8 reports the implied exchange rate impulse responses. The correlation for the technological disturbance is high (99%) and the response to the technological disturbance is essentially unchanged relative to the baseline. This extremely close match for the technological disturbance is natural because its recoverability requirement is less stringent: one only needs the restricted VAR to accurately reflect the (unrestricted) autocovariances of TFP. By contrast, for the noise series, the extracted series correlation of 79% is high-but-imperfect and the impulse responses are somewhat different. The reason is that recovering the noise disturbances requires the VAR to accurately reflect both autocovariances *and* expected productivity. Evidently, removing the exchange rate from the information set changes the forecast of TFP in a non-trivial, albeit modest, way. Still, the other endogenous variables in the VAR (e.g. investment, interest rates) also contain information about future TFP, hence the restricted VAR still has statistical power to (partially) identify the underlying noisy news.

Another indication that the exchange rate embeds additional information about future TFP is the fact that the exchange rate in Appendix Figure B.8 moves prior to the realization of a noise disturbance. This means that endogenous variables respond before the measured expectation has changed, indicating that agents in the economy hold more information than is reflected in the restricted VAR.

5 Implications for open-economy models

A central conclusion of our analysis is that several well-known exchange rate puzzles share a *common* and *fundamental* origin: noisy news about future TFP. In this section, we explore

the implications of our results for several popular classes of open-economy models.

We consider four types of two-country endowment economies, described in detail in Appendix C.1. The models vary in terms of their international asset-market structures and household preferences. The first class of models assumes complete financial markets. Within this framework, we consider two models with different household preferences: constant relative risk aversion (CRRA) preferences, as in [Backus et al. \(1994\)](#), and [Epstein-Zin](#) preferences, following [Colacito and Croce \(2011, 2013\)](#). The second class of models we analyze features incomplete international asset markets with CRRA preferences, drawing on [Corsetti et al. \(2008b\)](#), [Itskhoki and Mukhin \(2021\)](#), and [Kekre and Lenel \(2024\)](#). Within this setting, we consider a standard benchmark model and an extension in which households' preferences for a given good increase with the aggregate availability of that good in the economy—a feature whose motivation will become clear in the discussion of our results below.

In order to evaluate the models, we calibrate standard parameters to common values in the literature. In particular, we set the rate of time preference $\beta = 0.99$ to match the quarterly frequency of the data we will compare the models to. We set risk aversion $\gamma = 5$. In the case of [Epstein-Zin](#) preferences when the IES is a separate parameter we set the IES = 1.2 as in [Colacito et al. \(2018\)](#). Last, the trade elasticity $\sigma = 1$ and home bias in consumption preferences $\zeta = 0.95$ in line with typical calibrations in the international macro literature.

In all of these models, we embed the same signal structure and process for TFP. In particular, for home TFP, we use the noise representation of the information structure proposed by [Blanchard et al. \(2013\)](#). This process is nested within the general structure of (5)-(7) and has two useful properties: it introduces only three free parameters, and can be calibrated to closely match the joint evolution of TFP and expectations about TFP that we observe in the data. Lastly, we assume that foreign TFP is weakly cointegrated with home TFP. Details on the calibration of this information structure can be found in Appendix C.2. The top two rows of Figures 8 and 9 compare the responses of TFP and expectations that we find in the data to those implied by our calibrated process.

The remaining preference parameters are summarized in Table 4. We calibrate these parameters to be consistent across models, and we solve all of the models using a first-order approximation, except for the version with [Epstein and Zin \(1989\)](#) preferences. For this model, we use a third-order perturbation technique.

Overall, all models share the same parameterization for preferences, TFP, and information structure. We then evaluate the models by comparing the model-implied impulse responses to ε_t^a and ε_t^v for several key endogenous variables—such as the real exchange rate q_t . Our objective is to assess whether these open-economy models can replicate the *qualita-*

Table 4: Parameter Calibration

| Parameter | Description | Complete Markets | | Incomplete Markets | |
|-------------|------------------------------|------------------|------|--------------------|--------------|
| | | CRRA | EZ | Benchmark | Endo. Demand |
| β | Subjective Discount Factor | 0.99 | 0.99 | 0.99 | 0.99 |
| γ | Relative Risk Aversion | 5 | 5 | 5 | 5 |
| ψ | Elas. of Intertemporal Subs. | $1/\gamma$ | 1.2 | $1/\gamma$ | $1/\gamma$ |
| ς | Home Bias | 0.95 | 0.95 | 0.95 | 0.95 |
| σ | Trade Elasticity | 1 | 1 | 1 | 1 |
| ϑ | Elas. of Rel. Good Demand | - | - | - | 0.38 |
| ϕ | Elas. of Int. Rate Premium | - | - | 0.01 | 0.01 |

Notes: The models are calibrated at a quarterly frequency, with all parameters set to standard benchmark values. In the incomplete-market model with endogenous demand composition, the parameter ϑ is estimated using impulse response matching.

tive patterns observed in the data: a side-by-side comparison is provided in Figures 8 and 9. We now discuss the results for each of the four models in turn.

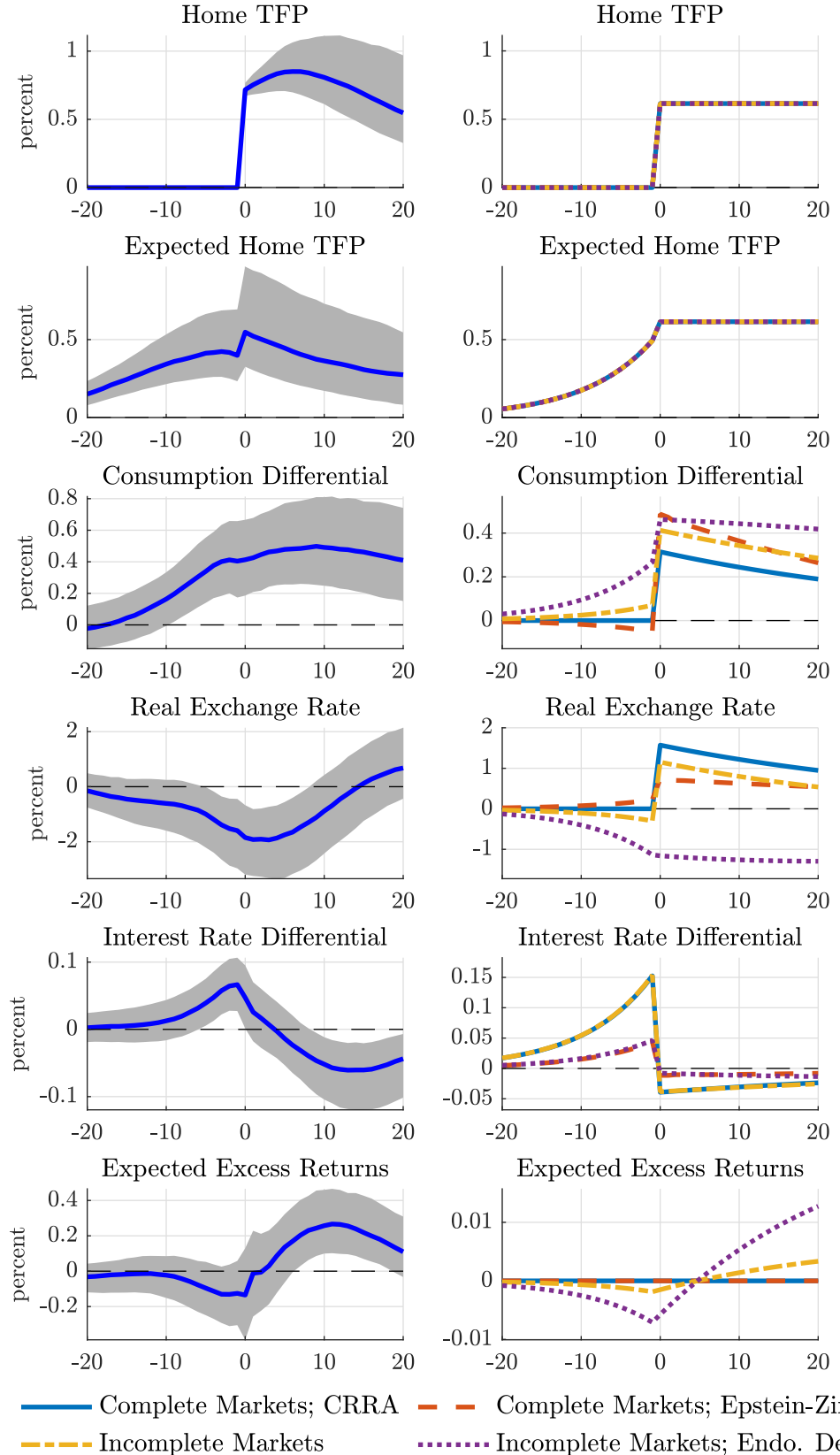
Complete Markets with CRRA Preferences We find that the benchmark complete markets model with CRRA preferences yields two main counterfactual implications.

First, expected future changes in TFP do not affect current consumption differentials or the real exchange rate (Figures 8–9). Under complete markets and time-separable preferences, all shocks are fully insured: marginal utilities are equalized across countries when expressed in common units. Therefore, even if home TFP is expected to rise in the future, this does not translate into a relative welfare or wealth gain for home agents today. As a result, allocations remain unchanged until TFP actually increases.

Second, when home TFP actually rises, the social planner allocates a larger share of the higher endowment to home agents due to home bias in preferences, increasing the home consumption differential and depreciating the real exchange rate. These responses are consistent with the standard [Backus-Smith](#) condition. However, empirically we observe the opposite pattern—a negative comovement between exchange rates and consumption in response to technological disturbances.

Complete Markets with Epstein-Zin Preferences A leading alternative to CRRA preferences in international finance is the recursive utility model of [Epstein and Zin \(1989\)](#).

Figure 8: Impulse responses to technology disturbances: data vs models



Notes: The left-hand panels present empirical impulse responses, and the right-hand panels present theoretical impulse responses. Details on the models can be found in Section 5 and Appendix C.

Under these preferences, marginal utility depends on the entire expected consumption path, allowing anticipated TFP changes to influence current outcomes as well as breaking the Backus-Smith condition, as shown by Colacito and Croce (2013).

However, while the complete markets model with Epstein-Zin preferences can generate anticipation effects and right sign for the Backus-Smith correlation, the responses of consumption differentials and exchange rates are inconsistent with those observed in the data. In the model, expectations of higher future home TFP lead to a decline of the consumption differential and a real exchange rate depreciation (Figures 8–9). This outcome stems from the recursive utility framework: households derive current utility from favorable news about future consumption. With complete risk-sharing, the resulting utility gain of home agents is immediately shared with foreign agents through resource transfers abroad, which lowers the consumption differential even before home TFP actually improves. The same mechanism depreciates the exchange rate. Thus, while the model succeeds in generating the negative correlation between consumption and the real exchange rate, it does so in a way that is qualitatively at odds with the data.

Importantly, these qualitative results are not tied to the specific structural TFP process we use. Appendix C.3 shows that similar dynamics arise under a TFP process with long-run risk features, as the one considered in Colacito and Croce (2011; 2013). In this case as well, anticipated TFP improvements reduce the consumption differential and depreciate the real exchange rate. The fluctuations in expected excess currency returns reinforce the exchange rate depreciation—opposite to the data, where the exchange rate instead appreciates in response to expected TFP gains.¹⁸

Incomplete Markets We now consider models with incomplete international asset markets, in which agents trade a single international bond and countries face a debt-elastic interest rate premium. The debt-elastic interest rate premium guarantees the stationarity of equilibrium dynamics (Schmitt-Grohé and Uribe, 2003) and generates fluctuations in expected excess currency returns linked to external borrowing, as in Gabaix and Maggiori (2015), Itskhoki and Mukhin (2021) and Kekre and Lenel (2024).

In Appendix C.1.2, we show that the benchmark incomplete market model can be represented as the following system of 3 equations:

$$q_t = -\frac{(2\varsigma - 1)^2}{4(1 - \varsigma)\sigma\varsigma}(c_t - c_t^*) + \frac{(2\varsigma - 1)}{4(1 - \varsigma)\sigma\varsigma}(a_t - a_t^*), \quad (11a)$$

¹⁸Appendices C.2 and C.3 provide an explicit mapping from the information structures in Blanchard et al. (2013) and Colacito and Croce (2013) to the noise structure in (5)–(7).

$$q_t = \gamma(c_t - c_t^*) - \phi \sum_{j=1}^{\infty} E_t b_{t+j}^*, \quad (11b)$$

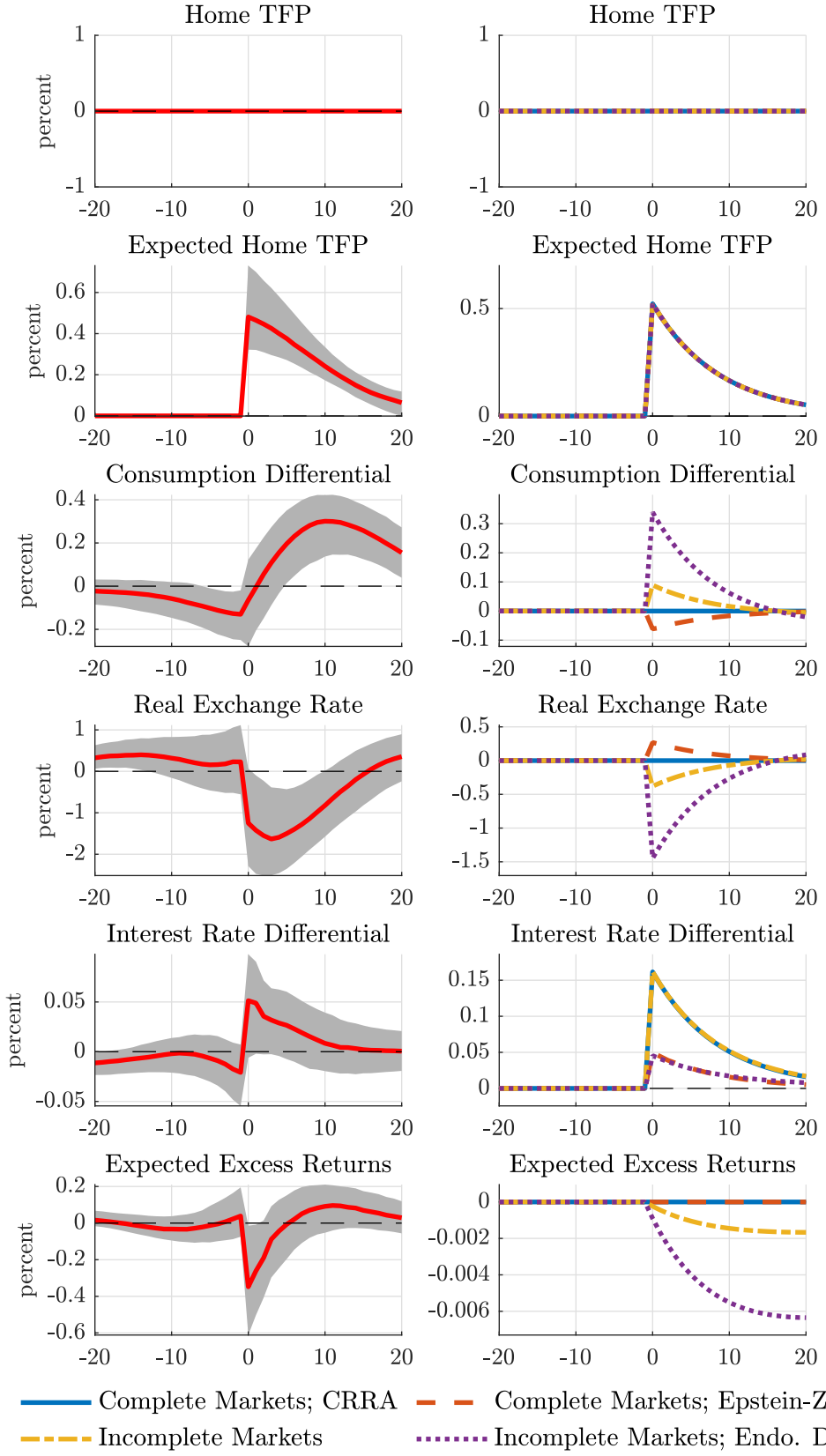
$$\beta b_{t+1}^* - b_t^* = (1 - \varsigma) \left[-(c_t - c_t^*) + \frac{(2\sigma\varsigma - 1)}{(2\varsigma - 1)} q_t \right]. \quad (11c)$$

Equation (11a) describes equilibrium in the goods market. Equation (11b) characterizes equilibrium in the asset market, given expectations about the future path of the net foreign asset position. Equation (11c) describes country's intertemporal budget constraint, and governs the evolution of net foreign assets. Equilibrium dynamics are shaped by standard parameters: home bias, ς , trade elasticity, σ , intertemporal elasticity of substitution, $1/\gamma$, and the elasticity of expected excess currency returns to the net foreign asset position, $\phi > 0$.

Together, equations (11a)–(11c) determine the joint dynamics of the consumption differential, $c_t - c_t^*$, the real exchange rate, q_t , and the country's net external position, b_{t+1}^* . In particular, we observe that the comovement between consumption and exchange rates depends on whether a disturbance primarily shifts the goods market equilibrium or the asset market equilibrium. Shifts to the goods market equilibrium (11a) generate a positive relationship between the consumption differential and the exchange rate. For example, when home goods supply increases ($a_t - a_t^* > 0$), equilibrium is restored through a higher consumption differential ($c_t - c_t^* > 0$) and a depreciation of the exchange rate ($q_t > 0$). Conversely, shifts to the asset market equilibrium (11b) induce a negative relationship between consumption and the exchange rate. For instance, a higher path of net external savings ($\sum_{j=1}^{\infty} E_t b_{t+j}^* > 0$) raises the path of expected excess returns on foreign assets, leading to an appreciation of the exchange rate ($q_t < 0$) and higher consumption differential ($c_t - c_t^*$). In the literature, shifts to the asset market equilibrium have been associated with noise trading shocks (Itskhoki and Mukhin, 2021) or relative discount factor shocks (Kkre and Lenel, 2024). Below, we discuss how technology and noise disturbances transmit within this framework.

The benchmark incomplete-markets model is successful in generating a high consumption differential and an appreciated real exchange rate in *anticipation* of a TFP improvement, as observed in the data (see the anticipation phase of the impulse responses in Figure 8, as well as Figure 9). Positive news about future TFP increases the expected future income of home households, thereby raising their consumption demand when their intertemporal elasticity of substitution is sufficiently low. Home households finance this initial rise in consumption by borrowing abroad, resulting in a negative net foreign asset position ($b_{t+1}^* < 0$). While next-period excess returns are expected to be negative (due to $b_{t+1}^* < 0$), their expected cumulative sum is positive, as households anticipate higher net external savings once the TFP improvement materializes (that is, $\sum_{j=1}^{\infty} E_t b_{t+j}^* > 0$). This behavior gives rise to

Figure 9: Impulse responses to noise disturbances: data vs models



Notes: The left-hand panels present empirical impulse responses, and the right-hand panels present theoretical impulse responses. Details on the models can be found in Section 5 and Appendix C.

expected excess currency return dynamics that are consistent with our empirical estimates (and also in line with the empirical response of the US trade balance in Figure B.1).

Since the endowment of home goods has not yet increased during the anticipation phase, these disturbances operate only through the asset market equilibrium condition, (11b). As a result, the consumption differential increases and the exchange rate appreciates. More broadly, the comovement upon arrival of news mirrors that generated by demand disturbances: higher consumption, elevated interest rates, and appreciated exchange rates, as emphasized by Kekre and Lenel (2024). Yet, in this case the exchange rate appreciation obtains through expectations of positive future excess foreign-currency returns, rather than through persistently higher interest differentials.

When a TFP improvement materializes, however, it now influences the economy through the goods market clearing condition, (11b), leading to an immediate depreciation of the real exchange rate. This prediction contrasts with the empirical evidence, which shows that the real exchange rate remains appreciated when TFP rises, before gradually depreciating thereafter. Although the expected increase in the net foreign asset position tends to appreciate the exchange rate for a given consumption differential (see eq. (11b)), the sharp increase in home-goods supply shifts the goods-market equilibrium (eq. (11a)), raising home consumption and depreciating the exchange rate. Because this latter effect dominates, the benchmark incomplete-markets model cannot simultaneously account for an appreciated real exchange rate and elevated home consumption following the actual TFP improvement.¹⁹ In Appendix C.1.2, we prove that the benchmark incomplete-markets model cannot generate an exchange rate appreciation in response to a contemporaneous increase in relative productivity.

Incomplete Markets with Endogenous Demand Composition To reconcile the model with the observed persistent exchange rate appreciation after TFP improvements, we introduce a mechanism linking higher home TFP to stronger global demand for home goods.²⁰ Specifically, we assume that the preference weights on individual goods in the consumption baskets of home and foreign agents are proportional to the current endowment of each good (see Appendix C.1.2 for details). This is not intended as a structural solution, but as a reduced-form illustration. To a first-order approximation, the modification operates entirely through the demand functions of home and foreign goods, where higher home productivity shifts global demand towards home-produced goods.

¹⁹In principle, a sustained real appreciation could be supported by expectations of higher future trade surpluses, which imply higher foreign asset accumulation and thus a higher foreign-currency premium (see eq. (11b)). However, higher trade surpluses require either a lower consumption differential or a real depreciation under conventional values of the trade elasticity (see eq. (11c)).

²⁰We thank Moritz Lenel and Rohan Kekre for suggesting this extension.

In Appendix C.1.2, we show that the 3-equations linear system in (11a)-(11c) becomes:

$$q_t = -\frac{(2\varsigma - 1)^2}{4(1-\varsigma)\sigma\varsigma}(c_t - c_t^*) + \frac{(2\varsigma - 1)}{4(1-\varsigma)\sigma\varsigma}(a_t - a_t^*) - \boxed{\frac{(2\varsigma - 1)}{2(1-\varsigma)\sigma}(\varsigma_t - \varsigma_t^*)}; \quad (12a)$$

$$q_t = \gamma(c_t - c_t^*) - \phi \sum_{j=1}^{\infty} E_t b_{t+j}^*; \quad (12b)$$

$$\beta b_{t+1}^* - b_t^* = (1-\varsigma) \left(-(c_t - c_t^*) + \frac{(2\sigma\varsigma - 1)}{(2\varsigma - 1)}(q_t) \right) + \boxed{\varsigma(\varsigma_t - \varsigma_t^*)} \quad (12c)$$

This system of equations differs from the benchmark counterpart (11a)-(11c) solely due to the presence of the $\varsigma_t - \varsigma_t^*$ terms in equations (12a) and (12c). The terms $\varsigma_t - \varsigma_t^*$ denotes shifts in the composition of demand between home and foreign goods. Bodenstein et al. (2024) and Mac Mullen and Woo (2025) introduce similar wedges—referred to as “trade shocks”—that are orthogonal to other structural shocks, including productivity. In contrast, in our framework these wedges are endogenous, given by:

$$\varsigma_t - \varsigma_t^* = \vartheta(a_t - a_t^*), \quad (13)$$

which captures that a rise in the home endowment raises world demand for home goods relative to foreign goods.

This extended model can generate a persistently appreciated real exchange rate even after the TFP increase, without compromising the otherwise realistic comovements implied by the benchmark incomplete-markets model (see Figure 8). Endogenous demand composition this dimension of the model through two channels. First, higher home good demand dampens the shift in the home goods market equilibrium, thereby weakening the depreciation pressure for a given consumption differential (see equation 12a). Intuitively, when the fruits of the home tree are more abundant ($a_t - a_t^* > 0$), they are also more desirable ($\varsigma_t - \varsigma_t^* > 0$). Second, the simultaneous increase in global demand for home goods allows the home economy to maintain persistent trade surpluses alongside higher consumption and an appreciated real exchange rate (see equation 12c). The resulting expansion in the net external position further increases the foreign-currency premium, supporting an equilibrium appreciation of the exchange rate along with a higher consumption differential (see equation 12b).²¹ Finally, because expected relative consumption growth turns negative upon the TFP improvement, the interest rate differential declines. Appendix C.4 demonstrates that expected excess currency returns—rather than interest rate movements—account for the real exchange rate appreciation.

²¹Proposition 1 in Appendix C.1.2 provides a sufficient condition on ϑ such that the incomplete markets model produces an exchange rate appreciation in response to a contemporaneous increase in relative productivity.

Overall, our analysis thus highlights that two ingredients are essential: *incomplete markets* and *time-varying currency premia*. Together, they explain why exchange rates appreciate in expectations of productivity gains, and how they can remain persistently appreciated even after productivity gains materialize.²²

6 Conclusions

This paper provides new empirical evidence that speaks to the apparent disconnect between exchange rates and macroeconomic fundamentals. Using a structural identification approach, we find that noisy news about future TFP account for a substantial share of the variation in both real exchange rates and macroeconomic aggregates. Our evidence reveals that the apparent disconnect arises not from an absence of linkage, but from differences in the timing of responses: exchange rates incorporate information about macro fundamentals well before these effects materialize in many other observable macro variables. In addition, our analysis explicitly accounts for expectational noise, *i.e.*, fluctuations in expectations that are not associated with actual subsequent changes in fundamentals. Ignoring this component of expectations may obfuscate the forward-looking nature of exchange rates.

Our analysis also shows that the responses to noisy news generate several well-known exchange rate puzzles—including violations of uncovered interest parity, the consumption-real exchange rate anomaly, and the excess volatility and persistence of exchange rates. This set of disturbances can therefore account for multiple empirical regularities that have long challenged open-economy models. Our theoretical results show that models with complete markets fail to reproduce the observed relationships between expected productivity, consumption differentials, and real exchange rate, whereas incomplete-market models provide a closer match to the data. In particular, incomplete-market frameworks that feature time-varying endogenous expected currency returns can successfully replicate the joint responses of consumption differentials, interest differentials, exchange rates, and excess currency returns to both expected and realized changes in TFP.

²²Huang et al. (2025) propose a model in which higher US productivity can cause the dollar to appreciate. With incomplete markets both domestically and internationally, productivity gains shift wealth from existing shareholders to a few US entrepreneurs. Under certain calibrations, this raises both aggregate US consumption and the average marginal utility of US consumers. Because the latter determines the exchange rate pricing, this implies a dollar appreciation.

References

- Akinci, O. and R. Chahrour (2025). Risk Sharing, International Comovement, and the Goldilocks Trade Elasticity.
- Alvarez, F., A. Atkeson, and P. J. Kehoe (2009). Time-varying risk, interest rates, and exchange rates in general equilibrium. *The Review of Economic Studies* 76(3), 851–878.
- Andersen, T. G., T. Bollerslev, F. X. Diebold, and C. Vega (2003). Micro effects of macro announcements: Real-time price discovery in foreign exchange. *American Economic Review* 93(1), 38–62.
- Angeletos, G.-M., F. Collard, and H. Dellas (2020). Business-cycle anatomy. *American Economic Review* 110(10), 3030–70.
- Ayres, J., C. Hevia, and J. P. Nicolini (2020). Real exchange rates and primary commodity prices. *Journal of International Economics* 122, 103261.
- Bacchetta, P. and E. van Wincoop (2006). Can information heterogeneity explain the exchange rate determination puzzle? *The American Economic Review* 96(3), 552.
- Bacchetta, P. and E. Van Wincoop (2010). Infrequent portfolio decisions: A solution to the forward discount puzzle. *The American Economic Review* 100(3), 870–904.
- Backus, D. K., P. J. Kehoe, and F. E. Kydland (1994). Dynamics of the Trade Balance and the Terms of Trade: The J-Curve? *American Economic Review* 84(1), 84–103.
- Backus, D. K. and G. W. Smith (1993). Consumption and real exchange rates in dynamic economies with non-traded goods. *Journal of International Economics* 35(3-4), 297–316.
- Baillie, R. T. and D. Cho (2014). Time variation in the standard forward premium regression: Some new models and tests. *Journal of Empirical Finance* 29, 52–63.
- Bansal, R. and I. Shaliastovich (2012). A long-run risks explanation of predictability puzzles in bond and currency markets. *Review of Financial Studies*, hhs108.
- Barsky, R. B. and E. R. Sims (2011). News Shocks and Business Cycles. *Journal of Monetary Economics* 58(3), 273 – 289.
- Basu, S., G. Candian, R. Chahrour, and R. Valchev (2021). Risky Business Cycles. NBER Working Papers 28693, National Bureau of Economic Research, Inc.
- Beaudry, P. and F. Portier (2006). Stock Prices, News, and Economic Fluctuations. *The American Economic Review* 96(4), pp. 1293–1307.
- Beaudry, P. and F. Portier (2014). News-Driven Business Cycles: Insights and Challenges. *Journal of Economic Literature* 52(4), 993–1074.
- Blanchard, O. J., J.-P. L'Huillier, and G. Lorenzoni (2013). News, Noise, and Fluctuations: An Empirical Exploration. *American Economic Review* 103(7), 3045–70.
- Bodenstein, M. (2011). Closing large open economy models. *Journal of International Economics* 84(2), 160–177.
- Bodenstein, M., P. Cuba-Borda, N. Gornemann, and I. Presno (2024). Exchange rate disconnect and the trade balance. *International Finance Discussion Paper* (1391).
- Boer, L., J. Lee, and M. Sun (2025). Dominant Drivers of Current Account Dynamics. *Working Paper*.
- Burnside, C. (2011). Carry trades and risk. *Working Paper*.
- Burnside, C., M. Eichenbaum, and S. Rebelo (2011). Carry trade and momentum in currency

- markets. *Annu. Rev. Financ. Econ.* 3(1), 511–535.
- Burnside, C., B. Han, D. Hirshleifer, and T. Y. Wang (2011). Investor overconfidence and the forward premium puzzle. *The Review of Economic Studies* 78(2), 523–558.
- Candian, G. and P. De Leo (2025). Imperfect exchange rate expectations. *The Review of Economics and Statistics* 107(5), 1406–1423.
- Chahrour, R., S. K. Chugh, and T. Potter (2023). Anticipated productivity and the labor market. *Quantitative Economics* 14(3), 897–934.
- Chahrour, R. and K. Jurado (2018). News or noise? the missing link. *American Economic Review* 108(7), 1702–36.
- Chahrour, R. and K. Jurado (2022). Recoverability and expectations-driven fluctuations. *The Review of Economic Studies* 89(1), 214–239.
- Chahrour, R. and K. Jurado (2025). Expectation response functions in dynamic linear economies. Technical report, National Bureau of Economic Research.
- Chari, V. V., P. J. Kehoe, and E. R. McGrattan (2002). Can sticky price models generate volatile and persistent real exchange rates? *The Review of Economic Studies* 69(3), 533–563.
- Chen, Y.-C., K. S. Rogoff, and B. Rossi (2010). Can Exchange Rates Forecast Commodity Prices? *The Quarterly Journal of Economics* 125(3), 1145–1194.
- Chernov, M. and D. Creal (2023). International yield curves and currency puzzles. *The Journal of Finance* 78(1), 209–245.
- Chernov, M., V. Haddad, and O. Itskhoki (2023). What do financial markets say about the exchange rate? *Working Paper*.
- Cheung, Y.-W., M. D. Chinn, and A. G. Pascual (2005). Empirical exchange rate models of the nineties: Are any fit to survive? *Journal of International Money and Finance* 24(7), 1150–1175.
- Colacito, R., M. Croce, S. Ho, and P. Howard (2018). BKK the EZ Way: International Long-Run Growth News and Capital Flows. *American Economic Review* 108(11), 3416–49.
- Colacito, R. and M. M. Croce (2011). Risks for the long run and the real exchange rate. *Journal of Political Economy* 119(1), 153–181.
- Colacito, R. and M. M. Croce (2013). International asset pricing with recursive preferences. *The Journal of Finance* 68(6), 2651–2686.
- Comin, D. A., J. Quintana, T. G. Schmitz, and A. Trigari (2023). Revisiting productivity dynamics in europe: A new measure of utilization-adjusted tfp growth. Technical report, National Bureau of Economic Research.
- Cormun, V. and P. De Leo (2024). Shocks and exchange rates in small open economies. *Working Paper*.
- Corsetti, G., L. Dedola, and S. Leduc (2008a). High exchange-rate volatility and low pass-through. *Journal of Monetary Economics* 55(6), 1113–1128.
- Corsetti, G., L. Dedola, and S. Leduc (2008b). International Risk Sharing and the Transmission of Productivity Shocks. *The Review of Economic Studies* 75(2), 443–473.
- Corsetti, G., L. Dedola, and S. Leduc (2014). The International Dimension of Productivity and Demand Shocks in the US Economy. *Journal of the European Economic Association*

- tion* 12(1), 153–176.
- Devereux, M. B. and C. Engel (2002). Exchange Rate Pass-Through, Exchange Rate Volatility, and Exchange Rate Disconnect. *Journal of Monetary Economics* 49(5), 913 – 940.
- Dieppe, A., N. Francis, and G. Kindberg-Hanlon (2021). The identification of dominant macroeconomic drivers: Coping with confounding shocks.
- Dou, L., P. Ho, and T. Lubik (2025). Max-share misidentification. *Federal Reserve Bank of Richmond Working Paper Series* (25-2).
- Du, W., A. Tepper, and A. Verdelhan (2018). Deviations from covered interest rate parity. *The Journal of Finance* 73(3), 915–957.
- Eaton, J. and S. Kortum (1999). International technology diffusion: Theory and measurement. *International Economic Review* 40(3), 537–570.
- Eichenbaum, M. and C. L. Evans (1995). Some empirical evidence on the effects of shocks to monetary policy on exchange rates. *The Quarterly Journal of Economics*, 975–1009.
- Engel, C. (2014). Exchange rates and interest parity. In *Handbook of international economics*, Volume 4, pp. 453–522. Elsevier.
- Engel, C. (2016). Exchange rates, interest rates, and the risk premium. *American Economic Review* 106.
- Engel, C., N. C. Mark, and K. D. West (2008). Exchange Rate Models Are Not As Bad As You Think. In *NBER Macroeconomics Annual 2007, Volume 22*, NBER Chapters, pp. 381–441. National Bureau of Economic Research, Inc.
- Engel, C. and J. H. Rogers (2006). The us current account deficit and the expected share of world output. *Journal of monetary Economics* 53(5), 1063–1093.
- Engel, C. and K. D. West (2005). Exchange rates and fundamentals. *Journal of Political Economy* 113(3), 485–517.
- Engel, C. and S. P. Y. Wu (2024). Exchange rate models are better than you think, and why they didn't work in the old days. *Working Paper*.
- Epstein, L. G. and S. E. Zin (1989). Substitution, Risk Aversion, and the Temporal Behavior of Consumption and Asset Returns: A Theoretical Framework. *Econometrica* 57(4), pp. 937–969.
- Evans, M. D. and R. K. Lyons (2008). How is macro news transmitted to exchange rates? *Journal of Financial Economics* 88(1), 26–50.
- Evans, M. D. D. and R. K. Lyons (2002). Order flow and exchange rate dynamics. *Journal of Political Economy* 110(1), 170–180.
- Fama, E. F. (1984). Forward and spot exchange rates. *Journal of Monetary Economics* 14(3), 319–338.
- Farhi, E. and X. Gabaix (2015). Rare disasters and exchange rates. *The Quarterly Journal of Economics*.
- Faust, J. (1998). The robustness of identified VAR conclusions about money. *Carnegie-Rochester Conference Series on Public Policy*.
- Faust, J., J. H. Rogers, S.-Y. B. Wang, and J. H. Wright (2007). The high-frequency response of exchange rates and interest rates to macroeconomic announcements. *Journal of Monetary Economics* 54(4), 1051–1068.
- Fernald, J. G. (2012). A quarterly, utilization-adjusted series on total factor productivity.

- Working Paper* (2012-19).
- Gabaix, X. and M. Maggiori (2015). International liquidity and exchange rate dynamics. *The Quarterly Journal of Economics* 130(3), 1369–1420.
- Gertler, M. and P. Karadi (2015). Monetary Policy Surprises, Credit Costs, and Economic Activity. *American Economic Journal: Macroeconomics* 7(1), 44–76.
- Gornemann, N., P. A. Guerrón Quintana, and F. Saffie (2025). Real exchange rates and endogenous productivity. *American Economic Journal: Macroeconomics* 17(4), 204–261.
- Gourinchas, P.-O., W. Ray, and D. Vayanos (2022). A preferred-habitat model of term premia, exchange rates, and monetary policy spillovers. *Working Paper*.
- Gourinchas, P.-O. and H. Rey (2007). International financial adjustment. *Journal of political economy* 115(4), 665–703.
- Gourinchas, P.-O. and A. Tornell (2004). Exchange rate puzzles and distorted beliefs. *Journal of International Economics* 64(2), 303–333.
- Greenwood, R., S. Hanson, J. C. Stein, and A. Sunderam (2023). A Quantity-Driven Theory of Term Premia and Exchange Rates. *The Quarterly Journal of Economics* 138(4), 2327–2389.
- Hassan, T. A. (2013). Country size, currency unions, and international asset returns. *The Journal of Finance* 68(6), 2269–2308.
- Hassan, T. A. and R. C. Mano (2019). Forward and spot exchange rates in a multi-currency world. *The Quarterly Journal of Economics* 134(1), 397–450.
- Hassan, T. A., T. M. Mertens, and T. Zhang (2016). Not so disconnected: Exchange rates and the capital stock. *Journal of International Economics* 99(S1), 43–57.
- Hau, H. and H. Rey (2006). Exchange rates, equity prices, and capital flows. *The Review of Financial Studies* 19(1), 273–317.
- Hoffmann, M., M. U. Krause, and T. Laubach (2019). The Expectations-driven US Current Account. *Economic Journal* 129(618), 897–924.
- Huang, Q., D. Papanikolaou, and L. Kogan (2025). Tech dollars: Technological innovation and exchange rates. *Working Paper*.
- Huo, Z., A. A. Levchenko, and N. Pandalai-Nayar (2023). Utilization-adjusted tfp across countries: Measurement and implications for international comovement. *Journal of International Economics*, 103753.
- Huo, Z., A. A. Levchenko, and N. Pandalai-Nayar (2025). International comovement in the global production network. *Review of Economic Studies* 92(1), 365–403.
- Ilut, C. (2012). Ambiguity aversion: Implications for the uncovered interest rate parity puzzle. *American Economic Journal: Macroeconomics* 4(3), 33–65.
- Itskhoki, O. and D. Mukhin (2021). Exchange rate disconnect in general equilibrium. *Journal of Political Economy*.
- Jeanne, O. and A. K. Rose (2002). Noise trading and exchange rate regimes. *The Quarterly Journal of Economics* 117(2), 537–569.
- Karabarounis, L. (2014). Home production, labor wedges, and international business cycles. *Journal of Monetary Economics* 64, 68–84.
- Kekre, R. and M. Lenel (2024). Exchange rates, natural rates, and the price of risk. *Working Paper*.

- Kollmann, R. (1995). Consumption, real exchange rates and the structure of international asset markets. *Journal of International Money and Finance* 14(2), 191–211.
- Kollmann, R. (2005). Macroeconomic effects of nominal exchange rate regimes: new insights into the role of price dynamics. *Journal of International Money and Finance* 24(2), 275–292.
- Kremens, L. and I. Martin (2019). The quanto theory of exchange rates. *American Economic Review* 109(3), 810–43.
- Kurmann, A. and C. Otrok (2013). News shocks and the slope of the term structure of interest rates. *American Economic Review* 103(6), 2612–32.
- Levchenko, A. A. and N. Pandalai-Nayar (2020). Tfp, news, and “sentiments”: The international transmission of business cycles. *Journal of the European Economic Association* 18(1), 302–341.
- Lilley, A., M. Maggiori, B. Neiman, and J. Schreger (2020). Exchange Rate Reconnect. *The Review of Economics and Statistics*, 1–28.
- Lloyd, S. and E. A. Marin (2020). Exchange rate risk and business cycles.
- Lustig, H., N. Roussanov, and A. Verdelhan (2014). Countercyclical currency risk premia. *Journal of Financial Economics* 111(3), 527–553.
- Lustig, H., A. Stathopoulos, and A. Verdelhan (2019). The term structure of currency carry trade risk premia. *American Economic Review* 109(12), 4142–77.
- Mac Mullen, M. and S. K. Woo (2025). Real exchange rate and net trade dynamics: Financial and trade shocks. *Journal of International Economics* 157, 104141.
- Meese, R. A. and K. Rogoff (1983). Empirical exchange rate models of the seventies: Do they fit out of sample? *Journal of International Economics* 14(1), 3–24.
- Menkhoff, L., L. Sarno, M. Schmeling, and A. Schrimpf (2012). Currency momentum strategies. *Journal of Financial Economics* 106(3), 660–684.
- Miyamoto, W., T. L. Nguyen, and H. Oh (2023). In Search of Dominant Drivers of the Real Exchange Rate. *The Review of Economics and Statistics*, 1–50.
- Moskowitz, T. J., Y. H. Ooi, and L. H. Pedersen (2012). Time series momentum. *Journal of Financial Economics* 104(2), 228–250. Special Issue on Investor Sentiment.
- Nam, D. and J. Wang (2015). The effects of surprise and anticipated technology changes on international relative prices and trade. *Journal of International Economics* 97(1), 162–177.
- Newey, W. K. and K. D. West (1987). A simple, positive semi-definite, heteroskedasticity and autocorrelation consistent covariance matrix. *Econometrica* 55(3), 703–708.
- Obstfeld, M. and K. Rogoff (2000). The six major puzzles in international macroeconomics: is there a common cause? *NBER Macroeconomics Annual* 15, 339–390.
- Rogoff, K. (1996). The purchasing power parity puzzle. *Journal of Economic literature* 34(2), 647–668.
- Rogoff, K. S. and V. Stavrakeva (2008). The continuing puzzle of short horizon exchange rate forecasting. *Working Paper*.
- Rossi, B. (2013). Exchange rate predictability. *Journal of Economic Literature* 51(4), 1063–1119.
- Sarno, L. (2005). Towards a solution to the puzzles in exchange rate economics: Where do

- we stand? *Canadian Journal of Economics* 38(3), 673–708.
- Sarno, L. and M. Schmeling (2014). Which fundamentals drive exchange rates? a cross-sectional perspective. *Journal of Money, Credit and Banking* 46(2-3), 267–292.
- Schmitt-Grohé, S. and M. Uribe (2003). Closing Small Open Economy Models. *Journal of International Economics* 61(1), 163 – 185.
- Siena, D. (2015). News shocks and international business cycles. *Working Paper*.
- Sims, C. A. (1972). Money, income, and causality. *American Economic Review* 62(4), 540–552.
- Sims, C. A., J. H. Stock, and M. W. Watson (1990). Inference in linear time series models with some unit roots. *Econometrica*, 113–144.
- Stavrakeva, V. and J. Tang (2020). A fundamental connection: Exchange rates and macroeconomic expectations. *Working Paper*.
- Steinsson, J. (2008). The dynamic behavior of the real exchange rate in sticky price models. *American Economic Review* 98(1), 519–33.
- Uhlig, H. (2003). What moves real GNP? Working paper, Humboldt University.
- Valchev, R. (2020). Bond convenience yields and exchange rate dynamics. *American Economic Journal: Macroeconomics* 12(2), 124–66.
- Verdelhan, A. (2010). A habit-based explanation of the exchange rate risk premium. *The Journal of Finance* 65(1), 123–146.

Appendix

A Data Sources

- Nominal exchange rate
 - Daily bilateral exchange rates, Foreign Currency/USD;
 - Source: *Datostream*;
 - Quarterly aggregation: period-average.
- Nominal interest rates
 - Daily Eurodollar deposit rates;
 - Source: *Datostream*;
 - Quarterly aggregation: period-average.
- Consumer Price Indexes
 - CPI Index (Chained 2010)
 - Source: *OECD*, https://stats.oecd.org/index.aspx?DataSetCode=PRICES_CPI
- Consumption
 - Real consumption;
 - Source: *OECD*, Private final consumption expenditure
- Investment
 - Real Investment;
 - Source: *OECD*, Gross Fixed Capital Formation (GFCF), Quarterly growth rates, <https://data.oecd.org/gdp/investment-gfcf.htm>.
- US TFP
 - US utilization-adjusted TFP as constructed in Fernald (2012);
 - Source: John Fernald's website, <https://www.johnfernald.net/TFP> (latest available vintage, downloaded on January 2, 2022);
- US R&D
 - Real R&D expenditure
 - Source: *US Bureau of Economic Analysis*, retrieved from *FRED*, <https://fred.stlouisfed.org/series/Y694RX1Q020SBEA>
- US trade balance (% of GDP)
 - Shares of gross domestic product: Net exports of goods and services
 - Source: *US Bureau of Economic Analysis*, retrieved from *FRED*, <https://fred.stlouisfed.org/series/A019RE1Q156NBEA>
- Equity prices and equity returns
 - MSCI price indexes and total returns indexes
 - Source: retrieved from *Datostream*

- Long-term bond yields
 - Interest Rates: Long-Term Government Bond Yields: 10-Year
 - Source: *Global Financial Data*

B Identification details and alternative specifications

B.1 Identification of TFP and expectational noise disturbances

Let the n_y -dimensional VAR(p)

$$y_t = B_1 y_{t-1} + \cdots + B_p y_{t-p} + u_t, \quad \mathbb{E}[u_t u'_t] = \Sigma$$

be stable. Its spectral density is

$$f_y(\lambda) = \frac{1}{2\pi} \left(I_{n_y} - B_1 e^{-i\lambda} - \cdots - B_p e^{-ip\lambda} \right)^{-1} \Sigma \left[\left(I_{n_y} - B_1 e^{-i\lambda} - \cdots - B_p e^{-ip\lambda} \right)^{-1} \right]^*. \quad (\text{B.1})$$

Let $a_t = e_a y_t$ pick the technology series from y_t and let $b_t = \sum_{s>0} \beta_s y_{t-s}$ be the forecast of a_{t+h} generated by VAR. Collecting, the spectral density of $\{a_t, b_t\}$ is

$$f(\lambda) = \begin{bmatrix} f_a(\lambda) & f_{ab}(\lambda) \\ f_{ba}(\lambda) & f_b(\lambda) \end{bmatrix} = \begin{bmatrix} e_a \\ \beta(\lambda) \end{bmatrix} f_y(\lambda) \begin{bmatrix} e'_a & \beta(\lambda)^* \end{bmatrix}, \quad (\text{B.2})$$

where $\beta(\lambda)$ is the Fourier transform of $\{\beta_s\}$. The spectral density $f(\lambda)$ can be factorized

$$f(\lambda) = \frac{1}{2\pi} \varphi(\lambda) \varphi(\lambda)^*, \quad \varphi(\lambda) = \begin{bmatrix} \varphi_{11}(\lambda) & 0 \\ \varphi_{21}(\lambda) & \varphi_{22}(\lambda) \end{bmatrix}. \quad (\text{B.3})$$

[Chahrour and Jurado \(2022\)](#) show that this factorization (B.3) is unique and, because of the zero in the top-right of $\varphi(\lambda)$, satisfies the two identification assumptions stated in Section 3.

Recovering disturbances Let the vector of structural disturbances be $\varepsilon_t = (\varepsilon_t^a, \varepsilon_t^v)'$. The disturbances are recovered from observables via the frequency-domain filter

$$\varepsilon(\lambda) = \psi(\lambda) Y(\lambda), \quad \psi(\lambda) = \varphi(\lambda)^{-1} \begin{bmatrix} e_a \\ \beta(\lambda) \end{bmatrix}. \quad (\text{B.4})$$

Impulse responses and variance shares The impulse response of variable k at horizon s to a unit innovation in component l of ε_t is given by $\text{IR}_{k,l}(s) = \text{Cov}(y_{k,t+s}, \varepsilon_{l,t})$. By the standard inversion from cross-spectra to cross-covariances,

$$\text{IR}_{k,l}(s) = \int_{-\pi}^{\pi} e^{i\lambda s} e_k f_y(\lambda) \psi(\lambda)^* e'_l d\lambda, \quad (\text{B.5})$$

where e_k selects component k of y_t and e_l selects component l of ε_t . The share of the variance in the process $\{y_{k,t}\}$ due to the disturbance $\{\varepsilon_{l,t}\}$ over the frequency range $\Delta = [\lambda_1, \lambda_2]$ is given by

$$\text{VS}_{kl}(\Delta) = \int_{\Delta} |e_k f_y(\lambda) \psi(\lambda)^* e_l'|^2 d\lambda \left(\int_{\Delta} f_{y,kk}(\lambda) d\lambda \right)^{-1}. \quad (\text{B.6})$$

B.2 Additional empirical evidence

Table B.1: Share of forecast error variance explained by the FX shock: target 2–1000 quarter periodicities

| | Forecast Horizon (Quarter) | | | | | |
|----------------------------|----------------------------|------|-------|-------|-------|--------|
| | $Q1$ | $Q4$ | $Q12$ | $Q24$ | $Q40$ | $Q100$ |
| Home TFP | 0.03 | 0.06 | 0.20 | 0.37 | 0.46 | 0.45 |
| Home Consumption | 0.02 | 0.04 | 0.21 | 0.49 | 0.53 | 0.45 |
| Foreign Consumption | 0.01 | 0.03 | 0.07 | 0.23 | 0.39 | 0.34 |
| Home Investment | 0.27 | 0.32 | 0.33 | 0.40 | 0.43 | 0.43 |
| Foreign Investment | 0.06 | 0.08 | 0.15 | 0.23 | 0.36 | 0.36 |
| Interest Rate Differential | 0.37 | 0.37 | 0.30 | 0.33 | 0.36 | 0.39 |
| Real Exchange Rate | 0.47 | 0.66 | 0.80 | 0.71 | 0.69 | 0.67 |
| Expected Excess Returns | 0.44 | 0.32 | 0.34 | 0.43 | 0.44 | 0.46 |

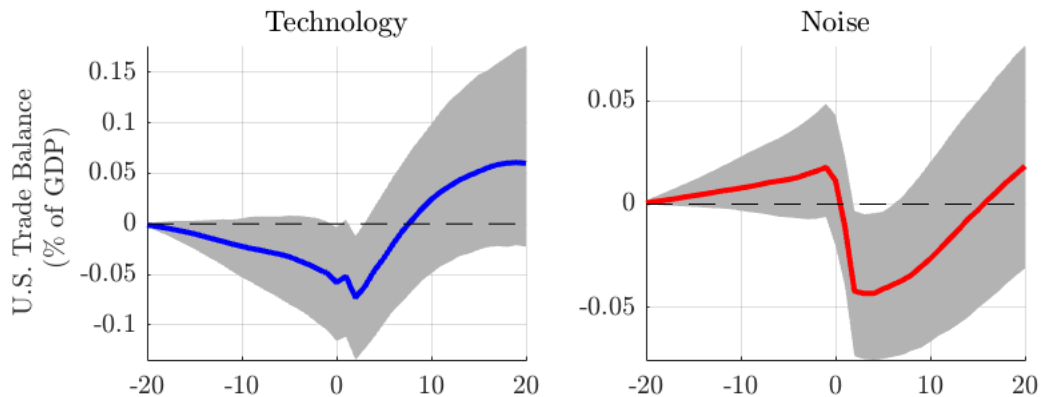
Notes: The table reports the estimated variance shares at different horizons accounted for by the exchange rate shock that explains most of the forecast error variance of the exchange rate over the [2,1000] quarter periodicity range.

Table B.2: Share of forecast error variance explained by the FX shock: target 6–32 quarter periodicities

| | Forecast Horizon (Quarter) | | | | | |
|----------------------------|----------------------------|------|------|------|------|------|
| | Q1 | Q4 | Q12 | Q24 | Q40 | Q100 |
| Home TFP | 0.02 | 0.03 | 0.13 | 0.18 | 0.21 | 0.21 |
| Home Consumption | 0.07 | 0.10 | 0.22 | 0.35 | 0.32 | 0.24 |
| Foreign Consumption | 0.01 | 0.01 | 0.05 | 0.22 | 0.27 | 0.18 |
| Home Investment | 0.11 | 0.17 | 0.15 | 0.19 | 0.20 | 0.21 |
| Foreign Investment | 0.01 | 0.02 | 0.05 | 0.13 | 0.22 | 0.18 |
| Interest Rate Differential | 0.28 | 0.22 | 0.21 | 0.24 | 0.24 | 0.23 |
| Real Exchange Rate | 0.89 | 0.93 | 0.73 | 0.58 | 0.55 | 0.50 |
| Expected Excess Returns | 0.32 | 0.20 | 0.41 | 0.43 | 0.42 | 0.41 |

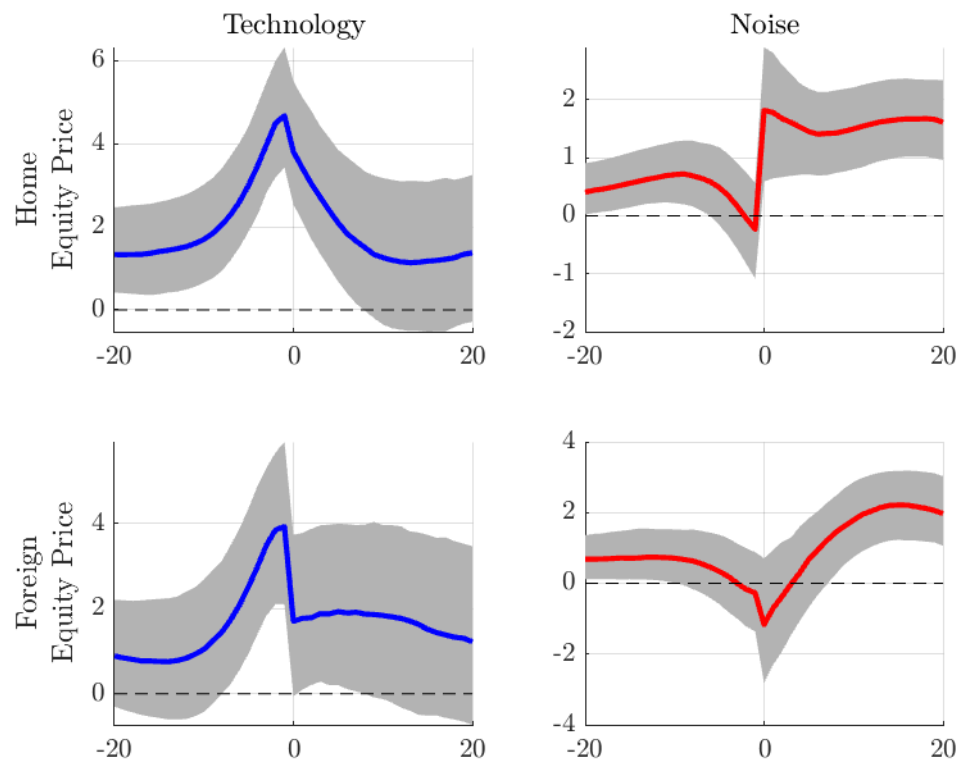
Notes: The table reports the estimated variance shares at different horizons accounted for by the exchange rate shock that explains most of the forecast error variance of the exchange rate over the [6,32] quarter periodicity range.

Figure B.1: Technology, Noise and the Trade Balance



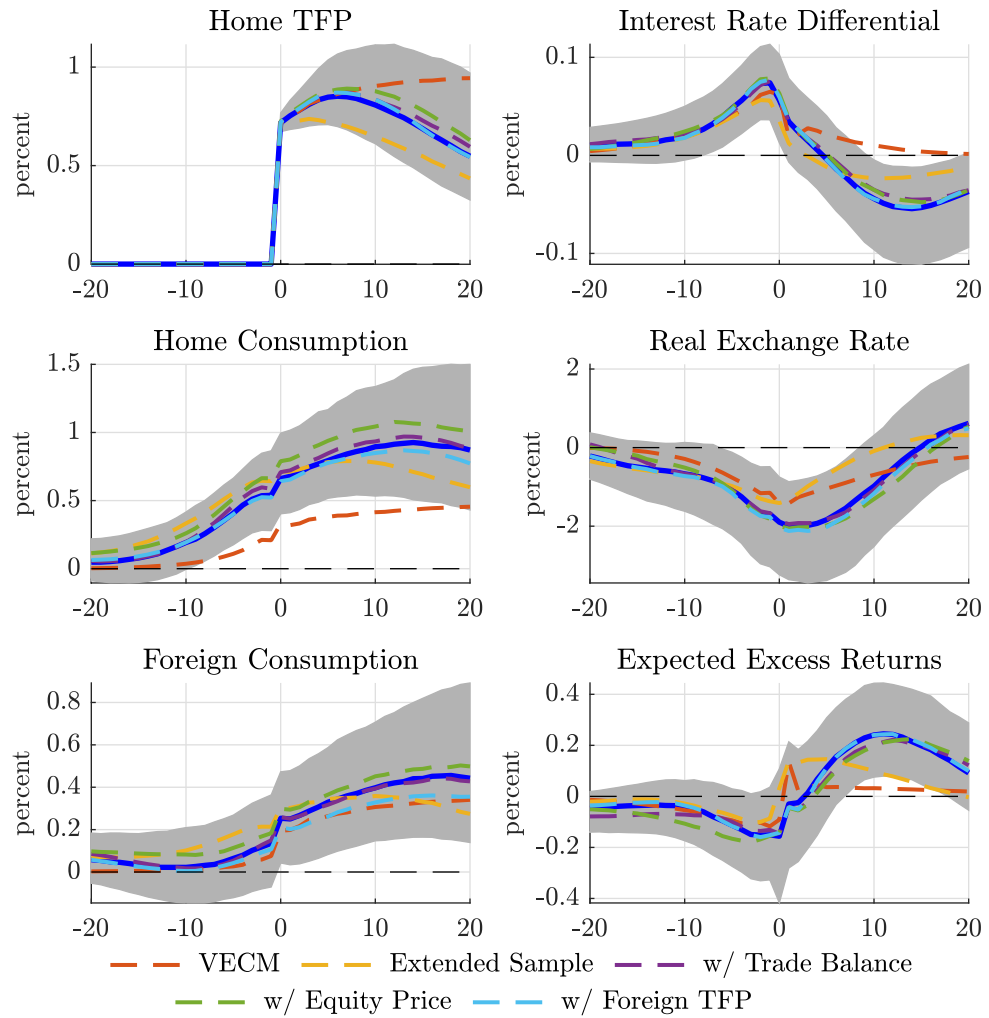
Notes: The figure displays the responses to a one standard deviation impulse in the technological disturbance (left column) and the expectational disturbance (right column) at time $t = 0$. The shaded areas are 16–84th percentile bands. Each period is a quarter. The trade balance data refer to the US trade balance in goods with the other G7 countries and are obtained from the International Monetary Fund, International Trade in Goods (by partner country), available at <https://data.imf.org/en/datasets/IMF.STA:IMTS>. The responses are computed by cumulating the estimated responses of the change in the trade balance starting from period $t = -20$.

Figure B.2: Technology, noise, and equity prices



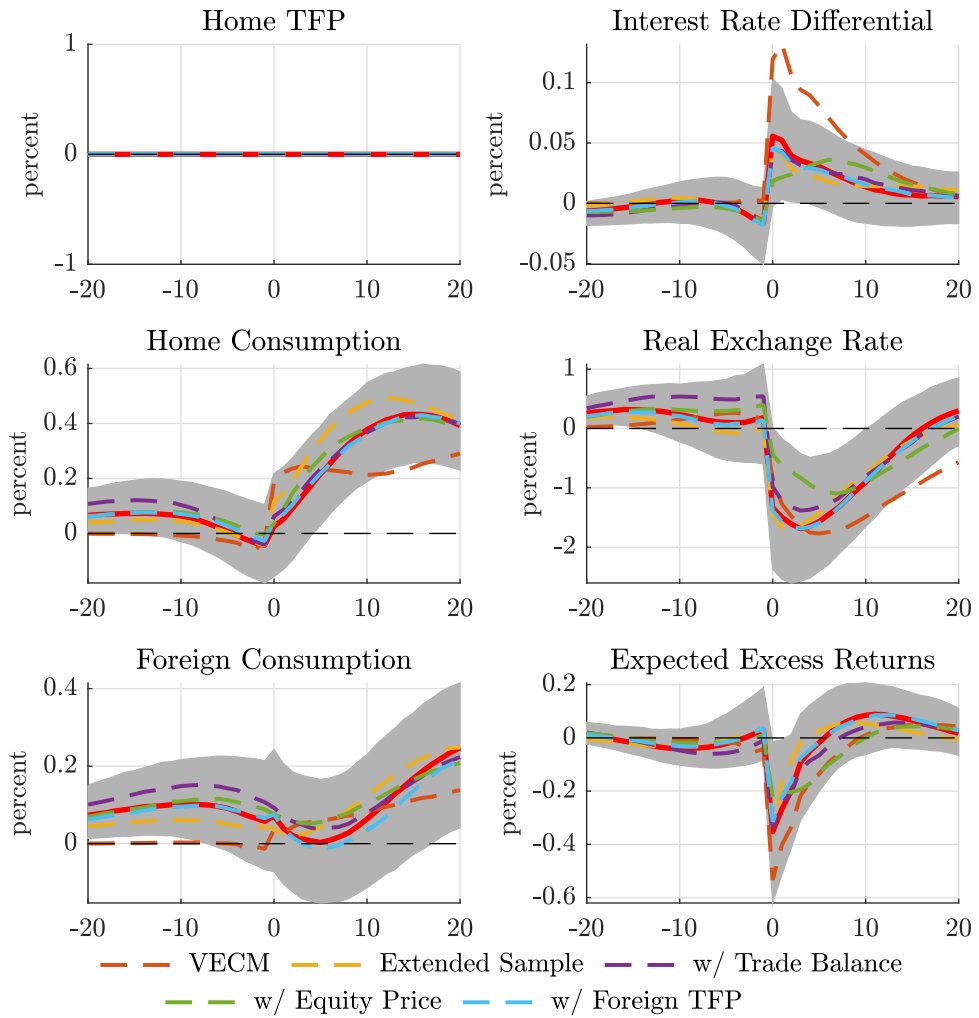
Notes: The figure displays the IRF a one standard deviation impulse in the technological disturbance (left column) and the expectational disturbance (right column) at time $t = 0$. The shaded area is the 16–84th. Each period is a quarter.

Figure B.3: Impulse responses to Technology disturbances (Alternative specifications)



Notes: The figure displays IRFs to a one standard deviation impulse in the technological disturbance at time $t = 0$ for the baseline sample (blue lines), where the shaded areas are 16–84th percentile bands. In addition the figure displays the point estimate of the responses obtained from the VAR applied to the extended sample (1978:Q4–2018:Q4) and from a VECM where the real exchange rate and interest rate differential are assumed stationary. The figure also displays the point estimate of the responses obtained from the baseline VAR with one additional variable. Each period is a quarter.

Figure B.4: Impulse responses to Noise disturbance (Alternative specifications)



Notes: The figure displays IRFs to a one standard deviation impulse in the expectational disturbance at time $t = 0$ for the baseline sample (blue lines), where the shaded areas are 16–84th percentile bands. In addition the figure displays the point estimate of the responses obtained from the VAR applied to the extended sample (1978:Q4–2018:Q4) and from a VECM where the real exchange rate and interest rate differential are assumed stationary. The figure also displays the point estimate of the responses obtained from the baseline VAR with one additional variable. Each period is a quarter.

Table B.3: Share of variance explained by the Main FX shock (Alternative specifications)

Panel A: Extended sample (1978:Q4-2018:Q4)

| | Forecast Horizon (Quarter) | | | | | |
|----------------------------|----------------------------|------|------|------|------|------|
| | Q1 | Q4 | Q12 | Q24 | Q40 | Q100 |
| Home TFP | 0.03 | 0.03 | 0.07 | 0.18 | 0.28 | 0.33 |
| Home Consumption | 0.04 | 0.07 | 0.26 | 0.45 | 0.48 | 0.43 |
| Foreign Consumption | 0.01 | 0.02 | 0.04 | 0.18 | 0.30 | 0.31 |
| Home Investment | 0.20 | 0.25 | 0.32 | 0.38 | 0.39 | 0.38 |
| Foreign Investment | 0.03 | 0.03 | 0.05 | 0.12 | 0.22 | 0.24 |
| Interest Rate Differential | 0.41 | 0.39 | 0.31 | 0.30 | 0.30 | 0.31 |
| Real Exchange Rate | 0.59 | 0.74 | 0.83 | 0.74 | 0.70 | 0.67 |
| Expected Excess Returns | 0.56 | 0.29 | 0.30 | 0.36 | 0.36 | 0.37 |

Panel B: Vector Error Correction Model

| | Forecast Horizon (Quarter) | | | | | |
|----------------------------|----------------------------|------|------|------|------|------|
| | Q1 | Q4 | Q12 | Q24 | Q40 | Q100 |
| Home TFP | 0.01 | 0.01 | 0.05 | 0.10 | 0.13 | 0.15 |
| Home Consumption | 0.09 | 0.13 | 0.25 | 0.41 | 0.50 | 0.58 |
| Foreign Consumption | 0.02 | 0.02 | 0.04 | 0.10 | 0.16 | 0.20 |
| Home Investment | 0.09 | 0.15 | 0.14 | 0.14 | 0.15 | 0.18 |
| Foreign Investment | 0.02 | 0.02 | 0.03 | 0.06 | 0.07 | 0.09 |
| Interest Rate Differential | 0.49 | 0.52 | 0.45 | 0.44 | 0.44 | 0.45 |
| Real Exchange Rate | 0.72 | 0.87 | 0.92 | 0.90 | 0.90 | 0.90 |
| Expected Excess Returns | 0.55 | 0.40 | 0.39 | 0.43 | 0.44 | 0.44 |

Panel C: Individual countries (Median)

| | Forecast Horizon (Quarter) | | | | | |
|----------------------------|----------------------------|------|------|------|------|------|
| | Q1 | Q4 | Q12 | Q24 | Q40 | Q100 |
| Home TFP | 0.03 | 0.06 | 0.11 | 0.26 | 0.44 | 0.45 |
| Home Consumption | 0.03 | 0.05 | 0.16 | 0.34 | 0.36 | 0.40 |
| Foreign Consumption | 0.04 | 0.04 | 0.15 | 0.20 | 0.38 | 0.38 |
| Home Investment | 0.02 | 0.04 | 0.20 | 0.34 | 0.34 | 0.36 |
| Foreign Investment | 0.05 | 0.05 | 0.10 | 0.19 | 0.32 | 0.37 |
| Interest Rate Differential | 0.08 | 0.07 | 0.11 | 0.22 | 0.26 | 0.32 |
| Real Exchange Rate | 0.27 | 0.42 | 0.68 | 0.80 | 0.76 | 0.72 |
| Expected Excess Returns | 0.21 | 0.18 | 0.29 | 0.32 | 0.39 | 0.43 |

Notes: The table reports the estimated variance shares accounted for by the main exchange rate shock at different horizons.

Table B.4: Variance decomposition (Alternative specifications)

Panel A: Extended sample 1978:Q4-2018:Q4

| | Periodicities of 2–100 Quarters | | | Periodicities of 6–32 Quarters | | |
|----------------------------|---------------------------------|-------|-------|--------------------------------|-------|-------|
| | Both | Tech. | Noise | Both | Tech. | Noise |
| Home TFP | 1.00 | 1.00 | 0.00 | 1.00 | 1.00 | 0.00 |
| Home Consumption | 0.67 | 0.42 | 0.25 | 0.33 | 0.07 | 0.26 |
| Foreign Consumption | 0.47 | 0.32 | 0.15 | 0.18 | 0.07 | 0.12 |
| Home Investment | 0.56 | 0.34 | 0.21 | 0.27 | 0.09 | 0.19 |
| Foreign Investment | 0.50 | 0.25 | 0.25 | 0.35 | 0.08 | 0.27 |
| Interest Rate Differential | 0.41 | 0.28 | 0.13 | 0.30 | 0.18 | 0.11 |
| Real Exchange Rate | 0.48 | 0.26 | 0.22 | 0.29 | 0.08 | 0.20 |
| Expected Excess Returns | 0.38 | 0.22 | 0.16 | 0.32 | 0.16 | 0.16 |

Panel B: Vector Error Correction Model

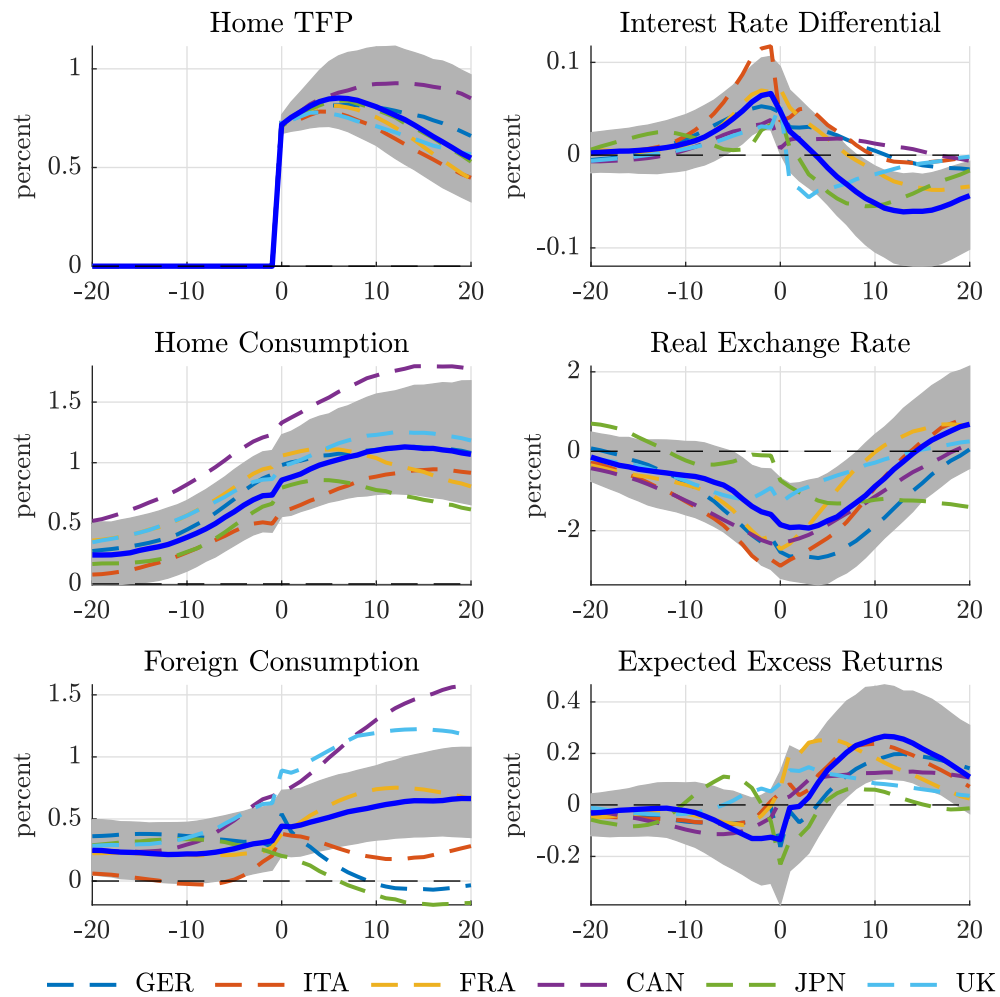
| | Periodicities of 2–100 Quarters | | | Periodicities of 6–32 Quarters | | |
|----------------------------|---------------------------------|-------|-------|--------------------------------|-------|-------|
| | Both | Tech. | Noise | Both | Tech. | Noise |
| Home TFP | 1.00 | 1.00 | 0.00 | 1.00 | 1.00 | 0.00 |
| Home Consumption | 0.28 | 0.12 | 0.16 | 0.25 | 0.05 | 0.20 |
| Foreign Consumption | 0.24 | 0.16 | 0.09 | 0.15 | 0.08 | 0.07 |
| Home Investment | 0.29 | 0.08 | 0.22 | 0.40 | 0.06 | 0.34 |
| Foreign Investment | 0.22 | 0.08 | 0.14 | 0.16 | 0.04 | 0.12 |
| Interest Rate Differential | 0.66 | 0.15 | 0.51 | 0.62 | 0.09 | 0.53 |
| Real Exchange Rate | 0.49 | 0.14 | 0.35 | 0.33 | 0.06 | 0.27 |
| Expected Excess Returns | 0.49 | 0.13 | 0.36 | 0.47 | 0.09 | 0.38 |

Panel C: Individual countries (Median)

| | Periodicities of 2–100 Quarters | | | Periodicities of 6–32 Quarters | | |
|----------------------------|---------------------------------|-------|-------|--------------------------------|-------|-------|
| | Both | Tech. | Noise | Both | Tech. | Noise |
| Home TFP | 1.00 | 1.00 | 0.00 | 1.00 | 1.00 | 0.00 |
| Home Consumption | 0.69 | 0.515 | 0.17 | 0.34 | 0.095 | 0.24 |
| Foreign Consumption | 0.54 | 0.41 | 0.12 | 0.29 | 0.12 | 0.145 |
| Home Investment | 0.62 | 0.455 | 0.16 | 0.375 | 0.2 | 0.18 |
| Foreign Investment | 0.56 | 0.43 | 0.145 | 0.355 | 0.105 | 0.205 |
| Interest Rate Differential | 0.395 | 0.27 | 0.125 | 0.245 | 0.11 | 0.13 |
| Real Exchange Rate | 0.59 | 0.395 | 0.195 | 0.37 | 0.11 | 0.245 |
| Expected Excess Returns | 0.415 | 0.25 | 0.145 | 0.31 | 0.13 | 0.18 |

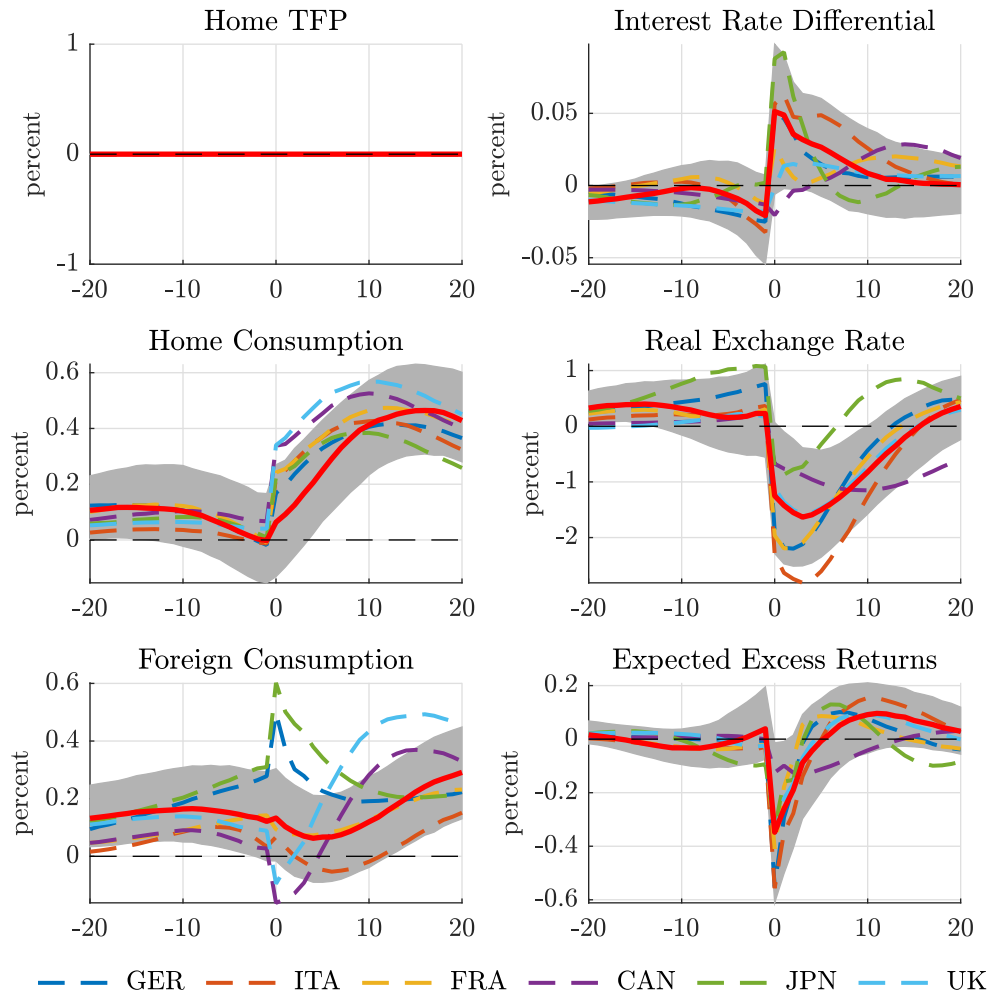
Notes: The table reports the estimated variance shares (at periodicities between 2 and 100 quarters and between 6 and 32 quarters) explained by technological disturbances (“Tech.”), expectational disturbances (“Noise”), and the combination of both.

Figure B.5: Impulse responses to Technology disturbances (Individual countries)



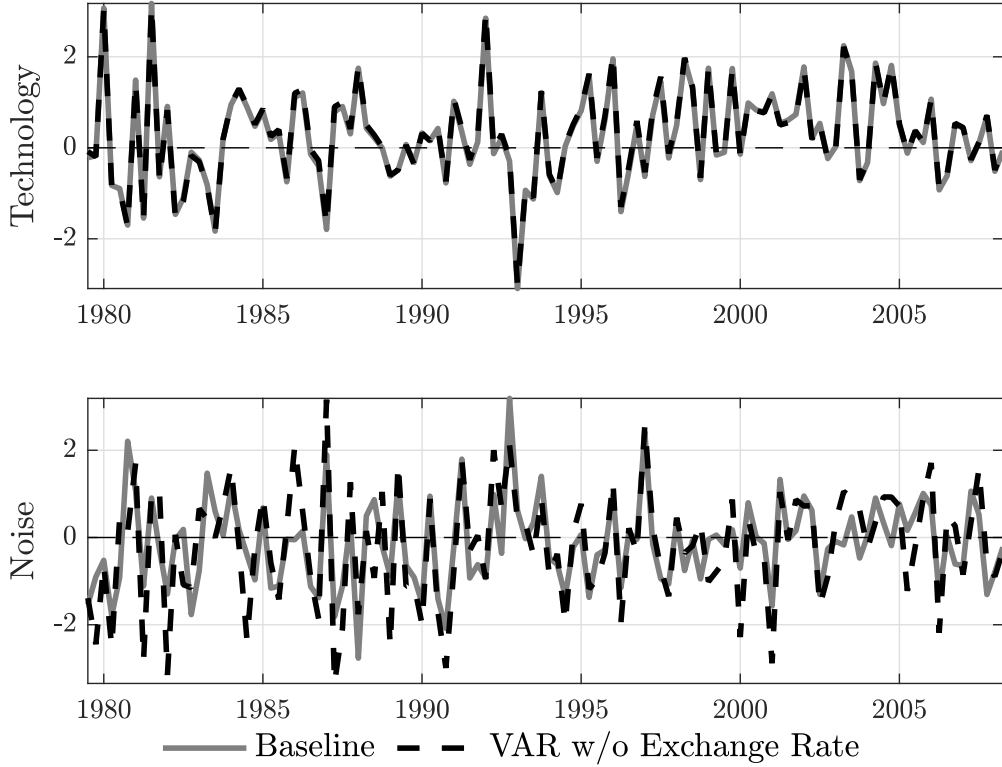
Notes: The figure displays IRFs to a one standard deviation impulse in the technological disturbance at time $t = 0$ for the baseline sample (blue lines), where the shaded areas are 16–84th percentile bands. In addition the figure displays the point estimate of the responses obtained from six different bilateral VARs. Each period is a quarter.

Figure B.6: Impulse responses to Noise disturbance (Individual countries)



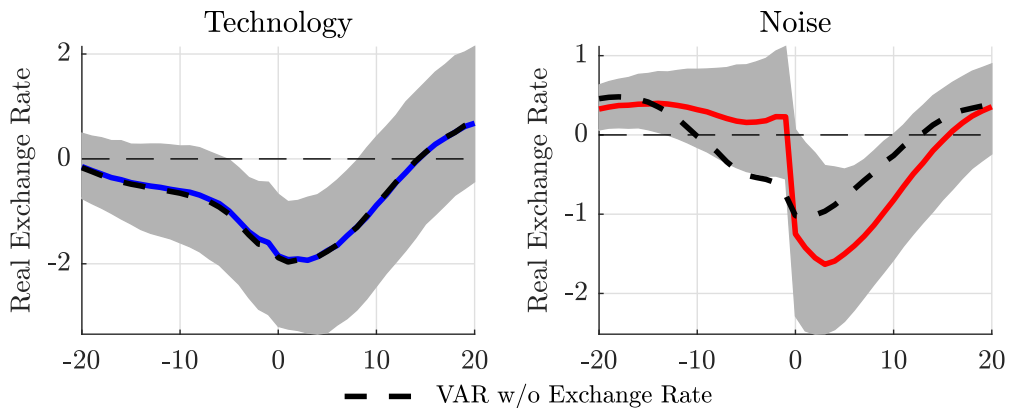
Notes: The figure displays IRFs to a one standard deviation impulse in the expectational disturbance at time $t = 0$ for the baseline sample (red lines), where the shaded areas are 16–84th percentile bands. In addition the figure displays the point estimate of the responses obtained from six different bilateral VARs. Each period is a quarter.

Figure B.7: Series of estimated technology and noise disturbances



Notes: The figure displays the series of technology and noise disturbances estimated by the baseline VAR as well as the VAR without the exchange rate (see Appendix B.4).

Figure B.8: The exchange rate response to technology and noise disturbances



Notes: The figure displays the IRF of the real exchange rate a one standard deviation impulse in the technological disturbance (left column) and the expectational disturbance (right column) at time $t = 0$. The dashed black line is the exchange rate response when the disturbances are estimated using a VAR without the exchange rate (see Appendix B.4). The shaded area is the 16–84th. Each period is a quarter.

Table B.5: Granger causality: exchange rates and TFP

Panel A: P-values testing whether exchange rates Granger-cause TFP

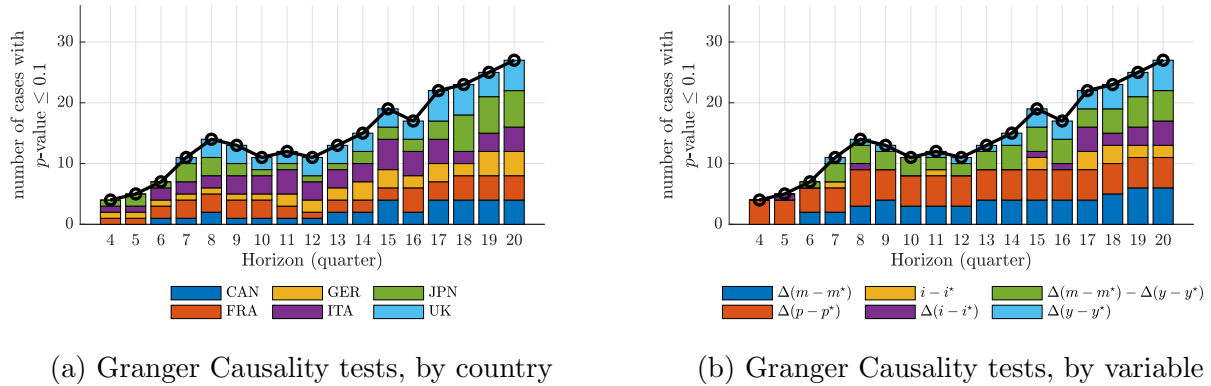
| h | Canada | France | Germany | Italy | Japan | UK | Aggregate |
|-----|--------|---------|---------|---------|---------|---------|-----------|
| 1 | 0.92 | 0.78 | 0.61 | 0.97 | 0.65 | 0.64 | 0.95 |
| 2 | 0.11 | 0.86 | 0.57 | 0.67 | 0.80 | 0.80 | 0.99 |
| 3 | 0.20 | 0.04** | 0.09* | 0.00*** | 0.17 | 0.00*** | 0.09* |
| 4 | 0.17 | 0.05** | 0.10* | 0.02** | 0.09* | 0.04** | 0.21 |
| 5 | 0.11 | 0.00*** | 0.00*** | 0.03** | 0.00*** | 0.04** | 0.00*** |

Panel B: P-values testing whether TFP Granger-cause exchange rates

| h | Canada | France | Germany | Italy | Japan | UK | Aggregate |
|-----|---------|--------|---------|-------|-------|------|-----------|
| 1 | 0.67 | 0.76 | 0.82 | 0.89 | 0.99 | 0.96 | 0.90 |
| 2 | 0.39 | 0.80 | 0.76 | 0.63 | 0.99 | 0.20 | 0.75 |
| 3 | 0.39 | 1.00 | 1.00 | 0.85 | 0.81 | 0.75 | 0.95 |
| 4 | 0.07* | 0.62 | 0.71 | 0.44 | 0.82 | 0.83 | 0.44 |
| 5 | 0.00*** | 0.83 | 0.88 | 0.49 | 0.70 | 0.97 | 0.76 |

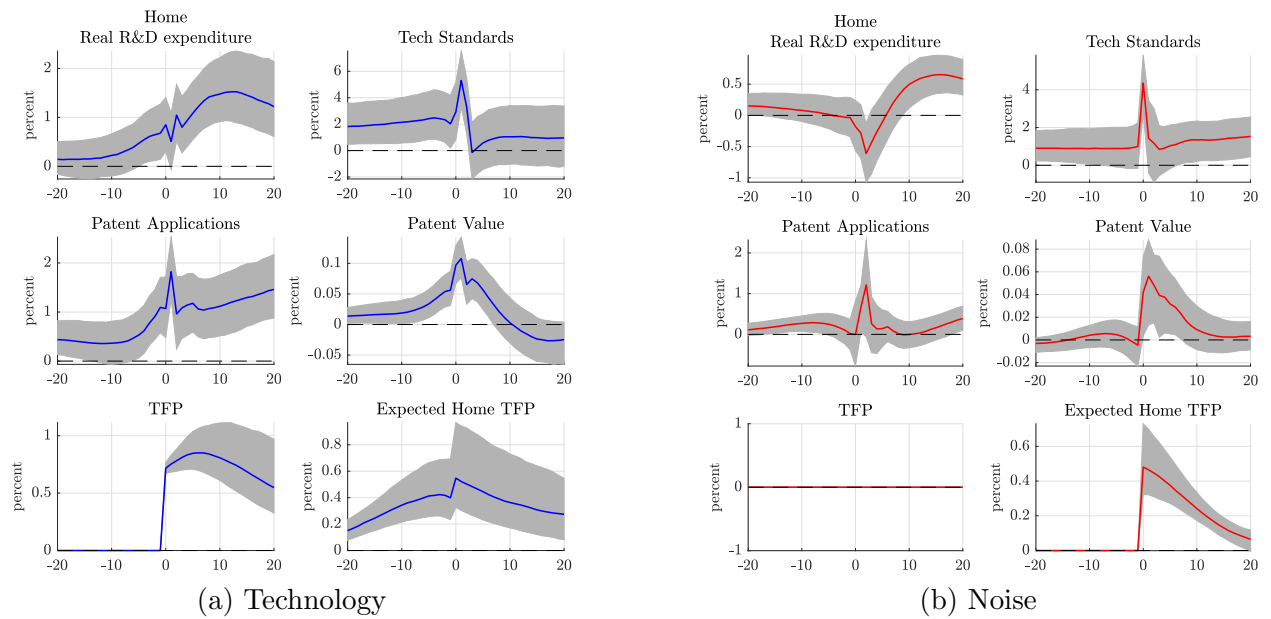
Notes: P-values from a Wald test of Granger causality as in Sims (1972). The test is based on the equation: $x_t = \alpha + \beta_0 y_t + \sum_{k=1}^h \beta_{-k}^{\text{lag}} y_{t-k} + \sum_{k=1}^h \beta_k^{\text{lead}} y_{t+k} + \varepsilon_t$, where x is the quarterly observation of the annual change in the log of the real exchange rate and y is the quarterly observation of the annual change of the log of TFP in Panel A; variables are reversed in Panel B. The null hypothesis is that $\beta_k^{\text{lead}} = 0$ for all $k = 1, \dots, h$. The sample period is 1976:Q1–2008:Q2. Newey-West standard errors are computed using a data-driven bandwidth, a Bartlett kernel, and prewhitening.

Figure B.9: Bivariate Granger causality tests *á la* Engel and West (2005) (1976:Q1–2018:Q4)



Notes: For each horizon, we report the number of cases in which the p -value from a Wald test of Granger causality is below 0.1. There are 36 cases per horizon: 6 countries (each compared to the US) and 6 macroeconomic fundamentals, following the data and methodology of Engel and West (2005). Each test is based on a bivariate VAR estimated using the quarterly change in the nominal exchange rate, Δs , and one fundamental variable, f . The horizon on the x -axis indicates the number of lags included in the VAR. The reported p -value corresponds to a Wald test of the joint significance of the lags of Δs in predicting f . The variables are defined as follows: Δm is the percentage change in M1 (M2 for the United Kingdom); Δy is the percentage change in real GDP; Δp is the percentage change in consumer prices; and i is the short-term government interest rate. Newey-West standard errors are computed using a data-driven bandwidth, a Bartlett kernel, and prewhitening. Panel (a) highlights the case in which p -value from the Wald test of Granger causality is below 0.1, *by country*, while Panel (b) highlights the corresponding cases *by variable*.

Figure B.10: Responses of technology proxy series to technological and noise disturbances



B.3 Performance of a VAR-based trading strategy

We construct trading strategies that exploit the predictable component of excess returns associated with the identified disturbances. Specifically, we consider a simple strategy in which a US investor takes a position in foreign currency proportional to the VAR-implied expectation of foreign excess return. The portfolio return from this strategy is given by the product of realized and expected excess foreign-currency returns, $\lambda_{t+1}\mathbb{E}_t(\lambda_{t+1})$. Note that $\mathbb{E}_t(\lambda_{t+1})$ can be negative, in which case the investor takes a long position in the dollar and a short position in the basket of foreign currencies. We estimate expected returns using a rolling window of N quarters, with an investment horizon of one quarter. After each quarter, the investor observes the new data and updates expectations accordingly.

Specifically, for each t we re-estimate the VAR on the rolling window of $t - N + 1 : t$, identify the disturbances, and form the prediction $\mathbb{E}_t(\lambda_{t+1})$. Then, we evaluate the resulting trading return $\lambda_{t+1}\mathbb{E}_t(\lambda_{t+1})$. The exercise constitutes a valid out-of-sample analysis that can be implemented by investors using variables dated until the beginning of the investment period.²³

Table B.6: Sharpe ratios and returns of VAR-based trading strategy

| Window (quarter) | Sharpe ratio | Portfolio return |
|------------------|--------------|------------------|
| 60 | 0.26 | 1.96 |
| 64 | -0.21 | -1.62 |
| 68 | -0.34 | -2.16 |
| 72 | 0.04 | 0.36 |
| 76 | 0.37 | 3.50 |
| 80 | 0.44 | 4.97 |
| 84 | 0.64 | 6.62 |
| 88 | 0.80 | 8.12 |
| 92 | 0.91 | 9.61 |
| 96 | 0.87 | 8.92 |
| 100 | 0.60 | 5.16 |

Notes: The table reports the annualized Sharpe ratios and corresponding portfolio returns for different estimation window lengths when conditioning on the two disturbances. The Sharpe ratios are estimated from the median expected excess returns from 1000 VAR parameter draws in each sampled window. Since the baseline dataset contains 119 quarterly observations, this procedure yields $119 - N$ observations of portfolio returns, where N is the length of the rolling window.

Table B.6 reports the annualized Sharpe ratios and corresponding portfolio returns for different estimation window lengths when conditioning on the two disturbances.

Our preferred specification uses a rolling window length of 80 quarters, a choice we justify below. In this case, the annualized Sharpe ratio is 0.44 when conditioning on the two

²³This procedure is equivalent to conditioning on both current and past values of TFP as well as on expected future TFP (five years ahead), all of which belong to investors' information set at time t .

disturbances. The magnitude of the Sharpe ratio is broadly comparable to those obtained from alternative trading strategies in the currency market that exploit related, but distinct, time variation in return predictability, such as the “Dollar trade” (Lustig et al., 2014; Hassan and Mano, 2019), and momentum strategies (Burnside et al., 2011; Menkhoff et al., 2012; Moskowitz et al., 2012).

Table B.6 also reports results for alternative window lengths (ranging from 60 to 100 quarters). With very short windows, the Sharpe ratios are small, reflecting the limited degrees of freedom adopted in the estimation of the VAR parameters. The Sharpe ratios are bigger for longer window sizes, but the number of forecast observations decreases, leading to uncertainty around the Sharpe ratio estimates. Thus, we consider a rolling window length of 80 quarters to be an appropriate choice.

B.4 Estimation of VAR without exchange rate

Let $y_t \in \mathbb{R}^n$ follow a stable VAR(p)

$$y_t = \sum_{\ell=1}^p B_\ell y_{t-\ell} + u_t, \quad \mathbb{E}[u_t u_t'] = \Sigma, \quad (\text{B.7})$$

with MA (reduced-form) transfer

$$\Psi(z) \equiv \left(I_n - B_1 z - \cdots - B_p z^p \right)^{-1}, \quad y(z) = \Psi(z) u(z), \quad (\text{B.8})$$

and spectral density

$$f_y(\lambda) = \frac{1}{2\pi} \Psi(e^{-i\lambda}) \Sigma \Psi(e^{-i\lambda})^*. \quad (\text{B.9})$$

Subset and selection matrices Partition variables into the kept subset S of size k and the excluded block Z of size $m = n - k$. Let $P_S \in \{0, 1\}^{k \times n}$ select S so that $y_t^S = P_S y_t$, and $P_Z \in \{0, 1\}^{m \times n}$ selects Z . We will use the block-partitions

$$\Psi(z) = \begin{bmatrix} \Psi_{SS}(z) & \Psi_{SZ}(z) \\ \Psi_{ZS}(z) & \Psi_{ZZ}(z) \end{bmatrix}, \quad f_y(\lambda) = \begin{bmatrix} f_{SS} & f_{SZ} \\ f_{ZS} & f_{ZZ} \end{bmatrix}.$$

Step 1. Implied restricted VAR on the subset S

Population autocovariances of y_t from the unrestricted VAR Form the companion state $x_t = [y'_t, y'_{t-1}, \dots, y'_{t-p+1}]'$, with transition $x_{t+1} = Fx_t + Gu_{t+1}$,

$$F = \begin{bmatrix} B_1 & B_2 & \cdots & B_{p-1} & B_p \\ I_n & 0 & \cdots & 0 & 0 \\ \ddots & \ddots & & \vdots & \vdots \\ 0 & \cdots & I_n & 0 & 0 \end{bmatrix}, \quad G = \begin{bmatrix} I_n \\ 0 \\ \vdots \\ 0 \end{bmatrix}.$$

Let $Q = G \Sigma G'$ and solve the discrete Lyapunov

$$\Sigma_x = F \Sigma_x F' + Q. \quad (\text{B.10})$$

Then for $\tau \geq 0$,

$$\Gamma(\tau) \equiv \text{Cov}(y_t, y_{t-\tau}) = J F^\tau \Sigma_x J', \quad J = \begin{bmatrix} I_n & 0 & \cdots & 0 \end{bmatrix}. \quad (\text{B.11})$$

Extract the subset autocovariances $\Gamma_S(\tau) = P_S \Gamma(\tau) P_S'$ for $\tau = 0, 1, \dots, p$.

Block Yule–Walker projection (best linear VAR(p) for y_t^S) Let

$$\Gamma_{S,p} = \begin{bmatrix} \Gamma_S(0) & \Gamma_S(1)' & \cdots & \Gamma_S(p-1)' \\ \Gamma_S(1) & \Gamma_S(0) & \cdots & \Gamma_S(p-2)' \\ \vdots & \vdots & \ddots & \vdots \\ \Gamma_S(p-1) & \Gamma_S(p-2) & \cdots & \Gamma_S(0) \end{bmatrix} \in \mathbb{R}^{kp \times kp}, \quad G_p = [\Gamma_S(1) \cdots \Gamma_S(p)] \in \mathbb{R}^{k \times kp}.$$

Then the population OLS/Yule–Walker coefficients are

$$[\tilde{B}_1 \cdots \tilde{B}_p] = G_p \Gamma_{S,p}^{-1} \in \mathbb{R}^{k \times kp}, \quad (\text{B.12})$$

and the implied restricted reduced-form covariance

$$\tilde{\Sigma} = \Gamma_S(0) - \sum_{\ell=1}^p \tilde{B}_\ell \Gamma_S(\ell)' = \Gamma_S(0) - [\tilde{B}_1 \cdots \tilde{B}_p] [\Gamma_S(1)'; \dots; \Gamma_S(p)']. \quad (\text{B.13})$$

Equations (B.12)–(B.13) define the *implied* restricted VAR(p) for y_t^S :

$$y_t^S = \sum_{\ell=1}^p \tilde{B}_\ell y_{t-\ell}^S + \tilde{u}_t, \quad \mathbb{E}[\tilde{u}_t \tilde{u}_t'] = \tilde{\Sigma}. \quad (\text{B.14})$$

With the restricted transfer and spectral density:

$$\tilde{\Psi}(z) \equiv (I_k - \tilde{B}_1 z - \cdots - \tilde{B}_p z^p)^{-1}, \quad f_S(\lambda) = \frac{1}{2\pi} \tilde{\Psi}(e^{-i\lambda}) \tilde{\Sigma} \tilde{\Psi}(e^{-i\lambda})^*. \quad (\text{B.15})$$

Step 2. Estimate Impulse Response Functions

We use our identification procedure to identify the impulse responses of the subset of $k \leq n$ variables, so that

$$\epsilon(\lambda) = \psi_S(\lambda) Y_S(\lambda) \quad (\text{B.16})$$

where $Y_S(\lambda) = P_S Y(\lambda)$. Thus,

$$\epsilon(\lambda) = \psi_S(\lambda) P_S Y(\lambda) \quad (\text{B.17})$$

The impulse response of all variables is the inverse Fourier transform of

$$T(\lambda) = \frac{S_{y,\epsilon}(\lambda)}{S_\epsilon(\lambda)} = \frac{E(Y(\lambda) Y(\lambda)^* P_S' \psi_S(\lambda)^*)}{S_\epsilon(\lambda)} = \frac{f_y(\lambda) P_S' \psi_S(\lambda)^*}{S_\epsilon(\lambda)} \quad (\text{B.18})$$

Note that when $k = n$, *i.e.*, we don't drop any variable from the VAR, then P_S is an identity matrix and we are back to the full VAR identification.

C Model Appendix

C.1 Environments

We study different classes of two-country endowment economies. We begin by outlining the preferences and technology, and then characterize the equilibria under complete and incomplete markets.

Utility function Let C_t denote consumption of the home country. The home-country preferences over an infinite horizon are:

$$U_t = \left[(1 - \beta) \cdot C_t^{1-1/\psi} + \beta \mathbb{E}_t \left[U_{t+1}^{1-\gamma} \right]^{\frac{1-1/\psi}{1-\gamma}} \right]^{\frac{1}{1-1/\psi}}. \quad (\text{C.1})$$

With these preferences, agents are risk averse in future utility as well as future consumption. The extent of such utility risk aversion depends on the preference for early resolution of uncertainty, measured by $\gamma - 1/\psi > 0$.

When $\gamma = 1/\psi$, the agent is utility-risk neutral and preferences collapse to the standard time-additive, constant relative risk aversion (CRRA) case. When the agent prefers early resolution of uncertainty, that is, $\gamma > 1/\psi$, uncertainty about continuation utility reduces welfare and generates an incentive to trade off future expected utility, $\mathbb{E}_t[V_{t+1}]$, for future utility risk, $\text{var}_t[V_{t+1}]$. This trade-off drives international consumption flows—a key element of Colacito and Croce (2011; 2013).²⁴ The utility of foreign households is symmetric.

Technology Let $\{X_t, Y_t\}$ and $\{X_t^*, Y_t^*\}$ denote the time t consumption of goods X and Y in the home and foreign countries, respectively. The consumption aggregates in the two countries are

$$C_t = \left((\varsigma)^{\frac{1}{\sigma}} (X_t)^{\frac{\sigma-1}{\sigma}} + (1 - \varsigma)^{\frac{1}{\sigma}} (Y_t)^{\frac{\sigma-1}{\sigma}} \right)^{\frac{\sigma}{\sigma-1}}, \quad C_t^* = \left((1 - \varsigma)^{\frac{1}{\sigma}} (X_t^*)^{\frac{\sigma-1}{\sigma}} + (\varsigma)^{\frac{1}{\sigma}} (Y_t^*)^{\frac{\sigma-1}{\sigma}} \right)^{\frac{\sigma}{\sigma-1}} \quad (\text{C.2})$$

The home (foreign) country produces good X (Y) so that $\varsigma > 1/2$ introduces consumption home bias, while $\sigma > 1$ represents the elasticity of substitution.

In this endowment economy, the following resource constraints apply:

$$A_t \geq X_t + X_t^* \quad (\text{C.3})$$

$$A_t^* \geq Y_t + Y_t^* \quad (\text{C.4})$$

²⁴When $\psi = 1$, preferences take the following form:

$$V_t = (1 - \beta) \cdot \log C_t + \frac{\beta}{1 - \gamma} \log \mathbb{E}_t [\exp \{V_{t+1} \cdot (1 - \gamma)\}]. \quad (9)$$

When $\psi = 1$, if $\log V_t$ is normally distributed, equation (7) has the following exact counterpart:

$$V_t = (1 - \beta) \cdot \log C_t + \beta \mathbb{E}_t[V_{t+1}] - \frac{(\gamma - 1)}{2} \beta \text{var}_t[V_{t+1}].$$

where A_t and A_t^* are the exogenous stochastic TFP processes that follow eq. (C.40).

C.1.1 Complete Markets

To find the solution under complete markets, we follow Colacito et al. (2018) and solve the Pareto problem. We solve the Pareto problem under the general utility function (C.1).

Pareto Problem This appendix suppresses notation denoting state and histories and retain only subscripts for time. We represent the Epstein and Zin (1989) utility preference in the following compact way:

$$U_t = W(C_t, U_{t+1}),$$

so that the dependence of current utility on j -step-ahead consumption can be denoted as:

$$\frac{\partial U_t}{\partial C_{t+j}} = W_{2,t+1} \cdot W_{2,t+2} \cdots W_{2,t+j} \cdot W_{1,t+j}, \quad (\text{C.5})$$

where $W_{2,t+j} \equiv \frac{\partial U_{t+j-1}}{\partial U_{t+j}}$ and $W_{1,t+j} \equiv \frac{\partial U_{t+j}}{\partial C_{t+j}}$.

The stochastic discount factor in C units, M_{t+1} , is:

$$M_{t+1} = \beta \left(\frac{C_{t+1}}{C_t} \right)^{-\frac{1}{\psi}} \left(\frac{U_{t+1}}{\mathbb{E}_t[U_{t+1}^{1-\gamma}]^{\frac{1}{1-\gamma}}} \right)^{\frac{1}{\psi}-\gamma}. \quad (\text{C.6})$$

The consumption aggregate combines two goods, X and Y :

$$C_t = C(X_t, Y_t).$$

The planner faces the following constraints (C.3) and (C.4) where A_t and A_t^* are the exogenous stochastic productivity processes.

The social planner chooses sequences of $\{X_t, X_t^*, Y_t, Y_t^*\}_t$ to maximize:

$$\mu_0 W_0 + (1 - \mu_0) W_0^*,$$

subject to (C.3)-(C.4). Let $\lambda_{i,t}$ be the Lagrangian multiplier for the respective constraint i . The Lagrangian is:

$$\Omega = \mu_0 W_0 + (1 - \mu_0) W_0^* + \lambda_{1,t}(A_t - X_t - X_t^*) + \lambda_{2,t}(A_t^* - Y_t - Y_t^*) + \dots$$

The optimality condition for good X_t for all t is:

$$\mu_0 \left(\prod_{j=1}^t W_{2,j} \right) W_{1,t} C_{x,t} = \lambda_{1,t} = C_{x^*,t}^* W_{1,t}^* \left(\prod_{j=1}^t W_{2,j}^* \right) (1 - \mu_0). \quad (\text{C.7})$$

Let μ_t be the time- t Pareto weight for the home country:

$$\mu_t = \mu_0 \left(\prod_{j=1}^t W_{2,j} \right) W_{1,t} C_t = \mu_{t-1} W_{2,t} \cdot \frac{W_{1,t}}{W_{1,t-1}} \cdot \frac{C_t}{C_{t-1}} = \mu_{t-1} M_t \cdot \frac{C_t}{C_{t-1}}.$$

Thus, equation (C.7) becomes:

$$S_t C_{x,t} \cdot \frac{1}{C_t} = C_{x^*,t}^* \cdot \frac{1}{C_t^*}.$$

where $S_t = \mu_t / \mu_t^*$. Similarly:

$$S_t C_{y,t} \cdot \frac{1}{C_t} = C_{y^*,t}^* \cdot \frac{1}{C_t^*}.$$

Real Exchange Rate and Real Interest Rates Under complete markets, the real exchange rate satisfies the Backus and Smith (1993) condition:

$$\frac{Q_{t+1}}{Q_t} = \frac{M_{t+1}^*}{M_{t+1}}$$

where the home stochastic discount factor, M_{t+1} , is reported in equation (C.6), and the foreign stochastic discount factor has an analogous structure.

The home and foreign risk-free rates are:

$$E_t(M_{t+1})R_t = 1; \quad E_t(M_{t+1}^*)R_t^* = 1.$$

C.1.2 Incomplete Markets

Under incomplete markets agents only trade one bond internationally. We first present the benchmark incomplete-market model, and then the extended model with endogenous demand composition.

Households Let C_t denote the consumption of the home country. A representative home household maximizes the discounted expected utility over consumption under CRRA preferences. The utility function is a special case of eq. (C.1) when $\psi = 1/\gamma$:

$$E_0 \sum_{t=0}^{\infty} \beta^t \left(\frac{C_t^{1-\gamma}}{1-\gamma} \right) \tag{C.8}$$

where γ represents the coefficient of relative risk aversion.

Home households allocate their within-period consumption expenditure $P_t C_t$ between home and foreign goods, defined by a constant elasticity of substitution (CES) aggregator featuring home bias in eq. (C.2). The households minimize expenditure, resulting in the

conventional constant elasticity demand schedules:

$$X_t = \varsigma \left(\frac{p_{X,t}}{P_t} \right)^{-\sigma} C_t, \quad Y_t = (1 - \varsigma) \left(\frac{p_{Y,t}}{P_t} \right)^{-\sigma} C_t,$$

The consumer price level is given by

$$P_t = [\varsigma p_{X,t}^{1-\sigma} + (1 - \varsigma) p_{Y,t}^{1-\sigma}]^{\frac{1}{1-\sigma}}.$$

where $p_{X,t}$ and $p_{Y,t}$ represent the home-currency prices of the home and foreign goods in the home market and P_t represents the home consumer price level.

The expenditure allocation of the foreign households is characterized by a symmetric demand system. In particular, the demand for home and foreign goods by foreign households is given by

$$Y_t^* = C_t^* \varsigma \left(\frac{p_{Y,t}^*}{P_t^*} \right)^{-\sigma}, \quad X_t^* = C_t^* (1 - \varsigma) \left(\frac{p_{X,t}^*}{P_t^*} \right)^{-\sigma},$$

and

$$P_t^* = [\varsigma p_{Y,t}^{*\,1-\sigma} + (1 - \varsigma) p_{X,t}^{*\,1-\sigma}]^{\frac{1}{1-\sigma}}.$$

where $p_{X,t}^*$ and $p_{Y,t}^*$ represent the foreign-currency prices of the home and foreign goods in the foreign market and P_t^* represents the foreign consumer price level.

The budget constraint for the home economy is:

$$\frac{B_{t+1}}{R_t} + \frac{Q_t B_{t+1}^*}{R_t^* \Phi(Q_t B_{t+1}^*)} = \frac{p_{X,t}}{P_t} A_t - \frac{p_{X,t}}{P_t} X_t - \frac{p_{Y,t}}{P_t} Y_t + B_t + Q_t B_t^* \quad (\text{C.9})$$

where B_{t+1} and B_{t+1}^* denote bonds denominated in the home and foreign consumption bundles, respectively; $\frac{p_{X,t}}{P_t}$ and $\frac{p_{Y,t}}{P_t}$ are the price of the domestic and imported bundles, all relative to its overall consumption bundle. The function $\Phi(\cdot)$ represents an additional cost from international borrowings. As common in the literature, we assume that higher foreign borrowing, that is lower B_{t+1}^* , implies higher cost from international borrowings, *i.e.* $\Phi'(\cdot) < 0$. Households take the overall cost of international borrowing as given. We further assume a zero steady-state intermediation cost by setting $\Phi(B^*) = 1$. Foreign households only trade foreign-good-denominated bonds, while home-good-denominated bonds are in zero net supply. That is, in reality only foreign-good-denominated bonds are traded in equilibrium. As a result, defining the intermediation costs over the foreign bonds only is sufficient to pin down the overall steady-state net foreign asset position.

The budget constraint for the foreign economy is:

$$-\frac{B_{t+1}^*}{R_t^*} = \frac{p_{Y,t}^*}{P_t^*} A_t^* - \frac{p_{X,t}^*}{P_t^*} X_t^* - \frac{p_{Y,t}^*}{P_t^*} Y_t - B_t^* + \Pi_t \quad (\text{C.10})$$

where Π_t are the intermediation profits, rebated lump-sum to the foreign household. $\frac{p_{Y,t}^*}{P_t^*}$ and $\frac{p_{X,t}^*}{P_t^*}$ are the price of the domestic and imported bundles, all relative to its overall consumption bundle.

The home household maximizes utility (C.8) subject to (C.9). The first order condition with respect to home and foreign bonds implies:

$$\beta E_t \left[\left(\frac{C_{t+1}}{C_t} \right)^{-\gamma} \right] R_t = 1; \quad (\text{C.11})$$

$$\beta E_t \left[\left(\frac{C_{t+1}}{C_t} \right)^{-\gamma} \frac{Q_{t+1}}{Q_t} \right] R_t^* \Phi(Q_t B_{t+1}^*) = 1. \quad (\text{C.12})$$

The foreign households' first-order condition for bonds is:

$$\beta E_t \left[\left(\frac{C_{t+1}^*}{C_t^*} \right)^{-\gamma} \right] R_t^* = 1. \quad (\text{C.13})$$

Combining equations (C.12) and (C.13):

$$E_t \left[\left(\frac{C_{t+1}}{C_t} \right)^{-\gamma} \frac{Q_{t+1}}{Q_t} \right] \Phi(Q_t B_{t+1}^*) = E_t \left[\left(\frac{C_{t+1}^*}{C_t^*} \right)^{-\gamma} \right]$$

The functional form of the interest rate premium is:

$$\Phi(Q_t B_{t+1}^*) = [1 + Q_t(B_{t+1}^* - B^*)]^{-\phi}$$

where $\phi > 0$. Under this specification, expected excess currency returns depend on the level of external borrowing, akin to the mechanisms highlighted in models of segmented international asset markets (Gabaix and Maggiori, 2015; Itskhoki and Mukhin, 2021; Kekre and Lenel, 2024). Last, the law of one price holds.

Solution We solve the model by taking a log-linear approximation of the equilibrium conditions around a symmetric steady state, where $A = A^*$, and a zero steady-state net foreign asset position $B^* = 0$, and thus $Q = 1$.

Log-linear equilibrium system We characterize the log-linear equilibrium system for the benchmark incomplete-market model as follows. The equilibrium system has 11 endogenous variables $(c_t, c_t^*, x_t, y_t, x_t^*, y_t^*, r_t, r_t^*, q_t, \text{tot}_t, b_{t+1}^*)$ with 11 equilibrium conditions:

$$c_t = \varsigma x_t + (1 - \varsigma) y_t; \quad (\text{C.14})$$

$$c_t^* = \varsigma y_t^* + (1 - \varsigma) x_t^*; \quad (\text{C.15})$$

$$E_t(c_{t+1}) = c_t + \frac{1}{\gamma} r_t; \quad (\text{C.16})$$

$$E_t(c_{t+1}^*) = c_t^* + \frac{1}{\gamma} r_t^*; \quad (\text{C.17})$$

$$E_t(q_{t+1}) - q_t = r_t - r_t^* + \phi b_{t+1}^*; \quad (\text{C.18})$$

$$\beta b_{t+1}^* - b_t^* = a_t - \varsigma x_t - (1 - \varsigma) y_t - (1 - \varsigma)(tot_t); \quad (\text{C.19})$$

$$a_t = \varsigma x_t + (1 - \varsigma)x_t^*; \quad (\text{C.20})$$

$$a_t^* = (1 - \varsigma)y_t + \varsigma y_t^*; \quad (\text{C.21})$$

$$q_t = (2\varsigma - 1)(tot_t); \quad (\text{C.22})$$

$$x_t - y_t^* = (c_t - c_t^*) + 2\sigma(1 - \varsigma)(tot_t); \quad (\text{C.23})$$

$$y_t - x_t^* = (c_t - c_t^*) - 2\sigma\varsigma(tot_t). \quad (\text{C.24})$$

Incomplete Markets with Endogenous Demand Composition The CES aggregator (C.2) in the extended model reads:

$$C_t = \left((\varsigma_t)^{\frac{1}{\sigma}} (X_t)^{\frac{\sigma-1}{\sigma}} + (1 - \varsigma_t)^{\frac{1}{\sigma}} (Y_t)^{\frac{\sigma-1}{\sigma}} \right)^{\frac{\sigma}{\sigma-1}}, \quad C_t^* = \left((1 - \varsigma_t^*)^{\frac{1}{\sigma}} (X_t^*)^{\frac{\sigma-1}{\sigma}} + (\varsigma_t^*)^{\frac{1}{\sigma}} (Y_t^*)^{\frac{\sigma-1}{\sigma}} \right)^{\frac{\sigma}{\sigma-1}}; \quad (\text{C.25})$$

where

$$\varsigma_t = \varsigma \left(\frac{A_t}{\frac{1}{2}A_t + \frac{1}{2}A_t^*} \right)^\vartheta, \quad \varsigma_t^* = \varsigma \left(\frac{A_t^*}{\frac{1}{2}A_t + \frac{1}{2}A_t^*} \right)^\vartheta; \quad (\text{C.26})$$

The reduced-form relationships between the consumption shares and the respective endowment shares imply that agents want to allocate a larger share of their consumption to the goods that are in more abundant supply. With highly persistent productivity changes, this mechanism captures the empirical tendency of larger economies' goods to occupy a greater share of the world consumption bundle.

To a first order approximation, this mechanism only changes the equilibrium eqs. (C.23)–(C.24), which now read:

$$x_t - y_t^* = (c_t - c_t^*) + 2\sigma(1 - \varsigma)(tot_t) + (\varsigma_t - \varsigma_t^*); \quad (\text{C.27})$$

$$y_t - x_t^* = (c_t - c_t^*) - 2\sigma\varsigma(tot_t) - \frac{\varsigma}{1 - \varsigma}(\varsigma_t - \varsigma_t^*); \quad (\text{C.28})$$

where

$$\varsigma_t - \varsigma_t^* = \vartheta(a_t - a_t^*). \quad (\text{C.29})$$

Thus, to a first-order approximation, the channel operates entirely through relative demand: for a given consumption differential and terms of trade, a rise in the home endowment raises world demand for home goods relative to foreign goods.

3-equation system (benchmark model) The benchmark incomplete market model can be expressed as the system of three equations (11a)–(11c). Equation (11a) combines the goods market clearing conditions (C.20)–(C.21) with the goods demand functions in the baseline model (C.23)–(C.24). Equation (11b) integrates the modified UIP condition (C.18) with the Euler equations (C.16)–(C.17). Finally, equation (11c) links the country's budget constraint (C.19) with the goods market condition (C.20) and the demand equation (C.23). Throughout, relationship (C.22) is used to express the terms of trade in terms of the real exchange rate.

3-equation system (model with endogenous demand composition) Throughout we suppose that $\varsigma \geq \frac{1}{2}$, *i.e.* that home preferences are weakly home biased, and that $\sigma > \frac{1}{2\varsigma}$, *i.e.* that the trade elasticity is not too low. The latter assumption excludes the extremely low trade elasticities emphasized by Corsetti et al. (2008b). Bodenstein (2011) and Akinci and Chahrour (2025) argue that the counter intuitive effects of productivity shocks under extremely low trade elasticities are driven by equilibrium multiplicity. Most micro estimates of trade elasticities satisfy this constraint. Finally, we assume that the endogenous response of demand composition to an increase in relative home productivity is non-negative, *i.e.* $\vartheta \geq 0$. Note that when $\vartheta = 0$, the effects of technology disturbances are the same as in our baseline incomplete markets economy.

Finally, we assume that the inverse intertemporal elasticity—the CRRA coefficient—is sufficiently high. Specifically, we make

Assumption 1.

$$\gamma > \frac{2\varsigma - 1}{2\sigma\varsigma - 1}.$$

When Assumption 1 holds, we can state the following proposition:

Proposition 1. *For any given initial bond holdings b_t^* ,*

1. *An expected future increase in relative productivity causes an increase in relative consumption and an appreciation of the home real exchange rate. That is,*

$$\frac{\partial(c_t - c_t^*)}{\partial E_t[a_{t+j}]} > 0 \quad \text{and} \quad \frac{\partial q_t}{\partial E_t[a_{t+j}]} < 0, \quad \forall j > 0.$$

2. *A current increase in relative productivity causes a depreciation of the real exchange rate whenever $\vartheta = 0$. That is*

$$\frac{\partial q_t}{\partial a_t} > 0 \quad \text{if } \vartheta = 0.$$

3. *A current increase in relative productivity causes an appreciation of the real exchange rate whenever $\vartheta > \frac{1}{2\varsigma}$. That is,*

$$\frac{\partial q_t}{\partial a_t} < 0 \quad \text{if } \vartheta > \frac{1}{2\varsigma}.$$

The proposition is stated in terms of the expectations response function defined by Chahrour and Jurado (2025). An advantage of this approach is that it isolates the effects of changes in expectations regardless of their source: the conclusions do not depend on any particular assumptions about the exogenous process for productivity or assumptions about the information that the agents hold.

Proof. To conserve space, define home-foreign differential variables by, *e.g.*, $\tilde{a}_t \equiv a_t - a_t^*$. Combine equations (12a) - (12c) to deliver a second-order difference equation in b_t^* :

$$(\beta^{-1}L^2 + \omega_{b,0}^b L + 1)b_{t+1}^* = E_t [\omega_{b,0}^a(\tilde{a}_{t+1} - \tilde{a}_t) + \omega_{b,0}^\varsigma(\tilde{\varsigma}_{t+1} - \tilde{\varsigma}_t)] \quad (\text{C.30})$$

where L represents the lag operator. The coefficient $\omega_{b,0}^b$ on the left-hand side of (C.30) is given by

$$\omega_{b,0}^b = \beta^{-1} \frac{A\vartheta^2 + (\phi - A)\vartheta - (\beta + \phi + 1)}{B\vartheta^2 - B + 1} \quad (\text{C.31})$$

where $A \equiv 4(\beta + 1)(\gamma\sigma - 1) + 2\phi(\sigma - 1)$ and $B \equiv 4(1 - \gamma\sigma)$. Moreover, the coefficients on the right-hand side of (C.30) are

$$\omega_{b,0}^a = \frac{1 - \varsigma}{\beta} \frac{\chi_0}{\chi_1} \quad (\text{C.32})$$

$$\omega_{b,0}^\varsigma = \frac{\varsigma}{\beta} \frac{\chi_2}{\chi_1}, \quad (\text{C.33})$$

where $\chi_0 \equiv \gamma(2\sigma\varsigma - 1) + (1 - 2\varsigma) > 0$ and $\chi_1 \equiv 4(\gamma\sigma - 1)\varsigma(1 - \varsigma) + 1 > 0$ by Assumption 1, and $\chi_2 \equiv 2\gamma(1 - \varsigma) + (2\varsigma - 1) > 0$ by our assumption that $\varsigma > 1/2$.

Factoring, rewrite the left-hand side of (C.30) as

$$(1 - r_1^{-1}L)(1 - r_2^{-1}L)b_{t+1}^* = E_t [\omega_{b,0}^a(\tilde{a}_{t+1} - \tilde{a}_t) + \omega_{b,0}^\varsigma(\tilde{\varsigma}_{t+1} - \tilde{\varsigma}_t)] \quad (\text{C.34})$$

where $r_1 \in (0, 1)$ is the smaller root of the quadratic equation $\beta^{-1}r^2 + \omega_{b,0}^0r + 1 = 0$, $r_2 > 1$ is the larger root, and $\beta = r_1r_2$. The unique stable solution to (C.34) is given by

$$b_{t+1}^* = r_2^{-1}b_t^* + r_1\omega_0^a a_t + r_1\omega_0^\varsigma \varsigma_t - (1 - r_1)E_t \left[\sum_{j=1}^{\infty} r_1^j (\omega_0^a \tilde{a}_{t+j} + \omega_0^\varsigma \tilde{\varsigma}_{t+j}) \right].$$

To derive implications for q_t and relative consumption c_t , substitute the solution for b_{t+1}^* back into (12a) and (12b) to find

$$q_t = \omega_q^b b_t^* + \omega_{q,0}^a \tilde{a}_t + \omega_{q,0}^\varsigma \varsigma_t + (1 - r_1)E_t \left[\sum_{j=1}^{\infty} r_1^t (\omega_{q,1}^a \tilde{a}_{t+j} + \omega_{q,1}^\varsigma \tilde{\varsigma}_{t+j}) \right] \quad (\text{C.35})$$

$$\tilde{c}_t = \omega_c^b b_t^* + \omega_{c,0}^a \tilde{a}_t + \omega_{c,0}^\varsigma \varsigma_t + (1 - r_1)E_t \left[\sum_{j=1}^{\infty} r_1^t (\omega_{c,1}^a \tilde{a}_{t+j} + \omega_{c,1}^\varsigma \tilde{\varsigma}_{t+j}) \right] \quad (\text{C.36})$$

We can now compute the derivatives in Part 1 of the proposition. For example, using the relationship between \tilde{a}_t and $\tilde{\varsigma}_t$,

$$\frac{\partial \tilde{c}_t}{\partial E_t[a_{t+j}]} = (1 - r_1)r_1^j \left(\omega_{c,1}^a + \omega_{c,1}^\varsigma \frac{\partial \tilde{\varsigma}_{t+j}}{\partial a_{t+j}} \right) = (1 - r_1)r_1^j (\omega_{c,1}^a + \omega_{c,1}^\varsigma \vartheta).$$

Moreover, $(1 - r_1) > 0$ and $r_1^j > 0$, so that a sufficient condition for the whole term to be positive is that both $\omega_{c,1}^a > 0$ and $\omega_{c,1}^\varsigma > 0$.

After somewhat lengthy algebra, we have that

$$\omega_{c,1}^a = \frac{4\sigma\varsigma(1 - \varsigma)}{(2\sigma\varsigma - 2\varsigma + 1)} \frac{\chi_0}{\chi_1} > 0$$

The inequality follows from observing that $(1 - \varsigma) > 0$ since $\varsigma \in (1/2, 1)$ and $(2\sigma\varsigma - 2\varsigma + 1) > 0$ by our assumption about the trade elasticity. Similarly, we can show that

$$\omega_{c,1}^z = \frac{\varsigma}{1 - \varsigma} \frac{\chi_2}{\chi_0} \omega_{c,1}^a > 0.$$

Additional algebra establishes that

$$\omega_{q,1}^a = -\chi_3 \omega_{c,1}^a < 0 \quad \text{and} \quad \omega_{q,1}^z = -\chi_3 \omega_{c,1}^z < 0,$$

where $\chi_3 \equiv \frac{(2\varsigma-1)^2}{4\sigma\varsigma(1-\varsigma)} > 0$. Hence \tilde{c}_t and q_t move in opposite directions in response to anticipated changes in productivity. This establishes Part 1 of the proposition.

For the second part of the proposition, note that in this case $\frac{\partial q_t}{\partial a_t} = \omega_{q,0}^a$ and compute $\omega_{q,0}^a = -r_1 \omega_{q,1}^a + \frac{2\varsigma-1}{2\varsigma(\sigma-1)+1} > 0$, since both $-\omega_{q,1}^a > 0$ and $\frac{2\varsigma-1}{2\varsigma(\sigma-1)+1} > 0$, implying that $\frac{\partial q_t}{\partial a_t} > 0$ whenever $\vartheta = 0$. This establishes part (2) of the proposition.

For the part (3) of the proposition, we want to show

$$\frac{\partial q_t}{\partial a_t} = \omega_{q,0}^a + \omega_{q,0}^\varsigma \frac{\partial \tilde{c}_t}{\partial a_t} = \omega_{q,0}^a + \omega_{q,0}^\varsigma \vartheta \quad (\text{C.37})$$

is negative. Next, observe that

$$\omega_{q,0}^a = -r_1 \omega_{q,1}^a + \frac{2\varsigma-1}{2\varsigma(\sigma-1)+1} < -\omega_{q,1}^a + \frac{2\varsigma-1}{2\varsigma(\sigma-1)+1} \quad (\text{C.38})$$

$$\omega_{q,0}^\varsigma = -r_1 \omega_{q,1}^\varsigma + \frac{\varsigma}{\varsigma-1} \cdot \frac{2\varsigma-1}{2\varsigma(\sigma-1)+1} < -\omega_{q,1}^\varsigma + \frac{\varsigma}{\varsigma-1} \cdot \frac{2\varsigma-1}{2\varsigma(\sigma-1)+1} \quad (\text{C.39})$$

where the inequalities in both (C.38) and (C.39) follow from $\omega_{q,1}^a < 0$ and $\omega_{q,1}^\varsigma < 0$ respectively. Combining these inequalities with (C.37) and rearranging, we find

$$\frac{\partial q_t}{\partial a_t} < -\omega_{q,1}^a + \frac{2\sigma\varsigma-1}{2\varsigma(\sigma-1)+1} + \vartheta \left(-\omega_{q,1}^\varsigma + \frac{\varsigma}{\varsigma-1} \cdot \frac{2\varsigma-1}{2\varsigma(\sigma-1)+1} \right).$$

But, evaluating the right-hand side of this expression simplifying, we find it is negative whenever $\vartheta > \frac{1}{2\varsigma}$ completing the proof. ■

C.2 Blanchard et al. (2013) process

With the [Blanchard et al. \(2013\)](#) process, log productivity, a_t , is the sum of a permanent component μ_t (with autocorrelated growth rates) and a transitory component θ_t , but agents only observe the realizations of productivity a_t and not the two components separately. In addition, agents observe a noisy signal of the current value of the persistent component, $s_t = \mu_t + \xi_t$, which helps them forecast future TFP growth. Specifically, all stochastic processes $\{a_t\}$ and $\{s_t\}$ evolve according to the following system:

$$\begin{aligned} a_t &= \mu_t + \theta_t, \\ s_t &= \mu_t + \xi_t, \\ \Delta\mu_t &= \rho\Delta\mu_{t-1} + \varepsilon_t^\mu, \\ \theta_t &= \rho\theta_{t-1} + \varepsilon_t^\theta, \end{aligned} \quad \begin{bmatrix} \varepsilon_t^\mu \\ \varepsilon_t^\theta \\ \xi_t \end{bmatrix} \sim \text{iid } \mathcal{N} \left(0, \begin{bmatrix} \sigma_\mu^2 & 0 & 0 \\ 0 & \sigma_\theta^2 & 0 \\ 0 & 0 & \sigma_\xi^2 \end{bmatrix} \right). \quad (\text{C.40})$$

Lastly, it is common to impose the parameter restriction $\rho\sigma_\mu^2 = (1 - \rho)^2\sigma_\theta^2$, which ensures that the univariate Wold representation of TFP is a random walk as is true in the data.²⁵

To properly isolate the independent contributions of beliefs (or the independent effects of technology and noise disturbances), we follow Chahrour and Jurado (2018) to construct a noise representation that is observationally equivalent to representation (C.40).

Lemma 1. *The representation of fundamentals and beliefs in system (C.40) is observationally equivalent to the noise representation:*

$$\begin{aligned} \Delta a_t &= \frac{1 - \alpha L}{1 - \rho L} \varepsilon_t^m \\ \Delta \tilde{s}_t &= \sum_{j=0}^{\infty} \alpha^j \varepsilon_{t+j}^m + \tilde{v}_t, \\ \tilde{v}_t &= \frac{\sigma_\theta^2}{\alpha\sigma_\mu^2} \frac{(1 - L)(1 - \bar{\delta}_1 L)(1 - \bar{\delta}_2 L)}{(1 - \alpha L)} \varepsilon_t^v, \\ \begin{bmatrix} \varepsilon_t^m \\ \varepsilon_t^v \end{bmatrix} &\stackrel{iid}{\sim} \mathcal{N} \left(0, \begin{bmatrix} \sigma_\theta^2/\alpha & 0 \\ 0 & \frac{\alpha\rho\sigma_\xi^2}{\bar{\delta}_1\bar{\delta}_2} \end{bmatrix} \right), \end{aligned}$$

where α is the stable root of $L^2 - (2 + \frac{\sigma_\mu^2}{\sigma_\theta^2})L + 1 = 0$, and $\bar{\delta}_1, \bar{\delta}_2$ are the two stable roots of the polynomial $D(L)$ (excluding the unit roots):

$$D(L) = (1 - \alpha L)(1 - \alpha L^{-1})\sigma_\mu^2 + (1 - \rho L)(1 - \rho L^{-1})(1 - \alpha L)(1 - \alpha L^{-1})(1 - L)(1 - L^{-1})\sigma_\xi^2 - \alpha \frac{\sigma_\mu^4}{\sigma_\theta^2}$$

Proof. First, let's derive the univariate Wold representation of Δa_t . The process can be written as:

$$\Delta a_t = \frac{1}{1 - \rho L} (\varepsilon_t^\mu + (1 - L)\varepsilon_t^\theta)$$

The autocovariance generating function of Δa is:

$$\Gamma_{\Delta a}(L) = \frac{\sigma_\mu^2 + \sigma_\theta^2(2 - L - L^{-1})}{(1 - \rho L)(1 - \rho L^{-1})}.$$

After factorizing the numerator, we obtain:

$$\Gamma_{\Delta a}(L) = \frac{\sigma_\theta^2}{\alpha} \cdot \frac{(1 - \alpha L)(1 - \alpha L^{-1})}{(1 - \rho L)(1 - \rho L^{-1})},$$

²⁵Blanchard et al. (2013) refer to ε_t^μ as a permanent productivity shock, ε_t^θ as a transitory productivity shock, and ξ_t as an information noise shock.

where $\alpha \in (0, 1)$ is the stable root of the quadratic equation $L^2 - (\frac{\sigma_\mu^2}{\sigma_\theta^2} + 2)L + 1 = 0$. This implies the Wold representation,

$$\Delta a_t = \frac{1 - \alpha L}{1 - \rho L} \varepsilon_t^m, \quad \varepsilon_t^m \stackrel{iid}{\sim} \mathcal{N}(0, \sigma_\theta^2 / \alpha).$$

The signal, written as a lag polynomial, is given by

$$\Delta s_t = \frac{1}{1 - \rho L} \varepsilon_t^\mu + (1 - L) \xi_t.$$

Projecting Δs_t onto the full past, present, and future Δa_t , we can write

$$\Delta s_t = B(L) \Delta a_t + v_t,$$

where

$$B(L) = \frac{\Gamma_{\Delta a, \Delta s}(L)}{\Gamma_{\Delta a}(L)} = \frac{\sigma_\mu^2}{(1 - \rho L)(1 - \rho L^{-1})} \frac{1}{\Gamma_{\Delta a}(L)} = \frac{\alpha}{(1 - \alpha L)(1 - \alpha L^{-1})} \frac{\sigma_\mu^2}{\sigma_\theta^2}$$

and v_t is a noise process, characterized below, that is orthogonal to all leads and lags of Δa_t . Substituting the Wold form of Δa_t we find,

$$B(L) \Delta a_t = \frac{\alpha}{(1 - \alpha L^{-1})(1 - \rho L)} \frac{\sigma_\mu^2}{\sigma_\theta^2} \varepsilon_t^m.$$

Therefore:

$$\Delta s_t = \frac{\alpha}{(1 - \alpha L^{-1})(1 - \rho L)} \frac{\sigma_\mu^2}{\sigma_\theta^2} \varepsilon_t^m + v_t. \quad (\text{C.41})$$

To simplify without changing the information content of Δs_t , we scale both sides of (C.41) by the invertible polynomial $F(L) \equiv \frac{\sigma_\theta^2(1 - \rho L)}{\alpha \sigma_\mu^2}$ to find

$$\Delta \tilde{s}_t \equiv \frac{\sigma_\theta^2(1 - \rho L)}{\alpha \sigma_\mu^2} \Delta s_t = \frac{1}{(1 - \alpha L^{-1})} \varepsilon_t^m + \tilde{v}_t = \sum_{j=0}^{\infty} \alpha^j \varepsilon_{t+j}^m + \tilde{v}_t.$$

Finally, to characterize \tilde{v}_t , compute its autocovariance generating function

$$\begin{aligned} \Gamma_{\tilde{v}}(L) &= F(L) F(L^{-1}) [\Gamma_{\Delta s}(L) - B(L) \Gamma_{\Delta a}(L) B(L^{-1})] \\ &= F(L) F(L^{-1}) \left[\frac{D(L)}{(1 - \rho L)(1 - \rho L^{-1})(1 - \alpha L)(1 - \alpha L^{-1})} \right] \end{aligned}$$

where the polynomial $D(L)$ is:

$$D(L) \equiv (1 - \alpha L)(1 - \alpha L^{-1}) \sigma_\mu^2 + (1 - \rho L)(1 - \rho L^{-1})(1 - \alpha L)(1 - \alpha L^{-1})(1 - L)(1 - L^{-1}) \sigma_\xi^2 - \alpha \frac{\sigma_\mu^4}{\sigma_\theta^2}.$$

Then $\Gamma_{\tilde{v}}(L)$ becomes:

$$\Gamma_{\tilde{v}}(L) = \left(\frac{\sigma_\theta^2}{\alpha\sigma_\mu^2} \right)^2 \left[\frac{D(L)}{(1-\alpha L)(1-\alpha L^{-1})} \right].$$

Since $\Gamma_{\tilde{v}}(L)$ is a spectral density, $D(L)$ is symmetric and non-negative on the unit circle, ensuring a symmetric factorization exists. Furthermore, because α is defined such that $\alpha^2 - (\frac{\sigma_\mu^2}{\sigma_\theta^2} + 2)\alpha + 1 = 0$, we have $D(1) = 0$. This implies that $(1-L)(1-L^{-1})$ is a factor of $D(L)$. Factoring out the unit root, the square root of $\Gamma_{\tilde{v}}(L)$ gives the following Wold representation:

$$\tilde{v}_t = \frac{\sigma_\theta^2}{\alpha\sigma_\mu^2} \frac{(1-L)(1-\bar{\delta}_1 L)(1-\bar{\delta}_2 L)}{(1-\alpha L)} \varepsilon_t^v, \quad \varepsilon_t^v \stackrel{iid}{\sim} \mathcal{N}(0, \frac{\alpha\rho\sigma_\xi^2}{\bar{\delta}_1\bar{\delta}_2}) \quad (\text{C.42})$$

where $\bar{\delta}_1$ and $\bar{\delta}_2$ are the remaining stable roots of $D(L)$. ■

Calibration We assume foreign TFP is cointegrated with home TFP, that is, $\Delta a^* = \tau(a_{t-1} - a_{t-1}^*)$, where the parameter τ captures cross-country convergence in TFP. Table C.1 summarizes the calibration of this process that we use in Section 5.

Table C.1: Calibration of [Blanchard et al. \(2013\)](#) process

| Parameter | Description | Value |
|-----------------|--|--------------------|
| ρ | Pers. “permanent shock” | 0.89 |
| σ_θ | Std. dev. “transitory shock” | 0.61 |
| σ_ξ | Std. dev. “noise shock” | 5×10^{-5} |
| σ_μ | Std. dev. “permanent shock” $\rho\sigma_\mu^2 = (1-\rho)^2\sigma_\theta^2$ | |
| τ | Co-integration parameter | 0.025 |

Notes: Models are calibrated to quarterly frequency. The rest of the parameters are calibrated according to Table 4.

C.3 Long-run risk process

In this appendix, we consider a long-run risk process, of the type studied in international finance and macroeconomics by [Colacito and Croce \(2011, 2013\)](#) and [Colacito et al. \(2018\)](#). Letting Δa_t denote the growth rate of productivity (in deviations from its mean), the process $\{\Delta a_t\}$ is assumed to follow the law of motion:

$$\begin{aligned} \Delta a_t &= z_{t-1} + \varepsilon_t^a, \\ z_t &= \rho z_{t-1} + \varepsilon_t^z, \end{aligned} \quad \begin{bmatrix} \varepsilon_t^z \\ \varepsilon_t^a \end{bmatrix} \stackrel{iid}{\sim} \mathcal{N} \left(\begin{bmatrix} 0 \\ 0 \end{bmatrix}, \begin{bmatrix} \sigma_z^2 & 0 \\ 0 & \sigma_a^2 \end{bmatrix} \right), \quad (\text{C.43})$$

where $0 < \rho < 1$. Colacito and Croce (2013) refer to ε_t^z as a long-run shock (or news shock), and ε_t^a as a short-run shock.

To properly isolate the independent contributions of beliefs (or the independent effects of technology and noise disturbances), we follow Chahrour and Jurado (2018) and construct a noise representation that is observationally equivalent to representation (C.43). The following lemma presents one such noise representation.

Lemma 2. *The representation of fundamentals and beliefs in system (C.43) is observationally equivalent to the noise representation*

$$\begin{aligned}\Delta a_t &= \rho \Delta a_{t-1} + \kappa \varepsilon_t^w - \kappa \alpha \varepsilon_{t-1}^w \\ \tilde{z}_t &= \sum_{j=0}^{\infty} \alpha^j \varepsilon_{t+1+j}^w + \tilde{v}_t \\ \tilde{v}_t &= \alpha \tilde{v}_{t-1} + \frac{\sigma_a}{\sigma_z} \varepsilon_t^v - \rho \frac{\sigma_a}{\sigma_z} \varepsilon_{t-1}^v \\ \begin{bmatrix} \varepsilon_t^w \\ \varepsilon_t^v \end{bmatrix} &\stackrel{iid}{\sim} \mathcal{N} \left(0, \begin{bmatrix} 1 & 0 \\ 0 & 1 \end{bmatrix} \right),\end{aligned}$$

where α is the stable root of $L^2 - \frac{1}{\rho}(1 + \rho^2 + \frac{\sigma_z^2}{\sigma_a^2})L + 1$ and $\kappa \equiv \sqrt{\frac{\rho}{\alpha}}\sigma_a$.

Proof. The proof follows the same logic as in Lemma 1. First, let's derive the univariate Wold representation of Δa_t . The autocovariance generating function (ACGF) of Δa is:

$$\Gamma_{\Delta a}(L) = \frac{\sigma_z^2}{(1 - \rho L)(1 - \rho L^{-1})} + \sigma_a^2 = \frac{\sigma_z^2 + \sigma_a^2(1 - \rho L)(1 - \rho L^{-1})}{(1 - \rho L)(1 - \rho L^{-1})}.$$

We can factor the numerator as a symmetric second-order polynomial:

$$\Gamma_{\Delta a}(L) = \frac{\rho \sigma_a^2}{\alpha} \frac{(1 - \alpha L)(1 - \alpha L^{-1})}{(1 - \rho L)(1 - \rho L^{-1})} \tag{C.44}$$

where α is the stable root of the quadratic equation $L^2 - \frac{1}{\rho}(1 + \rho^2 + \frac{\sigma_z^2}{\sigma_a^2})L + 1$. Taking the square root yields the Wold representation:

$$\Delta a_t = \frac{1 - \alpha L}{1 - \rho L} \sqrt{\frac{\rho}{\alpha}} \sigma_a \varepsilon_t^w \tag{C.45}$$

where $\varepsilon_t^w \stackrel{iid}{\sim} \mathcal{N}(0, 1)$ is the Wold innovation.

Second, let's represent the signal process as a function of ε_t^w and noise. Define the linear projection:

$$z_t = B(L)\Delta a_t + v_t \tag{C.46}$$

where $v_t \perp \Delta a_{t-j} \forall j \in \mathbb{Z}$, i.e., the noise component is orthogonal to all leads and lags of

technology. We can write

$$B(L) = \frac{\Gamma_{z,\Delta a}(L)}{\Gamma_{\Delta a}(L)} = \frac{\sigma_z^2 L^{-1}}{\sigma_z^2 + \sigma_a^2(1 - \rho L)(1 - \rho L^{-1})} = \frac{\sigma_z^2 \alpha L^{-1}}{\rho \sigma_a^2(1 - \alpha L)(1 - \alpha L^{-1})}.$$

The noise process v_t has autocovariance generating function:

$$\begin{aligned}\Gamma_v(L) &= \Gamma_z(L) - B(L)\Gamma_{\Delta a}(L)B(L^{-1}) \\ &= \frac{\sigma_z^2}{(1 - \rho L)(1 - \rho L^{-1})} - \Gamma_{z,\Delta a}(L) \frac{\sigma_z^2 \alpha L}{\rho \sigma_a^2(1 - \alpha L)(1 - \alpha L^{-1})} \\ &= \frac{\sigma_z^2 \left((1 - \alpha L)(1 - \alpha L^{-1}) - \frac{\sigma_z^2 \alpha}{\rho \sigma_a^2} \right)}{(1 - \alpha L)(1 - \alpha L^{-1})(1 - \rho L)(1 - \rho L^{-1})} \\ &= \frac{\sigma_z^2 \alpha}{\rho} \frac{1}{(1 - \alpha L)(1 - \alpha L^{-1})}\end{aligned}$$

where the last equality uses the factorization in eq.(C.44). This gives the Wold representation:

$$v_t = \frac{1}{1 - \alpha L} \sqrt{\frac{\alpha}{\rho}} \sigma_z \varepsilon_t^v \quad (\text{C.47})$$

with $\varepsilon_t^v \stackrel{iid}{\sim} \mathcal{N}(0, 1)$.

Plug eq. (C.47) and (C.45) into (C.46) and rearrange as:

$$\underbrace{\frac{\kappa}{\sigma_z^2}(1 - \rho L)z_t}_{\tilde{z}_t} = \frac{L^{-1}}{1 - \alpha L^{-1}} \epsilon_t^w + \underbrace{\frac{\kappa}{\sigma_z^2}(1 - \rho L)v_t}_{\tilde{v}_t} \quad (\text{C.48})$$

where $\kappa \equiv \sqrt{\frac{\rho}{\alpha}} \sigma_a$. Thus, the information structure can be written as:

$$\begin{aligned}\Delta a_t &= \rho \Delta a_{t-1} + \kappa \varepsilon_t^w - \kappa \alpha \varepsilon_{t-1}^w \\ \tilde{z}_t &= \sum_{j=0}^{\infty} \alpha^j \varepsilon_{t+1+j}^w + \tilde{v}_t \\ \tilde{v}_t &= \alpha \tilde{v}_{t-1} + \frac{\sigma_a}{\sigma_z} \varepsilon_t^v - \rho \frac{\sigma_a}{\sigma_z} \varepsilon_{t-1}^v\end{aligned}$$

■

Calibration We assume foreign TFP process follows an analogous process, and it is cointegrated with home TFP:

$$\begin{aligned}\Delta a_t^* &= z_{t-1}^* + \tau(a_{t-1} - a_{t-1}^*) + \varepsilon_{a,t}^*, & \begin{bmatrix} \varepsilon_{z,t}^* \\ \varepsilon_{a,t}^* \end{bmatrix} &\stackrel{iid}{\sim} \mathcal{N} \left(\begin{bmatrix} 0 \\ 0 \end{bmatrix}, \begin{bmatrix} \sigma_z^2 & 0 \\ 0 & \sigma_a^2 \end{bmatrix} \right), \\ z_t^* &= \rho z_{t-1}^* + \varepsilon_{z,t}^*,\end{aligned} \quad (\text{C.49})$$

Table C.2 summarizes the calibration of this process. Figure C.1 characterizes the impulse responses of the complete market model with Epstein-Zin preferences under the long-run risk process.

Table C.2: Calibration of Long-run risk process

| Parameter | Description | Value |
|------------|------------------------------|-----------------------|
| ρ | Pers. “permanent shock” | 0.99 |
| σ_a | Std. dev. “transitory shock” | 4.9×10^{-3} |
| σ_z | Std. dev. “permanent shock” | 3.85×10^{-2} |
| τ | Co-integration parameter | 0.0023 |

Notes: Models are calibrated to quarterly frequency. The rest of the parameters are calibrated according to Table 4.

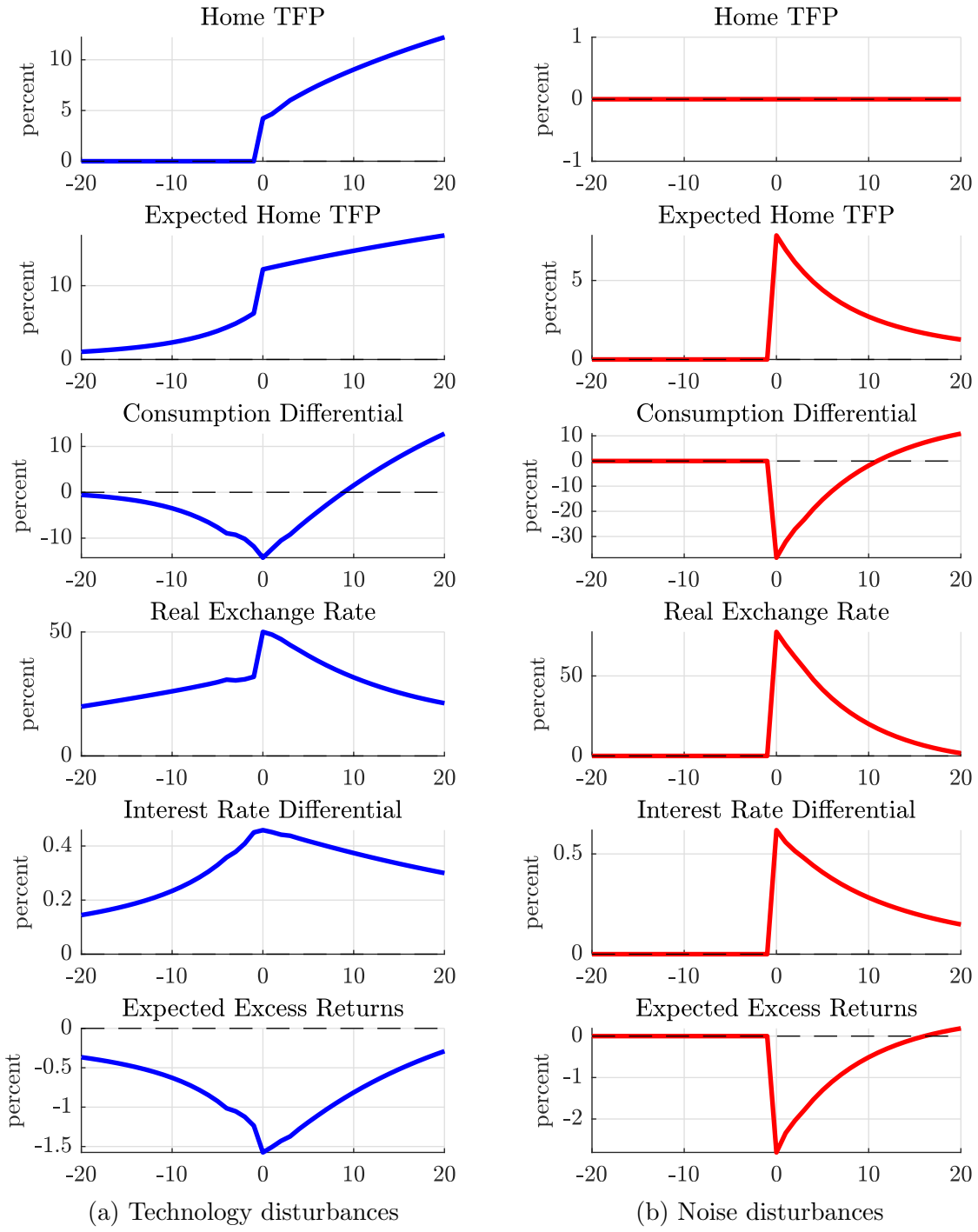


Figure C.1: Impulse response under Long-run risk process for TFP

Note: The model features complete markets with Epstein-Zin preferences. Table C.2 reports the parameter values of eq. (C.43). Model is calibrated to quarterly frequency.

C.4 The role of fluctuations in UIP deviations

In this appendix, we shed light on the channel through which the noisy news about future TFP transmit to the exchange rate in the incomplete-market model with endogenous demand composition. To begin with, we note that the real exchange rate can be decomposed into two terms, (i) the sum of expected future interest rate differentials; and (ii) the sum of future currency excess returns, as follows:

$$q_t = \underbrace{-\sum_{k=0}^{\infty} \mathbb{E}_t(r_{t+k} - r_{t+k}^*)}_{q_t^{UIP}} + \underbrace{\left(-\sum_{k=0}^{\infty} \mathbb{E}_t \lambda_{t+k+1} \right)}_{q_t^\lambda}. \quad (\text{C.50})$$

Thus, one can write the real exchange rate as the sum of the counter-factual exchange rate that would obtain if there are no deviations from interest parity, q_t^{UIP} , and the contribution of any predictable fluctuations in deviations from interest parity, q_t^λ .²⁶

We apply this decomposition in the model, and report the separate responses of q_t^{UIP} and q_t^λ to technological and expectational disturbances. Figure C.2 reports the results of this analysis.

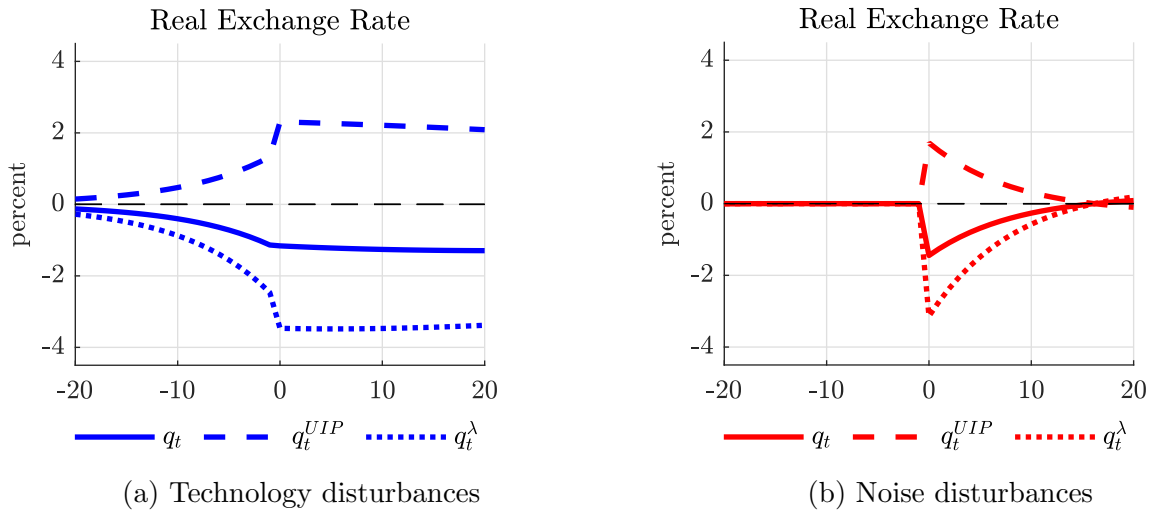


Figure C.2: Impulse response of exchange rate and its components

Note: The figure depicts the impulse response of the real exchange rate and its components (cf. eq. (C.50)) in the extended incomplete market model.

The main takeaway is that, in the model, noisy news primarily transmit to the exchange rate via fluctuations in the q_t^λ component, reflecting the importance of a time-varying “UIP wedge.” More specifically, technological disturbances are associated—both in the model and in the data—with expectations of low interest differentials, which occur when the productivity improvement materializes. Yet the real exchange rate remains appreciated not only in anticipation of, but also upon realization of, the productivity improvement, indicating that

²⁶In the model, the real exchange rate is stationary.

interest differentials alone cannot explain the observed exchange rate dynamics. Indeed, technological disturbances are associated—both in the model and in the data—with high expected excess foreign currency returns. In the model, this arises because the home economy becomes a net external creditor when TFP rises, a force that sustains an appreciated exchange rate both before and after the change in TFP materializes. Thus, the decomposition attributes most of the exchange rate variation to the expected path of excess currency returns, while the expected path of interest differentials acts in the opposite direction.